The Evolution of Plane Solitons

Michael A. Allen

Department of Physics
University of Warwick
Coventry CV4 7AL

This thesis is submitted to the University of Warwick
in partial fulfilment of the requirements
for admission to the degree of Doctor of Philosophy

September 1994

Abstract

In this work we use the Zakharov-Kuznetsov equation to study the evolution of a plane soliton subjected to a two-dimensional perturbation. The first part of the thesis is concerned with determining the growth rate of such a perturbation. We present two closely related methods which allow us to obtain rigorously the growth rates much more directly and simply than previous approaches. Both methods are general and hence applicable to other problems. If the perturbation is of a large enough wavelength, the plane soliton will evolve into more stable coherent structures of the form of two-dimensional solitons. This process is the subject of the remainder of the thesis. A weakly nonlinear analysis which fully describes the preliminary stages of the process is developed. We have studied how the eventual fate of a plane soliton is affected by the wavelength of the perturbation and obtained a simple formula for the variation of the number of cylindrical solitons formed with this wavelength.

The methods developed in this thesis have been used to obtain an analytical description of a soliton state that occurs in coupled optical fibres.

Acknowledgements

First and foremost I would like to thank Professor George Rowlands for his great supervision and guidance. I feel very fortunate to have had a supervisor with such enthusiasm and experience.

I am also indebted to all my friends and colleagues who have helped to make my time here enjoyable. In particular, many thanks go to Thanasis, with whom I shared the office in earlier days, for his encouragement and reassurance, and to my contemporaries Dej and Thanasi for many hours of discussion. Dej's TEXpertise, knowledge about Unix, 'C', and bicycle repairs, his extensive library, and his companionship have been very much appreciated over the years, as have Thanasi's Greek and cooking instruction, and encouragement in all things. I would also like to thank Julia for her support and encouragement.

Thanks are also due to the members of the UWSO with whom I spent many a happy hour, and also to Roger Coull for his violin lessons, which although few and far between, have been very beneficial.

Special thanks go to my parents who somewhere back in the mists of time must have sparked off my interest in science and nature, my grandparents, and my sister Jax for their love and support, and to Tanya for her interest and encouragement over the years.

I also acknowledge the Science and Engineering Research Council for providing the three year studentship.

Declaration

Except where otherwise indicated, this thesis contains an account of my own independent research undertaken in the Department of Physics, University of Warwick between January 1992 and September 1994, under the supervision of Professor George Rowlands. Some of Chapter 2 has appeared in the scientific literature (Allen & Rowlands 1993).

Contents

Chapter 1

Introduction

1.1 Self-organization and nonlinear physics

One of the central mysteries facing mankind is how structures as complicated as a living organism could arise as a consequence of physical laws which can be formulated so compactly. The incredible intricacy of the mechanism behind even the simplest life-forms have persuaded many that their origin must lie outside science. Our challenge is to see how much can be explained without having to resort to supernatural intervention.

According to the reductionist point of view, all processes can in principle be derived from the most basic laws. However, it is an enormous jump from quantum mechanics to the spontaneous formation of the simplest self-replicating system. This, amongst other difficulties, has prompted some to question whether the microscopic laws are truly 'fundamental' - perhaps it is a set of macroscopic laws that really belong in this elevated category (Prigogine 1980). There is also a growing feeling that at *each* level of complexity there is a set of laws which are fundamental in the sense that they cannot be derived from those governing another level (see e.g. Davies 1987).

Intimately connected with complexity is the phenomenon of self-organization. A self-organized state is a spontaneously appearing spatial pattern or temporal rhythm which has some degree of global co-operation. It seems that all the complex structures we see are a result of some sort of self-organizing process. If the simplest of such processes can be understood, we may gain some idea of what the new laws of complex systems are like. We would also be starting to bridge the gap to an understanding of more complicated structures resulting from self-organization, and problems such as morphogenesis or how DNA could form from a primordial soup.

The key requirement of a self-organizing system is nonlinearity. The term '*non*-linearity' might suggest that this property is the exception to the norm. It is in fact quite the opposite - as Stanislaw Ulam put it, calling it "nonlinear science" is like referring to zoology as "the study of non-elephant animals". Although the majority of phenomena involve nonlinearity as an essential ingredient, most of the results of physics, especially the earlier ones, are a product of linear analyses. This is because linear problems can be broken down into a sum of constituent parts and are therefore usually much more readily solved than nonlinear systems which in general can only be treated in a holistic manner. Physicists' success with linear models of certain macroscopic systems has tended to divert their attention away from other perhaps more physically important theories. Furthermore, constant application of linear methods is

bound to instill a reductionist way of thinking; and yet a world without nonlinearity and the self-organizing phenomena it results in would be (literally) lifeless.

In many self-organizing systems one finds localized coherent structures. The simplest type of self-organization in physics is the phase transition, an example of which occurs on cooling a ferromagnet to below its Curie temperature. The domain wall separating large regions of aligned spins is such a localized structure. While phase transitions occur close to equilibrium, the self-organization usually discussed in the literature occurs in driven dissipative systems far from equilibrium. Perhaps the most familiar example of this in physics is turbulent fluid flow. The coherent structures we see here are relatively long lived eddies or vortices. Both these and domain walls can be regarded as types of 'soliton'.

1.2 Solitons

A loose definition of a soliton would be a distortion of a medium, localized in at least one dimension, be it either spatial or temporal, that has a significant degree of permanence. The classic example of a soliton is the one observed by Scott Russell in 1834. He saw a canal boat come to an abrupt halt and as a result produce "a large solitary elevation, a rounded, smooth and well-defined heap of water which continued its course along the channel, apparently without change of form or diminution of speed" (Russell 1844). The fact that this persistent structure emerged from all the turbulence of the barge stopping is what is so remarkable - we here see the formation of a relatively stable state of matter lying between the microscopic and the global. The formation of solitons in general appears to occur via this self-organizing type behaviour - a fairly unspecific initial condition in a suitable régime will evolve to produce a number of solitons, as well as some uninteresting background disturbance in some cases. However, unlike the typical self-organizing systems, the most familiar examples of solitons exist in conservative systems close to equilibrium. Although solitons lack the complexity of the more traditional self-organizing systems, they are much more amenable to analysis. The study of solitons may therefore provide the preliminaries for an understanding of more complex structures.

The name soliton was coined by Zabusky & Kruskal (1965). They numerically followed the evolution of the same equation that governs the soliton observed by Russell. The initial condition they chose contained no solitons but after a while a number of pulse-like forms appeared whose speed was proportional to their amplitude. They discovered that the solitary pulses pass through one another unscathed apart from a change in phase. This was totally unexpected for a nonlinear equation. Perhaps it was because the space-time plots of the pulse maxima looked like Feynman diagrams for particle interactions that they added yet another '-on'-word to the menagerie.

The definition of a soliton we have given is so general that it encompasses a very wide variety of phenomena. It is helpful to divide them into two classes - topological and non-topological solitons. Topological solitons, also known as 'kinks', are the boundary layers (either in space or time) between different states of the medium. The domain wall mentioned before is an example of one - the spins are aligned in one direction on one side of the wall and in the opposite direction on the other side.

Non-topological solitons are like Russell's - the system remains in the same state after their passage as before. The solitons we will be considering in this thesis are all non-topological and are mostly derived from equations governing plasmas. However, non-topological solitons

of some variety occur in a very wide range of media. As will be discussed shortly, they occur in all fluids, and also, from the work of Krumhansl & Schrieffer (1975) it appears that, over a certain range of temperature, the thermal properties of solids are better accounted for using a model based on solitons than by using the usual (linear) phonon picture. Examples of solitons which are more directly observable can be induced in light propagating down optical fibres (see e.g. Hasegawa 1989), as Gunn domains in semiconductors (Butcher 1967), and as fluxons in Josephson junctions (Parmentier in Lonngren & Scott 1978). It has been postulated that the age-old problem of muscle-contraction may be explained by the passage of a soliton (Davydov 1982).

It is hardly surprising that the soliton struck Russell as a "singular and beautiful phenomenon" - an ordinary pulse-shaped waveform, which is equivalent to a superposition of a pulse-shaped distribution of wavelengths, soon spreads out due to the dispersive effect of the medium (the speed of a linear wave depends on its wavelength). The soliton, on the other hand, retains its shape as a result of some kind of nonlinearity which acts as to exactly oppose the dispersion. In all fluids nonlinearity arises quite naturally on applying Newton's second law to an individual particle in the flow. Since dispersion is also a generic property of such media, solitons are possible in any fluid. The presence of solitons, however, is usually far from obvious - although the physical system may contain a nonlinear element, as in the case of waves on a canal, its effect will only be apparent in phenomena with particular length and time scales. This is discussed further in the next section.

1.3 Approximation methods

In order to attempt to describe the universe, physics uses mathematical models. These are based on a hierarchy of approximations, the most fundamental of which is that rather than describing the system containing a large number of particles in terms of all of their positions and properties, we use just a handful of quantities, such as density and temperature, that are continuous functions of position and time. As a result, the mathematical models are generally based around differential or integral equations.

Given a sufficiently powerful computer and a sophisticated enough algorithm, an arbitrarily accurate solution to the model equations may be obtained using numerical methods. However, in doing so it is very easy to lose sight of the physics behind the phenomenon being modelled. It is therefore preferable to solve as much of the problem as possible analytically. The numerical results are then used in a complementary fashion, both as a check on the analytical results and to explore the regions of parameter space that the analysis cannot cope with.

In the event that the full model equations are too difficult to solve analytically, we can usually derive other equations from them which are valid for a limited range of the dependent variables. We must be careful to check that the solutions obey the assumptions used in deriving the approximate equations - it is quite possible that an amplitude which was assumed small in the derivation could grow large, at which point we have to stop using that equation. One common application of this technique used frequently in this work is linearization. Although the linearized equations are generally valid only in the limit of small times, they can be used to investigate the stability of equilibrium solutions of nonlinear equations.

Even the equations obtained after some form of surgery may not be solvable. We must then turn to inexact methods of solution. There are two basic approaches to obtaining

inexact solutions - using perturbation theory or a method based on a variational principle. Perturbation theory is the more widely applicable of the two in problems involving solitons. Not only is it used to obtain approximate solutions to equations, the equations themselves are often derived from the full equations using a perturbative approach.

Perturbation theory

Perturbation theory is applied to problems which cannot be solved analytically but deviate only slightly from problems whose solutions are known. The extent of this deviation is quantified by some small parameter ϵ. The basic idea behind perturbation theory is to expand the dependent variable(s) y as a power series in ϵ, for example

$$y = y_0 + \epsilon y_1 + \epsilon^2 y_2 + \ldots, \tag{1.1}$$

where y_0 is a known solution. The y_j, $j > 0$ are obtained by substituting (1.1) into the original equation and equating the coefficients of ascending powers of ϵ to zero. Provided ϵ is small enough, the first few terms of (1.1) should give a good approximation to the true solution. When the equations for non-zero ϵ differ fundamentally from those when $\epsilon = 0$, we have to choose a more sophisticated form of expansion. This expansion may well turn out to be asymptotic - that is, for a given ϵ, the solution only converges for a finite number of terms after which it diverges. Such cases are known as singular perturbation problems.

Even non-singular problems are not always free from difficulties. When applying ordinary perturbation theory to problems which are known to have periodic solutions we sometimes encounter secular terms of the form $tP(t)$ where $P(t)$ has period T. Such terms are evidently non-periodic and will dominate for sufficiently large t. If the secular terms cannot be eliminated by choice of arbitrary constants, as will be the case if the perturbation is nonlinear, their presence will restrict the validity of the expansion to $t \ll T$. One way to remove the secular terms is to allow the period to become dependent on ϵ. This is the essence of the Linstedt-Poincaré method (see e.g. Nayfeh & Mook 1979). We change variables to $\tau = \omega t$ and assume that

$$\omega = \omega_0 + \epsilon\omega_1 + \epsilon^2\omega_2 + \ldots$$

where $\omega_0 = 2\pi/T$. We then choose the values of the additional arbitrary constants ω_j, $j > 0$, in order to eliminate the secular terms. The amplitude-dependent frequency we are left with is the hallmark of a nonlinear perturbation.

A more powerful but more involved way of dealing with the secularities is the method of multiple scales (see e.g. Davidson 1972). This method can also cope with such terms arising in nonperiodic problems and is therefore applicable to the analysis of solitons. The basic idea behind a multiple-scale perturbation analysis is to effectively regroup the secular terms in the full expansion so that they form the series for a well behaved function of a 'scaled' independent variable. For example, if we apply straightforward perturbation analysis to a perturbed simple harmonic oscillator,

$$\ddot{y} + \omega_0^2 y + \epsilon y^3 = 0, \tag{1.2}$$

and ignore the fact that secular terms are arising, the sum of the most divergent terms at each successive order up to ϵ^2 is

$$A\cos(\omega_0 t + \phi) - \frac{3}{8}\frac{\epsilon A^3 t}{\omega_0}\sin(\omega_0 t + \phi) - \frac{9}{128}\frac{\epsilon^2 A^5 t^2}{\omega_0^2}\cos(\omega_0 t + \phi). \tag{1.3}$$

This is the same as the expansion to second order of

$$A\cos\left(\omega_0 t + \frac{3}{8}\frac{\epsilon A^2}{\omega_0}t + \phi\right).$$

We see that y varies on two time-scales: the original simple harmonic oscillator frequency ω_0 and a much slower amplitude-dependent variation of frequency $3\epsilon A^2/8\omega_0$. All secular terms can in fact be subsumed in a similar manner, giving rise to higher and higher order corrections to the overall frequency.

The power of the multiple-scale method lies in the fact that the regrouping of terms is carried out automatically. To achieve this, the dependent variable $y(t)$ is replaced by a function $y(t, t_1, t_2, ...)$ of the original independent variable and a series of scaled independent variables $t_m \equiv \epsilon^m t$, $m = 1, 2, \ldots$. These new scaled variables are treated as being independent of t and of one another. To introduce the scaled variables into the proceedings, any derivatives with respect to the original independent variable are replaced via an expansion of the type:

$$\frac{d}{dt} = \frac{\partial}{\partial t} + \epsilon\frac{\partial}{\partial t_1} + \epsilon^2\frac{\partial}{\partial t_2} + \ldots .$$

The arbitrary functions of the scaled variables which arise in the subsequent analysis are chosen to eliminate the secular terms.

Returning to our example, on applying the multiple-scale analysis to (1.2) we find to zeroth order

$$y_0 = A_0\cos(\omega_0 t + \phi_0)$$

where the arbitrary constants of the ordinary analysis have been replaced by the arbitrary functions $A_0 = A_0(t_1, t_2, ...)$ and $\phi_0 = \phi_0(t_1, t_2, ...)$. The first order equation will now include a term involving a partial derivative with respect to the scaled variable t_1:

$$\frac{\partial^2 y_1}{\partial t^2} + \omega_0^2 y_1 = -y_0^3 - 2\frac{\partial^2 y_0}{\partial t \partial t_1}.$$

Solving this gives

$$y_1 = \frac{A_0^3}{32\omega_0^2}\cos 3\Xi_0 - \frac{3}{8}\frac{A_0^3}{\omega_0}t\sin\Xi_0 + A_0\frac{\partial\phi_0}{\partial t_1}t\sin\Xi_0 + \frac{\partial A_0}{\partial t_1}t\cos\Xi_0 \qquad (1.4)$$

where $\Xi_0 \equiv \omega_0 t + \phi_0$. To remove the three secular terms, we merely make

$$\frac{\partial A_0}{\partial t_1} = 0 \quad \text{and} \quad \frac{\partial\phi_0}{\partial t_1} = \frac{3}{8}\frac{A_0^2}{\omega_0}.$$

This results in a phase of the form

$$\Xi_0 = \omega_0 t + \frac{3}{8}\frac{A_0^2}{\omega_0}\epsilon t + \phi_1(t_2, t_3, ...).$$

which is consistent with the terms (1.3) obtained via the ordinary perturbation theory expansion.

We shall demonstrate that the situation can be more complicated for non-periodic problems. Much of the work presented in this thesis concerns a *further* regrouping of terms in an expansion to which the multiple-scaling technique has already been applied.

Variational methods

If the problem does not lie close to one whose solution is known, and hence there is no small parameter with which to carry out a perturbative expansion, we can instead try a variational method. Variational methods are based around some physical quantity (that is dependent upon the unknown function) having a stationary value at the solution to the problem. In place of the unknown function, we use a trial function dependent on one or more parameters. At the parameter values corresponding to a stationary point, the trial function most closely resembles the true solution.

The equations of physics can in general be formulated using a variational principle. The physical quantity to be minimized (or maximized) is the action which is the integral of the Lagrangian density. At a stationary point, the first order variation in the action is zero. This condition is used to derive the Euler-Lagrange equations; if left in terms of the unknown functions, these are just the differential equations the Lagrangian density represents.

When a variation of action type method is used to find approximate results, a trial function is substituted into the Lagrangian density, and the Euler-Lagrange equations are obtained on taking variations with respect to the trial function parameters that are themselves functions of the integration variables which appear in the definition of the action. These new Euler-Lagrange equations are then generally simpler than the full equations and so more headway can be made with the analysis.

If we are interested only in the value of a quantity such as energy or growth rate, and not in the form of the unknown function, it is better to try and find a variational principle such that the quantity of interest is to be minimized (or maximized). This is because fairly good estimates of the true value can be obtained with only crude trial functions. A still more powerful technique can be employed if both a maximum and a minimum variational principle can be found for the same quantity. These so-called complementary variational principles then provide upper and lower bounds for the quantity. If the bounds coincide, an exact result is obtained.

1.4 Equations with soliton solutions

The simplest equation to admit solitons is the Korteweg-de Vries (KdV) equation,

$$u_t + uu_x + u_{xxx} = 0, \tag{1.5}$$

where subscripts denote partial derivatives. It was first derived for long surface waves in a channel of constant depth (Korteweg & de Vries 1895), and as a result explained Russell's observations, but has since been shown to be applicable to a wide variety of other systems. Many of the equations with soliton solutions mentioned in this thesis model plasmas. The KdV equation is the simplest of these - it was shown by Washimi and Taniuti (1966) to describe ion-acoustic waves in a magnetic-field-free plasma with u relating to the ion density. The existence of solitons in such a plasma was subsequently demonstrated experimentally by Ikezi, Taylor & Baker (1970). The equation usually arises with constant coefficients in front of the terms, but may always be transformed into (1.5) by a rescaling of u and x.

The general travelling wave solutions to the KdV equation are cnoidal waves of the form

$$u = V - 4\eta^2(2m-1) + 12\eta^2 m\,\mathrm{cn}^2\left(\eta(x - x_0 - Vt)\,|\,m\right) \tag{1.6}$$

with $0 \leq m \leq 1$. The soliton solutions correspond to a nonlinear wave with infinite period; as $m \rightarrow 1$, (1.6) becomes

$$u = 12\eta^2 \operatorname{sech}^2\eta\left(x - x_0 - 4\eta^2 t\right) \tag{1.7}$$

once we have set $V = 4\eta^2$ so that the integral of the solution is finite. In the case of ion-acoustic solitons, the x-axis is such that we are viewing the soliton from a reference frame moving at the speed of a long wavelength sound wave. In this frame the soliton speed is proportional to the amplitude, and as η must be real, the solitons always move to the right. It can also be seen that the pulse width is inversely proportional to the square root of the amplitude - in other words, tall solitons are thin.

The KdV equation was shown by Miura *et al.* (1968) to have an infinite family of conserved quantities. In the case of ordinary differential equations (o.d.e.'s), if there are the same number of degrees of freedom as conservation laws, the system is solvable or 'integrable'. Partial differential equations (p.d.e.'s) have an uncountably infinite number of degrees of freedom. The result of Miura *et al.* is therefore not a proof of integrability, but a strong indication. It was Gardner *et al.* (1967) who proved its integrability by devising an inverse scattering transform (IST) which could in principle be used to integrate any physically meaningful initial condition.

The basic idea behind the IST is to treat the solution $u(x,t)$ to the KdV equation as a potential in the time-independent Schrödinger equation. The scattering data, i.e. the eigenvalues and eigenfunctions, for the initial potential $u(x,0)$ are determined and are then allowed to evolve for time t, after which the quantum mechanical inverse scattering problem for the data is solved to obtain the evolved potential $u(x,t)$. The success of the method rests on the fact that for the KdV equation the time evolution of the scattering data only depends on the initial scattering data. More specifically, the number of bound states remains constant and their amplitudes, along with those of the continuum states, have a very simple time dependence.

An arbitrary initial condition (which decays sufficiently quickly at a large distance from the origin) will evolve into a number of solitons and a dispersive oscillatory disturbance which travels in the opposite direction. The number of solitons present is given simply by the number of bound states. Unfortunately, $u(x,t)$ can only be obtained in closed form for 'reflectionless' initial conditions where the system evolves into just solitons and nothing else. Nevertheless, in such a N-soliton solution we can analytically follow larger solitons overtaking smaller ones resulting in a phase shift but no change in form, just as was observed in the numerical work by Zabusky and Kruskal mentioned earlier.

The importance of the discovery of Gardner *et al.* lay in the realization that the solution of a particular *nonlinear* p.d.e. could be reduced to the task of solving of two *linear* problems: a second order ordinary differential equation and an integral equation. However, the real breakthrough was the generalization of the IST to accommodate a whole range of other nonlinear p.d.e.'s bearing soliton solutions (see Zakharov & Shabat 1974 and Ablowitz *et al.* 1974). Many important equations such as the cubic nonlinear Schrödinger (NLS) equation, which possibly has more applications than the KdV equation, and the sine-Gordon equation, which for example can describe fluxons, have as a result been shown to be integrable.

There still remain a number of physically important soliton equations for which an IST has not been found. Such equations also appear to have only a finite number of conservation laws. The presence of an infinite number of conserved quantities in the case of integrable p.d.e.'s places severe restrictions on the behaviour of their solutions - very complicated behaviour

such as chaos will certainly not occur. Hence if the (numerically determined) time evolution of a relatively simple initial condition gives rise to complicated structures, it would tend to indicate that the governing equation is non-integrable. A more analytical test for the integrability of p.d.e.'s has been proposed by Ablowitz *et al.* (1980). They conjecture that a nonlinear p.d.e. is solvable by an IST if, and only if, every o.d.e. derived from it (by exact reduction) can be transformed into an o.d.e. satisfying the Painlevé property. An o.d.e. has the Painlevé property if none of the critical points of the solution in the complex plane depend on the constants of integration (for a further discussion see Tabor 1989). Weiss *et al.* (1983) have since suggested an analogous Painlevé property for p.d.e.'s and hence have created a more direct conjectured test for their integrability.

As has been the case with solvable, linear theories, the scientific community has often focussed its attention on the integrable p.d.e.'s at the expense of equations of similar physical relevance to which the more elegant methods cannot be applied. It is, however, important to develop techniques for the analysis of non-integrable equations since many interesting phenomena such as chaotic dynamics and the traditional type of self-organizing processes cannot be modelled by integrable equations.

1.5 Higher dimensional solitons

We have so far explicitly considered only solitons whose shape depends just on one spatial variable. In a three-dimensional medium, such as a plasma where the KdV equation applies, one-dimensional solitons take the form of a planar localized increase in the ion density. In plasmas, along with a number of other media, it is also possible to have two- and three-dimensional solitons. In some cases the surfaces of constant ion density for these higher-dimensional solitons lack an angular dependence (once the axes have been appropriately scaled) - they are then referred to as cylindrical and spherical solitons respectively.

The Zakharov-Kuznetsov equation

The simplest looking equation which has been shown to admit one-, two-, and three-dimensional soliton solutions is the Zakharov-Kuznetsov (ZK) equation:

$$n_t + n\, n_x + \nabla^2 n_x = 0. \tag{1.8}$$

It was first derived for an ion-acoustic plasma permeated by a strong uniform magnetic field (Zakharov & Kuznetsov 1974), although the equation also governs long waves in thin liquid films (Melkonian & Maslowe 1989) and vortices in plasma drift waves (Nozaki 1981). For a low-β †, cold-ion plasma, with the magnetic field $\mathbf{B}$ directed along the x-axis, the ion motion is governed by the continuity equation, Newton's second law, and Poisson's equation:

$$\frac{\partial n}{\partial t} + \nabla.(n\mathbf{v}) = 0 \tag{1.9}$$

$$\frac{\partial \mathbf{v}}{\partial t} + (\mathbf{v}.\nabla)\mathbf{v} = -\nabla\varphi + \Omega\, \mathbf{v} \times \hat{\mathbf{x}} \tag{1.10}$$

$$\nabla^2\varphi = \exp(\varphi) - n \tag{1.11}$$

† $\beta = \mu_0^2 n_0 k T_e/\varepsilon_0 B^2$. For small β, we can use an electrostatic potential.

where the ion density n, the ion velocity $\mathbf{v}$, the electric potential φ, the spatial variables, and time are in units of the mean density, the ion sound velocity, kT_e/e, the Debye length, and the reciprocal of the plasma frequency (ω_{pi}), respectively. The quantity $\Omega = \Omega_i/\omega_{pi}$, where $\Omega_i = eB/m_i$ is the cyclotron frequency, is taken to be of order unity which implies that the magnetic field is strong. The ZK equation can be derived from the above equations by using a reductive perturbation technique. The dependent variables are expanded as

$$n = 1 + \epsilon n^{(1)} + \epsilon^2 n^{(2)} + \ldots$$

$$\mathbf{v} = (v_x, v_y, v_z) = (\epsilon v_x^{(1)} + \epsilon^2 v_x^{(2)} + \ldots,\ \epsilon^{3/2} v_y^{(1)} + \epsilon^2 v_y^{(2)} + \ldots,\ \epsilon^{3/2} v_z^{(1)} + \epsilon^2 v_z^{(2)} + \ldots)$$

$$\varphi = \epsilon \varphi^{(1)} + \epsilon^2 \varphi^{(2)} + \ldots,$$

and the independent variables are rescaled using $(x', y', z') = (\epsilon^{1/2}(x - t),\ \epsilon^{1/2} y,\ \epsilon^{1/2} z)$, $t' = \epsilon^{3/2} t$. Substituting these relations into equations (1.9)-(1.11) and equating the coefficients of ascending powers of ϵ to zero, the ZK equation is obtained at order $\epsilon^{5/2}$:

$$n_t^{(1)} + n^{(1)} n_x^{(1)} + \frac{1}{2}\left\{ n_{xxx}^{(1)} + (1 + \Omega^{-2})(n_{xyy}^{(1)} + n_{xzz}^{(1)}) \right\} = 0 \tag{1.12}$$

in which the primes have been dropped. After a further rescaling of the independent variables and on identifying n with $n^{(1)}$, equation (1.8) is recovered. Before turning to a version of the ZK equation where the dependence on the magnetic field has been scaled away, we note that the plane soliton solutions to (1.12) take the form

$$n^{(1)} = 6\eta^2 \operatorname{sech}^2 \left\{ \eta \left[1 + (1 + \Omega^{-2})(a^2 + b^2) \right]^{-1/2} (x + ay + bz - 2\eta^2 t) \right\} \tag{1.13}$$

(Shivamoggi 1989). It can be seen that the width of the soliton decreases with increasing magnetic field. This focussing of a soliton by a magnetic field agrees with the experimental studies on magnetized plasmas done by Raychaudhuri *et al.* (1987). Unfortunately there do not appear to be any further experimental results on magnetized-plasma ion-acoustic solitons in the literature.

The ZK equation is readily seen to be an extension of the KdV equation on suppressing the y and z dependences. Plane solitons travelling along the magnetic field therefore take the form of (1.7). However, plane solitons propagating at an angle to the field are also permitted and are given by

$$n = 12\eta^2 \operatorname{sech}^2 \eta((x - 4\eta^2 t)\cos\alpha \cos\lambda + y \sin\alpha \cos\lambda + z \sin\lambda)$$

where α and λ are respectively the azimuth and altitude angles of the direction of motion.

The cylindrical and spherical soliton solutions can be found by looking for solutions of the form $n = n(\xi, y, z)$ where $\xi = x - vt$. On substitution into (1.8) this leads to

$$\nabla^2 n + \frac{1}{2} n^2 - vn = 0 \tag{1.14}$$

where $\nabla^2 \equiv \partial_\xi^2 + \partial_y^2 + \partial_z^2$. On demanding cylindrical symmetry, (1.14) reduces to

$$\frac{1}{r}\frac{d}{dr}\left(r \frac{dn}{dr} \right) + \frac{1}{2} n^2 - vn = 0, \tag{1.15}$$

where $r = (\xi^2 + y^2)^{1/2}$, and for a spherically symmetric solution

$$\frac{1}{R^2}\frac{d}{dR}\left(R^2\frac{dn}{dR}\right) + \frac{1}{2}n^2 - vn = 0, \tag{1.16}$$

with $R = (\xi^2 + y^2 + z^2)^{1/2}$. The solutions of (1.15) and (1.16) cannot be expressed in terms of tabulated functions, but are readily determined numerically. In both cases n decreases monotonically from the origin, and at a large enough distance the decay is faster than exponential.

In contrast to the KdV equation, the ZK equation appears to have just five conservation laws. Four of them describe the conservation of familiar quantities:

$$M(y,z) \equiv \int n\,dx \tag{1.17}$$

$$P \equiv \iiint \frac{1}{2}n^2\,dx\,dy\,dz \tag{1.18}$$

$$H \equiv \frac{1}{2}\iiint \left\{(\nabla n)^2 - \frac{1}{3}n^3\right\} dx\,dy\,dz \tag{1.19}$$

$$\mathbf{I} \equiv \iiint (x\hat{\mathbf{x}} + y\hat{\mathbf{y}} + z\hat{\mathbf{z}})n\,dx\,dy\,dz - t\hat{\mathbf{x}}P\,, \tag{1.20}$$

where the integrals are over all space. $M(y,z)$, P, and H are the mass along an element parallel to the field, momentum, and energy respectively. $\mathbf{I}$ is related to the centre of mass motion. The fifth conservation law,

$$\frac{\partial}{\partial t}\iint \left\{n_y \int^{\infty} n\,dx\right\} dx\,dy = 0,$$

this time for the two-dimensional ZK equation, was noticed more recently (Shivamoggi, Rollins & Fanjul 1993) and doesn't appear to correspond to the conservation of any elementary physical quantity.

Collisions of parallel plane solitons of different amplitudes merely results in phase changes since this process is described by the N-soliton solution of the KdV equation. However, numerical studies by Iwasaki, Toh & Kawahara (1990) indicate that collisions of cylindrical solitons are slightly inelastic - a small amount of rippling is generated. Both this phenomenon and the existence of apparently only a finite number of constants of the motion suggest that the ZK equation is not integrable. Further evidence for its nonintegrability stems from work by Melkonian & Winternitz (1991) and Shivamoggi *et al.* (1993) who showed that the Painlevé property is possessed neither by, respectively, the o.d.e.'s generated from the ZK equation by reductions, nor by the p.d.e. itself.

In order to determine whether the ZK solitons are likely to be observable in nature, we need to investigate their stability to perturbations. Spherical solitons were shown by Zakharov & Kuznetsov in their original paper to be stable. Cylindrical solitons are stable with respect to dilations (Frycz & Infeld 1989) and in two-dimensional numerical simulations they are never seen to disintegrate on encountering a variety of perturbations. Finally, in a one dimensional system, KdV solitons are stable (Benjamin 1972) which ensures the stability of plane ZK solitons to perturbations with no y- or z-dependence. However, such solitons become unstable if a transverse disturbance of sufficient wavelength is present (Spatschek, Shukla & Yu 1975). Similarly, numerical studies have shown that a cylindrical soliton breaks up when perturbations are applied along its axis of symmetry (Frycz, Infeld & Samson 1992).

The inverse scattering method showed that for the (one-dimensional) KdV equation an arbitrary localized initial condition will eventually evolve into a state containing a number of solitons. These solitons are basically indestructible since their number is fixed. Although the ZK equation does not appear to have an IST, by analogy we might suppose that the supreme stability of spherical solitons would result in their formation from a random initial state of sufficient size. As demonstrated by the computer simulations of Frycz *et al.* (1992), a perturbed plane or cylindrical soliton does indeed eventually produce spherical solitons. For the two-dimensional system governed by the ZK equation, the unstable one-dimensional soliton is instead destined to become an array of cylindrical solitons (Frycz & Infeld 1989).

It is this self-organizing type transition from lower to higher dimensional solitons which is of particular interest. In this thesis we concentrate on the simpler case of the evolution in two dimensions. In the hope of gaining some insight into the mechanism of cylindrical soliton formation, we attempt to characterize the evolution of perturbed ZK plane solitons.

The Kadomtsev-Petviashvili equations

The instability of one-dimensional solitons to perpendicular perturbations is not an uncommon phenomenon. It also occurs for the plane solitons of the most straightforward higher-dimensional forms of the cubic NLS and sine-Gordon equations (Zakharov & Rubenchik 1974; Makhankov 1978). Like the ZK equation both these two- and three-dimensional analogues appear to be non-integrable.

There are, however, a few *integrable* higher-dimensional versions of integrable equations with one spatial variable. Perhaps the most important of these are the KP equations (Kadomtsev & Petviashvili 1970):

$$(n_t + nn_x + n_{xxx})_x = \sigma n_{yy} \tag{1.21}$$

where $\sigma = +1$ for a medium with positive dispersion (i.e. the group velocity increases with wavenumber), and $\sigma = -1$ for media where the dispersion is negative. Without the y-dependence, we see that (1.21) reduces to the KdV equation. The sign of the dispersion greatly affects the form and behaviour of the solutions. The most striking feature about both the KP equations is that they admit an N-soliton solution in which the solitons can propagate at arbitrary angles to one another. This, however, is where the similarity ends; when these solitons collide, the results differ according to the sign of the dispersion (see Infeld & Rowlands 1990 for a thorough survey).

The KP equation with positive dispersion (which we will refer to as the KP$^+$ equation) is of greater interest to us because, in direct contrast to the KP$^-$ equation, the KP$^+$ plane solitons are unstable to transverse perturbations (Zakharov 1975) and the KP$^+$ equation has two-dimensional soliton solutions[†] (Manakov *et al.* 1977). It would therefore seem to be very much the integrable cousin of the ZK equation, although Melkonian & Maslowe (1989) proved that the ZK equation cannot have intersecting plane soliton solutions. The connection between the two equations has recently been strengthened by the work of Pelinovsky & Stepanyants (1993a). They have shown *analytically* that a periodically perturbed plane soliton solution of the KP$^+$ equation will evolve into a line of cylindrical solitons. This has now also been demonstrated numerically (Infeld, Senatorski & Skorupski 1994). The analytical

[†]In this case the solitons are not cylindrical.

results should prove useful as a guide to the type of behaviour that one might expect from the ZK equation.

1.6 Outline

For a small amplitude perturbation applied to a known solution, the evolution is initially determined by the linearized equation. We therefore start by looking at the growth rate of linear instabilities. In Chapter 2 we find the growth rate γ of a periodic disturbance to a ZK plane soliton propagating in the same direction as the magnetic field. The usual analytical methods of determining γ either fail or give incorrect results at higher order. To overcome this, we develop an extension to the usual multiple-scale perturbation method which involves a regrouping of a certain type of secular term in the expansion of the solution. The growth rate is also determined numerically using a fast and accurate technique similar to the shooting method. We express $\gamma(k)$ for all $\gamma > 0$ in terms of a Padé approximant. This is found to give much better agreement with the numerical results than the growth rate curves obtained previously using variational methods.

In Chapter 3, we apply the new method to the KP$^+$ equation and a two-dimensional generalization of the Boussinesq equation, and find that a multiple-scale analysis can lead us to exact solutions of the linearized equations. As a result, an exact expression for the growth rate as a function of wavenumber can be determined more simply than by the conventional methods. We also examine some unusual soliton states in fibre optic cable couplers. In general, these states can only be written down as a perturbative expansion. The new analytic method is used to give us the correct ordering of such an expansion in a case where the usual technique of checking the consistency conditions cannot be employed.

We return to the linear analysis of the ZK equation in Chapter 4 and now look at the instability of plane solitons travelling at an angle to the field. We find that they are less unstable than those travelling parallel to the field. The analytical determination of the growth rate again requires an explicit regrouping of secular terms. However, this time there are two types of secularities that must be regrouped. Owing to the greater complexity of the linearized equation for the oblique solitons, our eventual analytical description of the growth rate curves is less complete than that obtained in Chapter 2, and we also have to extend the numerical method of that chapter.

In Chapter 5 we perform a nonlinear analysis on the perturbed plane soliton and find that the nonlinearity gives rise to a bending of the initial perturbation. The results of this are compared with numerical simulations of the full two-dimensional ZK equation. We also use the numerical calculations to investigate the dependence on wavenumber of cylindrical soliton formation and verify their speed-amplitude relationship. An attempt is made to account for some of our observations on physical grounds.

Finally, in Chapter 6 we present our conclusions and outline some ideas for further investigation.

Chapter 2

Stability of Zakharov-Kuznetsov plane solitons propagating along the magnetic field

In this chapter we start our investigation of the soliton solutions to the ZK equation by determining the initial response of a plane soliton propagating parallel to the magnetic field to a small perturbation. Since we will be performing a linear analysis, it is only necessary to study the effect of a periodic perturbation since any small disturbance may be decomposed into a sum of periodic components which can be treated independently. Those associated with the greatest instability will rapidly predominate.

Laedke & Spatschek (1982) have shown analytically that plane solitons are unstable with respect to perpendicular perturbations of sufficiently large wavelength, but are stable for $k^2 \geq k_c^2$, where k is the wavenumber of the perturbation. They found that the cut-off wavenumber, k_c, is $\sqrt{5}\eta$ where η is the soliton parameter (see equation (1.7)). The first step in the study of the region where perturbations grow is to determine the growth rate γ associated with such linear instabilities.

For plane solitons, the growth rate curve, γ as a function of k, has already been obtained numerically (Infeld & Frycz 1987) and placed within fairly close upper and lower bounds through the numerical evaluation of complementary variational principles (Laedke & Spatschek 1982). Makhankov (1978) also found an approximation to the curve by using a standard variational principle. The later two studies confirmed the analytical results for γ obtained so far, and showed that it has a maximum at around $k^2 = 1.7\eta^2$.

There are four basic techniques available for determining the growth rate of a periodic wave; Whitham I, Whitham II, the Hayes method, and the small-k expansion (for further details on these see Infeld & Rowlands 1990). The first three methods require the use of either conservation laws or the Lagrangian for the equation, and can only be used to find the growth rate to first order in k. The small-k expansion method (Rowlands 1969) suffers from none of these restrictions and is therefore the most generally applicable of the techniques. It also has the advantage of being the easiest to use.

The difficulty in obtaining the growth rate for a non-periodic wave of infinite extent analytically using a small-k expansion, due to the appearance of certain types of secular terms, was noted in Infeld & Rowlands (1977). This can be overcome by performing the analysis for nonlinear waves and then proceeding to the soliton (infinite wavelength) limit.

Using this method, Infeld (1985) derived the correct value of the growth rate of perturbations with $k \to 0$ applied at a general angle θ to a ZK plane soliton. However this approach is algebraically very involved because of the need to manipulate elliptic functions even in the simplest of cases.

Laedke & Spatschek (1982) also determined the small-k growth rate analytically, but by employing complementary variational principles which are again far from trivial to implement. The basis of this chapter is the presentation of a new method that can be used to obtain the growth rate of perturbations to pulse-like solutions such as solitons and kinks directly and fairly simply.

In §2.1 we introduce the linearized equation and show how ordinary perturbation analyses about both $k = 0$ and $k^2 = 5\eta^2$ fail. A new method is introduced in §2.2 and is then illustrated by applying it to the determination of the growth rate for small k. We also discuss why the conventional multiple-scale approach fails. We apply the new method again in §2.3 to find $\gamma(k)$ in the neighbourhood of $k^2 = 5\eta^2$, its other zero. In §2.4 we deal with the numerical evaluation of the growth rate curve, and the analytical results for $k^2 \to 0$ and $k^2 \to 5\eta^2$ are used to obtain a two-point Padé approximant for γ for all k in the range $0 \leq k^2 \leq 5\eta^2$. This is found to give excellent agreement with the numerical results. The effect of perturbations applied at a general angle θ to the field are dealt with in §2.5. In §2.6 we attempt to improve upon the variational calculations done by Infeld & Frycz (1987). The chapter is concluded with a discussion.

2.1 Ordinary perturbation analysis

In the linear analysis of a periodic perturbation to a plane soliton, it is only necessary to study the two-dimensional version of the equation since a perturbation applied at any angle may be made a function of two variables by appropriately rotating the y and z axes. The two-dimensional ZK equation is

$$n_t + n\, n_x + n_{xxx} + n_{xyy} = 0. \tag{2.1}$$

Since the plane soliton solution of (2.1) to which we will be applying a perturbation is of the form $n = 12\eta^2 \operatorname{sech}^2\eta(x - x_0 - 4\eta^2 t)$, we will find it convenient to transform the equation to a reduced variables coordinate system moving with the unperturbed soliton. This is accomplished by means of the transformation:

$$(x, y, t) \mapsto \left(\frac{x + 4t}{\eta}, \frac{y}{\eta}, \frac{t}{\eta^3}\right), \qquad n \mapsto \eta^2 n$$

which gives

$$n_t + (n - 4)n_x + n_{xxx} + n_{xyy} = 0. \tag{2.2}$$

To apply a sinusoidal perturbation perpendicular to the direction of propagation we write

$$n = n_0 + \varepsilon\Phi(x)e^{iky}e^{\gamma t} \tag{2.3}$$

where $n_0 \equiv 12\operatorname{sech}^2 x$ is now the stationary plane soliton solution. Substituting (2.3) into (2.2) and choosing $\varepsilon \ll k^2$, so that the nonlinearity in Φ can be neglected, we obtain

$$\frac{d}{dx}L_o\Phi = -\gamma\Phi + k^2\frac{d\Phi}{dx}, \tag{2.4}$$

where we have denoted $d^2/dx^2 + n_0 - 4$ by L_o.

On putting $\gamma \equiv 0$ and substituting $T = \tanh x$ and $k^2 = \lambda - 4$ into (2.4) integrated once, we obtain the associated Legendre equation

$$(1-T^2)\frac{d}{dT}\left((1-T^2)\frac{d\Phi}{dT}\right) + \left(N(N+1)(1-T^2) - \lambda\right)\Phi = 0 \tag{2.5}$$

with N=3. The only bounded solutions with $\lambda > 0$ are for $\lambda = \nu^2$ where $\nu = 1, 2, ..N$ (see p.46 of Drazin & Johnson 1989). The corresponding solutions are Legendre polynomials. Hence, as pointed out by Laedke & Spatschek (1982), equation (2.4) has exactly two marginally stable bounded solutions. They are $\Phi = \operatorname{sech}^2 x \tanh x$ when $k = 0$, and $\Phi = \operatorname{sech}^3 x$ for $k^2 = 5$.

Expansion about $k = 0$

Using the small-k expansion method we expand about the $k = 0$ marginally stable solution by writing Φ and γ as

$$\Phi = \varphi_0 + k\varphi_1 + k^2\varphi_2 + ... \tag{2.6}$$

$$\gamma = k\gamma_1 + k^2\gamma_2 + ... \tag{2.7}$$

and substituting these expansions into (2.4). Equating coefficients of zeroth order in k, we obtain

$$\frac{d}{dx}L_o\varphi_0 = 0. \tag{2.8}$$

The solution is just our marginally stable solution to (2.4):

$$\varphi_0 = \operatorname{sech}^2 x \tanh x. \tag{2.9}$$

Equating the terms of order k in (2.4), we obtain

$$\frac{d}{dx}L_o\varphi_1 = -\gamma_1\varphi_0 \tag{2.10}$$

from which

$$L_o\varphi_1 = \frac{d^2\varphi_1}{dx^2} + (n_0 - 4)\varphi_1 = \frac{\gamma_1}{2}\operatorname{sech}^2 x + C_1 \tag{2.11}$$

where C_1 is the constant of integration. An equation of the form

$$\frac{d^2u}{dx^2} + P(x)\frac{du}{dx} + Q(x)u = R(x)$$

can be solved if we know a solution u_0 to the equation with $R \equiv 0$ (p.86 of Forsyth 1888). The general solution is then

$$u = A\,u_0(x) + B\,u_0(x)\int^x \frac{dx'}{u_0(x')^2} + u_0(x)\int^x \frac{\int^{x'} u_0(x'')R(x'')\,dx''}{u_0(x')^2}\,dx' \tag{2.12}$$

where A and B are arbitrary constants. The u_0 in our case is just the solution to the zeroth order equation (2.8), namely φ_0. With $R(x)$ equal to the right hand side of (2.11), using (2.12) we obtain

$$\varphi_1 = \frac{\gamma_1}{8}(\operatorname{sech}^2 x - x\varphi_0) + B_1\psi + C_1\chi, \tag{2.13}$$

where

$$\chi = \frac{1}{4}(3x\,\mathrm{sech}^2 x \tanh x - 3\,\mathrm{sech}^2 x + 1)$$

and

$$\psi = \frac{1}{4}\cosh^2 x - \frac{5}{2}\chi.$$

Only by equating both the arbitrary constant B_1 and the constant of integration C_1 to zero do we get a φ_1 which vanishes at infinity. Although we have not encountered any difficulties so far, γ_1 has yet to be determined.

The solution of the second order relation

$$\frac{d}{dx}L_o\varphi_2 = -\gamma_2\varphi_0 - \gamma_1\varphi_1 + \frac{d\varphi_0}{dx} \tag{2.14}$$

is obtained in an analogous manner. Immediately discarding the arbitrary amount of ψ leaves us with

$$\begin{aligned}\varphi_2 \;=\; & \frac{1}{128}\left(\frac{64}{15} - \gamma_1^2\right)\sinh x\cosh x + \frac{1}{640}(64 - 5\gamma_1^2)\tanh x + \frac{\gamma_1^2}{128}x^2\varphi_0 \\ & + \frac{\gamma_2}{8}(\,\mathrm{sech}^2 x - x\varphi_0) + C_2\chi.\end{aligned} \tag{2.15}$$

We choose γ_1^2 so as to remove the most divergent quantity, namely, the $\sinh x \cosh x$ term.

We should point out that the value of γ_1^2 could also have been obtained less directly by the use of a consistency condition. The importance of checking that consistency conditions are satisfied has been stressed in Infeld & Rowlands (1977) - missing such a condition could lead to incorrect results. A family of consistency conditions for the present problem can be derived by using the self-adjoint property of L_o and the fact that $L_o\varphi_0 = 0$:

$$\int_{-\infty}^{\infty}\left(\int^{x}\varphi_0(x')\,dx'\right)\frac{d}{dx}L_o\varphi_j\,dx = -\int_{-\infty}^{\infty}\varphi_0 L_o\varphi_j\,dx = -\int_{-\infty}^{\infty}\varphi_j L_o\varphi_0\,dx = 0. \tag{2.16}$$

Hence multiplying the right hand side of (2.14) by $\mathrm{sech}^2 x$ (since this is proportional to the integral of φ_0) and integrating over all x will give an equation for γ_1^2. The corresponding consistency condition for the periodic case was used by Infeld (1985) to obtain the growth rate to first order for nonlinear waves.

Choosing γ_1 to remove the most offensive terms is equivalent to applying the consistency condition because the latter is only satisfied when the solution behaves sufficiently well as $x \to \pm\infty$. The advantage of using consistency conditions is that we have less algebra to do - in particular, if we do not wish to proceed to next order, we no longer need to solve the differential equation. However, as we shall see shortly, they cannot always be applied, and in some cases (as will be shown in §4.2) if their use were insisted upon, the eventual appropriate method of solution would be obscured.

Both methods give $\gamma_1^2 = 64/15$ and to obtain a positive growth rate, we must have

$$\gamma_1 = \mathrm{sgn}(k)\frac{8}{\sqrt{15}}, \tag{2.17}$$

which is the result arrived at by Laedke & Spatschek (1982) and Infeld (1985). However, before accepting this result, we should note that there is another secular term in (2.15) in

addition to the one we removed[†]; the $\tanh x$ term means that φ_2 cannot be made to vanish both as $x \to +\infty$ and $x \to -\infty$. Hence the method fails at this point and the validity of the derivation of (2.17) is called into question. Nevertheless, the closeness to obtaining a physically acceptable form for φ_2 (C_2 can be chosen so that φ_2 only fails to vanish at one infinity) and the appearance in successive orders of the first few terms in the expansion of an exponential (i.e. the leading coefficients of φ_0 in (2.9), (2.13), and (2.15)), suggests that a multiple-scale perturbation approach might be fruitful.

Expansion about $k^2 = 5$

Before attempting a multiple-scale expansion, we see how far we can proceed with the ordinary perturbation analysis about the other zero of $\gamma(k^2)$. The small quantity we expand in now is $\bar{k}$ where $\bar{k}^2 = 5 - k^2$. (We make this substitution rather than $\bar{k} = \sqrt{5} - k$ so that the analysis continues to apply to k of both signs.) We rewrite (2.4) as

$$\frac{d}{dx}\bar{L}_o\Phi = -\gamma\Phi - \bar{k}^2\frac{d}{dx}\Phi, \tag{2.18}$$

where $\bar{L}_o \equiv d^2/dx^2 + n_0 - 9$. For k^2 near the second zero we expand Φ and γ in the form

$$\Phi = \bar{\varphi}_0 + \bar{k}\bar{\varphi}_1 + \bar{k}^2\bar{\varphi}_2 + \ldots$$

$$\gamma = \bar{k}\bar{\gamma}_1 + \bar{k}^2\bar{\gamma}_2 + \ldots .$$

and substitute these expressions into (2.18).

This time we have $\bar{L}_o\bar{\varphi}_0 = 0$ and $\bar{\varphi}_0 = \operatorname{sech}^3 x$. Integrating the first order equation,

$$\frac{d}{dx}\bar{L}_o\bar{\varphi}_1 = -\bar{\gamma}_1\bar{\varphi}_0$$

gives

$$\bar{L}_o\bar{\varphi}_1 = -\frac{\bar{\gamma}_1}{2}\left\{\operatorname{sech} x \tanh x + \tan^{-1}\sinh x\right\} + \bar{C}_1. \tag{2.19}$$

We again use (2.12) but with $u_0 = \operatorname{sech}^3 x$ to obtain the following results for the inverse of the differential operator:

$$\bar{\psi} \equiv \bar{L}_o^{-1}(0) = \frac{1}{6}\sinh x \cosh^2 x + \frac{5}{24}\sinh x + \frac{5}{16}\operatorname{sech} x \tanh x + \frac{5}{16}x\operatorname{sech}^3 x \tag{2.20}$$

$$\bar{\chi} \equiv \bar{L}_o^{-1}(1) = \frac{1}{2}\bar{\psi}\tan^{-1}\sinh x + \frac{1}{12}\cosh^2 x - \frac{5}{144} - \frac{5}{32}\operatorname{sech}^2 x - \frac{5}{32}\operatorname{sech}^3 x \int^x x' \operatorname{sech} x'\, dx' \tag{2.21}$$

$$\bar{L}_o^{-1}(\operatorname{sech} x \tanh x) = -\frac{1}{8}\operatorname{sech} x \tanh x - \frac{1}{8}x\bar{\varphi}_0. \tag{2.22}$$

The quantities $\bar{\psi}$ and $\bar{\chi}$ have the following limiting forms as $x \to \pm\infty$:

$$\bar{\psi}_{\pm\infty} = \pm\frac{1}{8}\left(\frac{1}{6}e^{\pm 3x} + e^{\pm x}\right)$$

$$\bar{\chi}_{\pm\infty} = \frac{\pi}{32}\left(\frac{1}{6}e^{\pm 3x} + e^{\pm x}\right) - \frac{1}{9}.$$

[†]For a non-periodic problem, we define a secular term as a term which does not vanish at infinity.

The inverse of the remaining term on the right hand side of (2.19) has the limiting form

$$\bar{L_o}^{-1}(\tan^{-1}\sinh x)_{\pm\infty} = \pm\frac{\pi}{2}\left\{\frac{\pi}{64}\left(\frac{1}{6}e^{\pm 3x}+e^{\pm x}\right)-\frac{1}{9}\right\}. \tag{2.23}$$

The arbitrary constant, C_1, on the right hand side of (2.19) will lead to exponentially growing terms in $\bar{\varphi}_1$ which cannot be counteracted by the other terms since they are of opposite parity. Thus $\bar{C}_1 = 0$. By adding some $\bar{\psi}$, which we are permitted to do since $\bar{L_o}\bar{\psi} = 0$, we can cancel out the exponentially growing part of (2.23), but the overall expression for φ_1 will still be non-zero at infinity. We therefore have to put

$$\bar{\gamma}_1 = 0. \tag{2.24}$$

Using the above result, the second order equation becomes

$$\frac{d}{dx}\bar{L_o}\bar{\varphi}_2 = -\bar{\gamma}_2\bar{\varphi}_0 + \frac{d\bar{\varphi}_0}{dx}. \tag{2.25}$$

We note at this point that a consistency condition of the type given by (2.16) cannot be implemented. On integrating by parts the left hand side of an analogous expression, we obtain:

$$\left[\left(\int^x \bar{\varphi}_0(x')\,dx'\right)\bar{L_o}\bar{\varphi}_j\right]_{-\infty}^{\infty} - \int_{-\infty}^{\infty}\bar{\varphi}_0\bar{L_o}\bar{\varphi}_j\,dx. \tag{2.26}$$

The first term of (2.26) is no longer necessarily zero and so the rest of the derivation in (2.16) cannot be applied. To see whether we can determine $\bar{\gamma}_2$, we must therefore find $\bar{\varphi}_2$ explicitly. Integrating (2.25) and applying $\bar{L_o}^{-1}$ gives

$$\begin{aligned}\bar{\varphi}_2 &= -\frac{\bar{\gamma}_2}{2}\left\{\bar{L_o}^{-1}(\tan^{-1}\sinh x)-\frac{1}{8}(\operatorname{sech} x\tanh x + x\bar{\varphi}_0)\right\}+\frac{4}{45}\cosh^3 x \\ &\quad +\frac{1}{15}\cosh x+\frac{1}{10}\operatorname{sech} x+\bar{B}_2\bar{\psi}+\bar{C}_2\bar{\chi}\end{aligned} \tag{2.27}$$

whose limiting form is given by

$$(\bar{\varphi}_2)_{x\to\pm\infty} = \left(\frac{1}{15}+\frac{\pi\bar{C}_2}{32}\pm\frac{\bar{B}_2}{8}\mp\frac{\pi^2\bar{\gamma}_2}{256}\right)\left(\frac{1}{6}e^{\pm 3x}+e^{\pm x}\right)-\frac{\bar{C}_2}{9}\mp\frac{\pi\bar{\gamma}_2}{36}. \tag{2.28}$$

No matter how $\bar{B}_2$, $\bar{C}_2$, and $\bar{\gamma}_2$ are chosen, we cannot make $\bar{\varphi}_2$ vanish at both infinities. Hence, as in the small-k expansion about $k = 0$, the method fails at second order. However, unlike in the previous case, $\bar{\gamma}_1$ is determined the order before the analysis breaks down, and so we can at least accept (2.24).

2.2 Multiple-scale perturbation analysis about $k = 0$

In the expressions for both φ_2 and $\bar{\varphi}_2$ derived using ordinary perturbation theory the exponentially diverging terms can be removed by an appropriate choice of the arbitrary constants. Problems arise because there are additional secular terms which cannot be removed and result in the expressions not decaying at large distances from the origin. However, these secularities are not as 'serious' as the exponential ones - the expressions are still finite at infinity.

In §1.3 it was demonstrated that for periodic problems, mildly secular terms can be regrouped with terms at other orders to give expansions of slowly varying functions. This also turns out to be the case when we are seeking a solution that is no longer periodic but vanishes exponentially as $x \to \pm\infty$. However this situation is more complicated; we find two types of 'true' secular terms and also terms which are reminiscent of the secular terms commonly found in the analysis of periodic problems.

Firstly there are terms which diverge exponentially. These *exponentially secular* terms must be removed, and it is found that their removal gives us the values of γ_m to all orders. We also find terms of the form $x^m\varphi_0$, where $m = 1, 2, ...$ and φ_0 is the zeroth order solution. As they have a similar appearance to the secular terms found in the periodic case, but are now bounded, vanishing at infinity, we shall call them *ghost secular* terms. Such terms may be regrouped using the multiple-scale approach into the form $h_0\varphi_0$ where h_0 is a function of the scaled independent variables only.

The other type of true secular term is proportional to x^n as $x \to \pm\infty$ ($n = 0, 1, 2, ...$) and we will therefore refer to such terms as *algebraically secular*. Some care must be taken when dealing with them. For example, as we shall see shortly, the lowest order algebraically secular term that arises in the multiple-scale analysis applied to the present problem is proportional to

$$e^{-\alpha kx}(\tanh x + C) \tag{2.29}$$

where C is a constant of integration to be chosen and α is real, greater than zero, and of order one. The conventional approach would be to put $C = 1$ so that (2.29) is bounded. This, however, does not lead to a solution having the correct asymptotic form. To obtain this we must in fact choose $C = -1$, which results in (2.29) considered by itself not vanishing as $x \to -\infty$. However, regrouping this term with other algebraically secular terms that appear at higher order results in an expression that has the required behaviour as $x \to \pm\infty$. Thus at each stage we choose constants of integration, such as C, that appear in the algebraically secular terms by demanding that the overall solution has the correct asymptotic forms for large $|x|$.

We now expand on our method further by applying it to the analytical determination of γ for small k. Our first step is to find the asymptotic behaviour of Φ. For large $|x|$, the linearized ZK equation (2.4) reduces to

$$\frac{d^3\Phi}{dx^3} - (4 + k^2)\frac{d\Phi}{dx} + \gamma\Phi = 0. \tag{2.30}$$

The solutions to this are $e^{p_1 x}$, $e^{-p_2 x}$, and $e^{p_3 x}$, where $p_1, p_2, p_3 > 0$ for $k^2 \leq 5$. For small k and γ we find $p_1 \simeq 2 - \gamma/8$, $p_2 \simeq 2 + \gamma/8$, and $p_3 \simeq \gamma/4$. Any physically acceptable solution of (2.4) should eventually decay exponentially and so we would expect it to tend to a sum of the two positive exponentials for large negative x and to $e^{-p_2 x}$ for large positive x. Hence for small k, the underlying or zeroth order asymptotic form which all terms in the solution must possess is e^{-2x} as $x \to +\infty$ and either e^{2x} or e^0 as $x \to -\infty$.

To ensure that subsequent terms in the perturbation expansion have the correct underlying asymptotic form for $x > 0$, given that the zeroth order solution already does so, we perform the integration of $\delta_x L\Phi_i$ (where $L \equiv \delta_x^2 + n_0 - 4$) between the limits ∞ and x, and use (2.12) to define

$$L^{-1}R(x) \equiv \varphi_0(x)\int^x \frac{\int_\infty^{x'} R(x'')\varphi_0(x'')\,dx''}{\varphi_0^2(x')}\,dx' \mod \varphi_0(x) \tag{2.31}$$

for any function $R(x)$ which decays exponentially as $x \to \infty$. (The mod $\varphi_0(x)$ operation is employed to remove any φ_0 terms which inadvertently appear as a result of the integration and are unwanted since $L\varphi_0 = 0$.) Then the correct choice of the constants of integration, such as the C in (2.29), is automatic.

The corrections involving γ to the e^{2x} and e^{-2x} underlying asymptotic forms arise naturally as a consequence of the multiple scaling. The algebraically secular terms are associated with the 'e^0' underlying form, and to obtain the dependence for large negative x of the form $e^{\gamma x/4}$, we need to regroup these explicitly.

As we are performing a multiple-scale expansion we must write

$$\Phi = \Phi_0(x, x_1, x_2, ...) + k\Phi_1(x, x_1, x_2, ...) + k^2\Phi_2(x, x_1, x_2, ...) + ..., \tag{2.32}$$

where x, $x_1 \equiv kx$, $x_2 \equiv k^2x$, etc. are the scaled independent variables. To introduce these into the analysis we re-express the derivatives by writing

$$\frac{d}{dx} \equiv \frac{\partial}{\partial x} + k\frac{\partial}{\partial x_1} + k^2\frac{\partial}{\partial x_2} + ... \tag{2.33}$$

from which it follows that, for instance,

$$\frac{d^3}{dx^3} \equiv \frac{\partial^3}{\partial x^3} + 3k\frac{\partial^3}{\partial x_1 \partial x^2} + 3k^2\left\{\frac{\partial^3}{\partial x_2 \partial x^2} + \frac{\partial^3}{\partial x_1^2 \partial x}\right\} + ...$$

In the following we employ the notation $\Phi_{0,x} \equiv \partial\Phi_0/\partial x$, $\Phi_{0,1} \equiv \partial\Phi_0/\partial x_1$, etc. A similar style is used for perturbative expansions throughout the thesis; the first subscript of a constant or undetermined function gives the order at which it is first introduced, and the subscripts after the comma signify partial derivatives. This notation allows us to carry out a check on any equation in which none of the quantities have been replaced by their numerical values; once any products have been expanded, the sum of the numerals in the subscripts contained in each term plus a correction must equal the order to which the equation applies. The correction is just the order of the expansion parameter in the corresponding term in the original equation. For example, consider equation (2.39). As it is a second order equation, the numeral subscripts in each term add up to two except for the last term which corresponds to the $k^2\, d^2\Phi/dx^2$ term in (2.4) and hence has a correction of two.

We substitute the expansions (2.7), (2.32), and (2.33) into (2.4) and equate terms of the same order in k. The solution of the zeroth order equation

$$\partial_x L\Phi_0 = 0, \tag{2.34}$$

is now

$$\Phi_0 = h_0\varphi_0 = h_0(x_1, x_2, ...)\,\mathrm{sech}^2 x \tanh x. \tag{2.35}$$

On integrating the first order equation

$$\partial_x L\Phi_1 = -3\Phi_{0,xx1} - (n_0 - 4)\Phi_{0,1} - \gamma_1\Phi_0 = -2\Phi_{0,xx1} - \gamma_1\Phi_0 \tag{2.36}$$

and then applying the inverse operator L^{-1} given by (2.31), we obtain

$$\Phi_1 = \frac{\gamma_1}{8}h_0\,\mathrm{sech}^2 x - \left(\frac{\gamma_1}{8}h_0 + h_{0,1}\right)x\varphi_0, \tag{2.37}$$

where the second term is a ghost secularity. Removing it by setting the coefficient of $x\varphi_0$ to zero gives us an equation for $h_{0,1}$:

$$h_{0,1} = -\frac{\gamma_1}{8} h_0$$

from which

$$h_0 = h_0^{(1)}(x_2, x_3, \ldots) e^{-\gamma_1 x_1/8}. \tag{2.38}$$

Notice that with h_0 of this form, Φ_0 and Φ_1 have the correct asymptotic form to first order in k.

The second order equation is:

$$\partial_x L\Phi_2 = -2\Phi_{0,xx2} - 3\Phi_{0,x11} - 3\Phi_{1,xx1} - (n_0 - 4)\Phi_{1,1} - \gamma_2\Phi_0 - \gamma_1\Phi_1 + \Phi_{0,x}. \tag{2.39}$$

Integrating and applying L^{-1} leads to a Φ_2 containing the first instance of exponentially secular terms:

$$\begin{aligned}\Phi_2 \;=\; & h_0 \left\{ \frac{1}{256}\left(\gamma_1^2 - \frac{64}{15}\right) e^{-2x} + \frac{1}{640}(64 - 5\gamma_1^2)(\tanh x - 1) \right. \\ & \left. + \left(\frac{1}{4} - \frac{3\gamma_1^2}{256} + \frac{\gamma_2}{8}\right) \operatorname{sech}^2 x \right\} - \left(\frac{h_0}{4} - \frac{3\gamma_1^2 h_0}{256} + \frac{\gamma_2 h_0}{8} + h_{0,2}\right) x\varphi_0. \end{aligned} \tag{2.40}$$

This time the exponentially secular terms are proportional to e^{-2x} and can be removed by demanding that

$$\gamma_1^2 = \frac{64}{15}. \tag{2.41}$$

As with the ordinary perturbation theory (see (2.16)), we could obtain this from (2.39) by using the consistency condition:

$$\int_{-\infty}^{\infty} \operatorname{sech}^2 x \; \partial_x L\Phi_2 \, dx = 0 \tag{2.42}$$

where the scaled variables x_1, etc. are treated as constants. As with the first order analysis, we again equate the $x\varphi_0$ coefficient to zero to obtain:

$$h_{0,2} = \left(-\frac{1}{5} - \frac{\gamma_2}{8}\right) h_0 \tag{2.43}$$

after substituting in (2.41). Our expression for Φ_2 now takes the form:

$$\Phi_2 = \frac{1}{15} h_0 (\tanh x - 1) + \left(\frac{1}{5} + \frac{\gamma_2}{8}\right) h_0 \operatorname{sech}^2 x. \tag{2.44}$$

The first term in (2.44) is algebraically secular and results in Φ_2 tending to a non-zero constant (to zeroth order in k) as $x \to -\infty$. However, for the time being we disregard this unphysical behaviour.

The third order equation derived from (2.4) is:

$$\begin{aligned}\partial_x L\Phi_3 \;=\; & -2\Phi_{0,xx3} - 6\Phi_{0,x12} - \Phi_{0,111} - 3\Phi_{1,xx2} - 3\Phi_{1,x11} - 3\Phi_{2,xx1} \\ & -(n_0 - 4)(\Phi_{1,2} + \Phi_{2,1}) - \gamma_3\Phi_0 - \gamma_2\Phi_1 - \gamma_1\Phi_2 + \Phi_{0,1} + \Phi_{1,x}.\end{aligned}$$

On integrating and then applying L^{-1} we have

$$\begin{aligned}\Phi_3 &= h_0\left\{\frac{\gamma_1}{128}\left(\frac{4}{15}+\gamma_2\right)e^{-2x}+\frac{\gamma_1}{40}\mathcal{A}_1+\frac{\gamma_1}{320}(4-5\gamma_2)\mathcal{A}_0\right.\\ &\quad\left.+\left(\frac{5\gamma_1}{96}-\frac{3\gamma_1\gamma_2}{128}+\frac{\gamma_3}{8}-\frac{3\gamma_1}{40}\mathcal{A}_1\right)\operatorname{sech}^2 x+\frac{3\gamma_1}{40}\mathcal{A}_2\varphi_0\right\}\\ &\quad+\left(\frac{11\gamma_1 h_0}{480}+\frac{3\gamma_1\gamma_2 h_0}{128}-\frac{\gamma_3 h_0}{8}-h_{0,3}\right)x\varphi_0. \qquad (2.45)\end{aligned}$$

in which we have introduced the quantities $\mathcal{A}_n = \mathcal{A}_n(x)$. These are defined by

$$\mathcal{A}_n(x) = \int_{\infty}^{x}\mathcal{A}_{n-1}(x')\,dx' \quad \text{and} \quad \mathcal{A}_0(x) = \tanh x - 1 \qquad (2.46)$$

from which we have

$$\begin{aligned}\mathcal{A}_1(x) &= \ln\cosh x - x + \ln 2\\ \mathcal{A}_2(x) &= \int_0^x \ln\cosh x'\,dx' - \frac{1}{2}x^2 + x\ln 2 - \frac{\pi^2}{24}.\end{aligned}$$

On considering the asymptotic behaviour of $\mathcal{A}_0$ for large $|x|$, it follows from definition (2.46) that the asymptotic behaviour of the $\mathcal{A}_n$ in general is given by

$$(\mathcal{A}_n)_{x\to\infty} \simeq (-2)^{1-n}e^{-2x} + O(e^{-4x}) \qquad (2.47)$$

$$(\mathcal{A}_n)_{x\to-\infty} \simeq -\frac{2}{n!}x^n + O(e^{2x}). \qquad (2.48)$$

From the above we see that any term proportional to $\mathcal{A}_n$ is an algebraic secularity.

As before, to remove terms of the form e^{-2x} from (2.45) we have to demand that

$$\gamma_2 = -\frac{4}{15}.$$

It turns out that if we had carried out the conventional multiple-scale analysis, choosing the constant of integration so that the second order term vanishes at both infinities, we would have obtained a γ_2 of the same magnitude but opposite sign.

After removing the unwanted ghost secularities in (2.45) by assigning them to $h_{0,3}$

$$h_{0,3} = \left(\frac{\gamma_1}{60}-\frac{\gamma_3}{8}\right)h_0 \qquad (2.49)$$

we are left with

$$\Phi_3 = h_0\left\{\frac{\gamma_1}{40}\mathcal{A}_1+\frac{\gamma_1}{60}\mathcal{A}_0+\left(\frac{7\gamma_1}{120}+\frac{\gamma_3}{8}-\frac{3\gamma_1}{40}\mathcal{A}_1\right)\operatorname{sech}^2 x+\frac{3\gamma_1}{40}\mathcal{A}_2\varphi_0\right\}. \qquad (2.50)$$

Now the first two terms in (2.50) are of the algebraically secular type.

In order to convincingly demonstrate the regrouping of algebraic secularities we need to proceed to yet higher order. The fourth order results are derived in Appendix A. In these higher order analyses the number of terms involved becomes quite large, and so the algebraic manipulating functions in the computer program *Mathematica* (Wolfram 1991) were used. For further details see Appendix B.

We now turn our attention to the asymptotic behaviour of the terms in the expansion of Φ. All such terms have h_0 as a factor. From equations (2.38), (2.43), (2.49), and (A.4) we see that $h_0 \simeq e^{-\gamma x/8}$. Since we have performed the integrations so that all terms have e^{-2x} as the basic asymptotic form for positive x, all terms decay as $h_0 e^{-2x} = e^{-p_2 x}$ as $x \to +\infty$. The asymptotic form to first order is therefore in agreement with that derived from (2.30).

As for their behaviour as $x \to -\infty$, the terms fall into two classes. Firstly those containing $\mathrm{sech}^2 x$ or its derivatives decay as $h_0 e^{2x} = e^{p_1 x}$. From the second order onwards we also get terms which do not decay exponentially; these are the algebraic secularities. With the use of (2.48) we now examine the leading algebraically secular terms at each order in the limit as $x \to -\infty$. From (2.44), (2.50), and (A.5) we see that they give a contribution to $(\Phi)_{x \to -\infty}$, to order k^4, of the form

$$-\frac{2}{15}h_0k^2 - \frac{\gamma_1}{20}h_0k^3x - \frac{1}{25}h_0k^4x^2 = -\frac{2}{15}h_0k^2\left(1 + \frac{3}{8}\gamma_1 kx + \frac{9}{128}\gamma_1^2k^2x^2\right). \tag{2.51}$$

To this order, the polynomial can be re-expressed as $-(2/15)h_0k^2e^{3\gamma_1 kx/8}$. Since $h_0 = e^{-\gamma_1 kx/8}$ to first order, the regrouped terms (2.51) have an overall asymptotic form $e^{\gamma_1 kx/4}$ for $x \to -\infty$. This is in agreement with the third solution of (2.30), namely $e^{p_3 x}$, for small k.

Unlike the case of multiple-scale analysis in which the ghost secularities are automatically regrouped to give an expression for the $\gamma_1 x_1$ dependence to all orders, we have had to regroup the algebraically secular terms ourselves. However, on examining the terms up to fourth order giving rise to (2.51), we find that they are consistent with a contribution to Φ of the form

$$\begin{aligned}\Phi_{\text{alg.sec.}} &\equiv \frac{1}{15}h_0k^2\left\{\mathcal{A}_0(x) + \frac{3}{8}k\gamma_1\int_{\infty}^{x}\mathcal{A}_0(x')\,dx' + \frac{9}{64}k^2\gamma_1^2\int_{\infty}^{x}\int_{\infty}^{x'}\mathcal{A}_0(x'')\,dx'\,dx'' + \ldots\right\} \\ &\equiv \frac{1}{15}h_0k^2\Lambda(k,x)\end{aligned} \tag{2.52}$$

where

$$\Lambda(k,x) \equiv \left\{1 - \frac{3}{8}k\gamma_1\left[\int_{\infty}^{x}dx\right]\right\}^{-1}\mathcal{A}_0(x) \tag{2.53}$$

and see no reason why (2.52) is not true to all orders. Operating on (2.53) with the contents of the curly brackets and then differentiating gives the differential equation

$$\frac{d\Lambda}{dx} - \frac{3}{8}k\gamma_1\Lambda = \mathrm{sech}^2 x \tag{2.54}$$

whose solution is

$$\Lambda = e^{\frac{3}{8}k\gamma_1 x}\int_{\infty}^{x}e^{-\frac{3}{8}k\gamma_1 x'}\,\mathrm{sech}^2 x'\,dx'. \tag{2.55}$$

Even after using the above to express $\Phi_{\text{alg.sec.}}$ in a more conventional way, it has not been found possible to formulate the analysis so that such an expression emerges explicitly.

Looking back at the analysis in §2.1, we are now in a position to understand why simple perturbation theory gave the correct value for γ_1. In both perturbation methods γ_1 is obtained by removing exponentially secular terms. The constants of integration in the algebraically secular terms are chosen so that the algebraic secularities have the correct asymptotic form as $x \to \infty$. Such constants arising at mth order will appear in $\partial_x L\Phi_{m+1}$ and as a result will generate an exponential secularity. Hence the value of γ_m will depend on the constant of integration. In the case of the first order contribution to Φ, there were no algebraically

secular terms and hence the constant of integration was zero for both methods. This results in the two methods giving the same expression for γ_1. However, as an algebraic secularity arises at second order, our choice of its asymptotic form will critically affect the value of γ_2.

In spite of both methods giving the same first order growth rate, the x-dependence of Φ to finite order is different in the two methods. This is because in a multiple-scale type expansion, the ghost secular states present in the ordinary expansion have been removed and replaced by the h_0 factor. Although the ghost secularities are not truly secular, it is necessary to remove them in order to determine the behaviour of h_0. We can then use this to show that both the non-secular terms and the regrouped algebraic secularities have the correct asymptotic form to first order in k.

In conclusion, we see that only after treating the three types of secularity does one obtain a Φ that can be seen to be bounded and possess the correct asymptotic form.

2.3 Multiple-scale perturbation analysis about $k^2 = 5$

We use a similar procedure to that given in the previous section to determine the growth rate around $k^2 = 5$. Rewriting the asymptotic equation (2.30) in terms of $\bar{k}^2 \equiv 5 - k^2$, we obtain

$$\frac{d^3\Phi}{dx^3} - (9 - \bar{k}^2)\frac{d\Phi}{dx} + \gamma\Phi = 0. \tag{2.56}$$

The asymptotic solutions to the linearized equation (2.18) are therefore $e^{\bar{p}_1 x}$, $e^{-\bar{p}_2 x}$, and $e^{\bar{p}_3 x}$, where $\bar{p}_1 \simeq 3 - \gamma/18$, $\bar{p}_2 \simeq 3 + \gamma/18$, and $\bar{p}_3 \simeq \gamma/9$ for small $\bar{k}$. The underlying asymptotic forms are now e^{-3x} for $x \to +\infty$ and either e^{3x} or e^0 for $x \to -\infty$.

After substituting

$$\Phi = \bar{\Phi}_0(x, \bar{x}_1, \bar{x}_2, ...) + \bar{k}\bar{\Phi}_1(x, \bar{x}_1, \bar{x}_2, ...) + \bar{k}^2\bar{\Phi}_2(x, \bar{x}_1, \bar{x}_2, ...) + ...\,,$$

where $\bar{x}_m \equiv \bar{k}^m x$, and

$$\gamma = \bar{k}\bar{\gamma}_1 + \bar{k}^2\bar{\gamma}_2 + ...$$

into (2.18) we obtain to zeroth order the equation:

$$\partial_x \bar{L}\bar{\Phi}_0 = 0, \tag{2.57}$$

where $\bar{L} \equiv \partial_x^2 + n_0 - 9$. The solution of (2.57) is

$$\bar{\Phi}_0 = \bar{h}_0\bar{\varphi}_0 = \bar{h}_0(\bar{x}_1, \bar{x}_2, ...)\,\mathrm{sech}^3 x.$$

On integrating the first order equation,

$$\partial_x \bar{L}\bar{\Phi}_1 = -3\bar{\Phi}_{0,xx1} - (n_0 - 9)\bar{\Phi}_{0,1} - \bar{\gamma}_1\bar{\Phi}_0 = -2\bar{\Phi}_{0,xx1} - \bar{\gamma}_1\bar{\Phi}_0\,, \tag{2.58}$$

we find:

$$\bar{L}\bar{\Phi}_1 = -\bar{\gamma}_1\bar{h}_0\int_\infty^x \bar{\varphi}_0\,dx - 2\bar{h}_{0,1}\bar{\varphi}_{0,x}\,, \tag{2.59}$$

in which we have not evaluated the integral due to the complexity of $\bar{L}^{-1}(\int\bar{\varphi}_0)$. Instead we will only need to use the following results for large negative x:

$$\bar{\varphi}_0 = 8\,e^{3x} + O(e^{5x}) \qquad \bar{\varphi}_0^2 = 64\,e^{6x} + O(e^{8x})$$
$$\int_\infty^x \bar{\varphi}_0\,dx = -\frac{\pi}{2} + \frac{8}{3}e^{3x} + O(e^{5x}) \qquad \int_\infty^x \bar{\varphi}_0^2\,dx = -\frac{16}{15} + \frac{32}{3}e^{6x} + O(e^{8x}). \tag{2.60}$$

Using $\bar{L}(x\bar{\varphi}_0) = 2\bar{\varphi}_{0,x}$ and applying $\bar{L}^{-1}$ to the remaining term on the right hand side of (2.59) results in†

$$\bar{\Phi}_1 = -\frac{\bar{\gamma}_1\bar{h}_0}{2}\bar{\varphi}_0\int^x \frac{\left(\int_\infty^{x'}\bar{\varphi}_0(x'')\,dx''\right)^2}{\bar{\varphi}_0^2(x')}\,dx' - \bar{h}_{0,1}\,x\bar{\varphi}_0. \tag{2.61}$$

The expression automatically has the correct asymptotic form for $x > 0$. However, since the numerator inside the integral tends to a constant as $x \to -\infty$, the first term in (2.61) will tend to e^{-3x} in this limit. We must therefore choose $\bar{\gamma}_1 = 0$. Our insistence on the removal of the $x\bar{\varphi}_0$ terms means that $\bar{h}_{0,1}$ also vanishes. This leaves $\bar{\Phi}_1 = 0$.

Because of the first order results, the second order equation simplifies to

$$\partial_x\bar{L}\bar{\Phi}_2 = -2\bar{\Phi}_{0,xx2} - \bar{\gamma}_2\bar{\Phi}_0 - \bar{\Phi}_{0,x}\,. \tag{2.62}$$

The extra term, comparing the above with (2.58), enables us to remove the exponential growth for negative x. Integrating (2.62) gives

$$\bar{L}\bar{\Phi}_2 = -\bar{\gamma}_2\bar{h}_0\int_\infty^x\bar{\varphi}_0\,dx - 2\bar{h}_{0,2}\bar{\varphi}_{0,x} - \bar{h}_0\bar{\varphi}_0\,, \tag{2.63}$$

from which

$$\bar{\Phi}_2 = -\bar{h}_0\bar{\varphi}_0\int^x \frac{\frac{\bar{\gamma}_2}{2}\left(\int_\infty^{x'}\bar{\varphi}_0(x'')\,dx''\right)^2 + \int_\infty^{x'}\bar{\varphi}_0^2(x'')\,dx''}{\bar{\varphi}_0^2(x')}\,dx' - \bar{h}_{0,2}x\bar{\varphi}_0\,, \tag{2.64}$$

where the integrals need only be evaluated if an explicit expression for $\bar{\Phi}_2$ is required or if we wish to continue to next order and find $\bar{\gamma}_3$. Using the results (2.60), we find that the numerator in the integrand of (2.64) for large negative x is equal to

$$\frac{\bar{\gamma}_2}{2}\left(\frac{\pi^2}{4} - \frac{8\pi}{3}e^{3x}\right) - \frac{16}{15} + O(e^{5x}). \tag{2.65}$$

We can remove the constant term of (2.65) which would have resulted in an exponential secularity by demanding that

$$\bar{\gamma}_2 = \frac{128}{15\pi^2}. \tag{2.66}$$

The next largest term in (2.65) now results in a contribution to $\bar{\Phi}_2$ equal to $64/(135\pi)$. On re-examining our ordinary perturbation analysis about $k^2 = 5$, we see that (2.28) gives this value for $x \to -\infty$ if the exponential terms are removed by appropriate choice of $\bar{B}_2$ and $\bar{C}_2$, and $\bar{\gamma}_2$ is chosen so that the expression vanishes at $+\infty$. This constant term, which occurs only for large *negative* x, signals the presence of an algebraic secularity and it can presumably be dealt with in an analogous manner to those in the expansion in §2.2.

As $x \to \infty$, the integrand of (2.64) tends to

$$\frac{\bar{\gamma}_2}{18} - \frac{1}{6} + O(e^{-2x}). \tag{2.67}$$

† L^{-1} is given by (2.31) with φ_0 replaced by $\bar{\varphi}_0$

The constant terms will generate an $x\bar{\varphi}_0$ term in $\bar{\Phi}_2$. To remove this and the other ghost secularity, we must have

$$\bar{h}_{0,2} = \left(\frac{1}{6} - \frac{\bar{\gamma}_2}{18}\right)\bar{h}_0 \quad \text{or} \quad \bar{h}_0 = \bar{h}_0^{(2)}(\bar{x}_3, \ldots)e^{(1/6-\bar{\gamma}_2/18)\bar{x}_2}. \tag{2.68}$$

We see that the $\bar{\gamma}_2$ dependence of $\bar{h}_0$ is in agreement with that of the $e^{\bar{p}_1 x}$ and $e^{-\bar{p}_2 x}$ solutions to the asymptotic equation (2.56).

This is the first time an analytical form for the growth rate about $k^2 = 5$ has been derived. The complicated form of $\bar{L}^{-1}(1)$ and $\bar{L}^{-1}(\int \bar{\varphi}_0)$ (see (2.21) and (2.23)) suggests that the approach of finding the growth rate for a soliton by considering the limit for nonlinear waves mentioned in the introduction would be very much more difficult than the already involved small-$\bar{k}$ type calculation that we have just used. Note that our approach of dealing only with the leading terms of the expansions of functions at the final order could also have been employed in the $k = 0$ analysis. However, the second order equation in that case had more terms and this approach would be quite cumbersome compared with the method that was actually used.

It will be noticed from the results of §2.2 that besides the variation of Φ on approximately the same scale as the equilibrium solution, there is a slowly decaying exponential for $x < 0$ resulting from the regrouped algebraically secular terms. This is apparent in the plots of the numerically derived eigenfunctions given in the next section and is particularly prominent as k^2 approaches 5. The reason for this can be understood on integrating the linearized equation (2.4) over all space to give the consistency condition

$$\gamma \int_{-\infty}^{\infty} \Phi \, dx = 0 \tag{2.69}$$

when Φ vanishes at both infinities. We see that for non-zero γ, the integral of the eigenfunction must vanish. For $k^2 = 5$, this integral is non-zero. For neighbouring k, the presence of a small amount of a very slowly decaying exponential whose amplitude is of the opposite sign to the $\gamma = 0$ eigenfunction ensures that (2.69) is satisfied. This slowly decaying exponential is provided by the algebraic secularities.

Before presenting our numerical results, we collect together our analytical results. For small k we find that the growth rate is given by:

$$\gamma = \frac{8}{\sqrt{15}}|k| - \frac{4}{15}k^2 - \frac{7}{15\sqrt{15}}|k|^3 - \frac{8}{225}k^4 + O(k^5) \tag{2.70}$$

and the eigenfunction by:

$$\begin{aligned}
\Phi \;=\; & h_0 \Bigg\{ \operatorname{sech}^2 x \tanh x + \left(\frac{|k|}{\sqrt{15}} + \frac{k^2}{6} + \frac{49|k|^3}{120\sqrt{15}} + \frac{73k^4}{1800}\right)\operatorname{sech}^2 x \\
& + \left(\frac{1}{15}k^2 + \frac{2}{15\sqrt{15}}|k|^3 + \frac{7k^4}{1800}\right)\mathcal{A}_0 + \left(\frac{|k|^3}{5\sqrt{15}} + \frac{k^4}{75}\right)\mathcal{A}_1 + \frac{k^4}{25}\mathcal{A}_2 \\
& + \left(\sqrt{\frac{3}{125}}|k|^3 + \frac{3k^4}{100}\right)\left(\mathcal{A}_2 \operatorname{sech}^2 x \tanh x - \mathcal{A}_1 \operatorname{sech}^2 x\right) - \frac{k^4}{50}\mathcal{A}_1 \tanh x \\
& + \frac{k^4}{300}\left(\mathcal{A}_1 e^{2x} - 1\right) - \frac{2k^4}{25}\mathcal{A}_2 \operatorname{sech}^2 x + \frac{3k^4}{25}\mathcal{A}_3 \operatorname{sech}^2 x \tanh x \Bigg\} + O(k^5)
\end{aligned} \tag{2.71}$$

where

$$h_0 = h_0^{(4)}(x_5, x_6, \ldots)e^{-\left(|k|/\sqrt{15}+k^2/6-23|k|^3/40\sqrt{15}+19k^4/1800\right)x}.$$

Even if we replace the leading algebraically secular terms at each order by the single term $(k^2/15)\Lambda(k,x)$ we suggested earlier, (2.71) is still very complicated. The possibility of finding an explicit expression valid for all k therefore seems very remote.

In the neighbourhood of $k = k_c$, the growth rate is given by:

$$\gamma = \frac{128}{15\pi^2}\bar{k}^2 + O(\bar{k}^3) \tag{2.72}$$

and the eigenfunction by:

$$\Phi = \bar{h}_0 \operatorname{sech}^3 x + O(\bar{k}^2) \tag{2.73}$$

where $\bar{k}^2 = 5 - k^2$ and

$$\bar{h}_0 = \bar{h}_0^{(2)}(\bar{x}_3, \ldots)e^{-(\gamma/18-\bar{k}^2/6)x}.$$

2.4 Comparison of the analysis with the numerical results

The numerical determination of γ given by Infeld & Frycz (1987) was carried out using a relaxation method. An initial guess of the eigenfunction $\Phi(x)$ of the linearized equation (2.4) is allowed to evolve under the discrete-Fourier equivalent equation until its entire profile grows at the same rate which is then identified as the growth rate γ. The method is computationally expensive, particularly when the eigenfunction becomes much less localized as k^2 approaches the cut-off value. In order to verify our analytic work, we have developed a much faster and more accurate way of determining both γ and the eigenfunction. Our method, which is essentially a shooting method, does not involve the restriction to a periodic domain, and as initial conditions requires only a value for γ and the first two derivatives of the eigenfunction at a single point x_0.

The numerical method

In our scheme, given k, we guess a value for γ and integrate the equations using an adaptive stepsize 4th-order Runge-Kutta technique (see e.g. Press *et al.* 1988). To generate the solution we are looking for, we need good estimates of the boundary conditions $\Phi'(x_0)$ and $\Phi''(x_0)$ given an arbitrary value for $\Phi(x_0)$. We obtain these by choosing x_0 large enough for us to be able use the asymptotic form of $\Phi(x)$. As this is a sum of two exponentials whose ratio is not known for $x \to -\infty$, but only one exponential, $e^{-p_2 x}$, for $x \to +\infty$, we choose x_0 to be large and positive. The latter asymptotic form can therefore be used to give the initial boundary conditions:

$$\Phi'(x_0) = -p_2\Phi(x_0) \quad \text{and} \quad \Phi''(x_0) = p_2^2\Phi(x_0) \tag{2.74}$$

where $-p_2$ is the negative solution of the auxiliary equation

$$p^3 - (4 + k^2)p + \gamma = 0 \tag{2.75}$$

derived from (2.30).

We start with an initial guess $\gamma_{[0]}$ for the growth rate and find the boundary conditions using (2.75) and (2.74). We then integrate from x_0 towards negative x until, once we have

passed the origin, $\Phi(x)$ grows exponentially. We then repeat the process but with other values of the growth rate until we find a $\gamma_{[1]}$ such that the sign of Φ at the end of the integration is opposite to that for $\gamma_{[0]}$. To obtain an eigenfunction which starts to grow exponentially at a greater distance from the origin and is therefore closer to the true Φ, we choose our next guess of γ to lie between $\gamma_{[0]}$ and $\gamma_{[1]}$. We continue to improve our approximation to the desired $\Phi(x)$, and hence refine our estimate of the growth rate, by choosing a $\gamma_{[n]}$ which lies between the most recent estimates which gave final values of Φ of the opposite sign until we have reached the required tolerance.

To determine the full growth rate curve, we start with a small value of k and use the analytical result for γ_1 (2.17) as our starting estimate of γ. We gradually increase k and use the values of γ for the two previous points on the growth rate curve to generate an estimate of γ for the present value of k. A good estimate is not strictly required by the method - once two values ($\gamma_{[0]}$ and $\gamma_{[1]}$) have been found which give a Φ of opposite sign for large negative x, the method will eventually converge to the correct γ. However, a good initial guess will mean that fewer iterations are necessary.

The accuracy of the numerical method was tested in two ways. First the method was applied to a similar equation whose solution is known exactly. Replacing the associated Legendre-type operator L in the linearized ZK equation by the $N = 2$ analogue (see equation (2.5)) gives

$$\frac{d}{dx}L_o^{(6)}\Phi^{(6)} = -\gamma^{(6)}\Phi^{(6)} + k^2\frac{d\Phi^{(6)}}{dx} \tag{2.76}$$

in which

$$L_o^{(6)} \equiv \frac{d^2}{dx^2} + 6\,\mathrm{sech}^2 x - 1.$$

It was serendipitously discovered that (2.76) has the exact solution

$$\Phi^{(6)} = e^{-kx/\sqrt{3}}\left(\mathrm{sech}\,x\tanh x + \frac{k}{\sqrt{3}}\mathrm{sech}\,x\right) \tag{2.77}$$

with

$$\gamma^{(6)} = \frac{2}{3\sqrt{3}}k(3-k^2) \tag{2.78}$$

for $k^2 \leq 3$.

It can be seen from (2.77) that the variation in the form of the eigenfunction with k is similar to that of the linearized ZK equation. The eigenfunctions always have a single maximum and are odd and even at $k = 0$ and $k = k_c$ respectively. For k^2 close to 3, the $e^{-kx/\sqrt{3}}\,\mathrm{sech}\,x\tanh x$ part of $\Phi^{(6)}$ generates a slowly decaying exponential for $x < 0$ just as is produced by the algebraic secularities in the case of Φ. Given also that the behaviour of γ near its zeros matches the form dictated by (2.78), it would seem reasonable to gauge the expected accuracy of the method in determining γ by applying it to (2.76). We find that the numerically derived $\gamma^{(6)}$ agrees with (2.78) to better than 1 part in 10^9 over the entire range of k between the two zeros of $(\gamma^{(6)})^2$.

As a further test, we looked at the effect of increasing the starting value of x so as to decrease the error in the derivatives of Φ. Again, this affected the values of γ by at most a few parts in 10^9. In contrast, Infeld & Frycz estimate that their numerical results are accurate to within 2.5%. Furthermore, our experience in using their method suggests that it is very much more computationally intensive than ours.

The growth rate curve obtained using our numerical method is shown as the solid line in Figure 2.1 and is in general agreement with that obtained by Infeld & Frycz (1987).

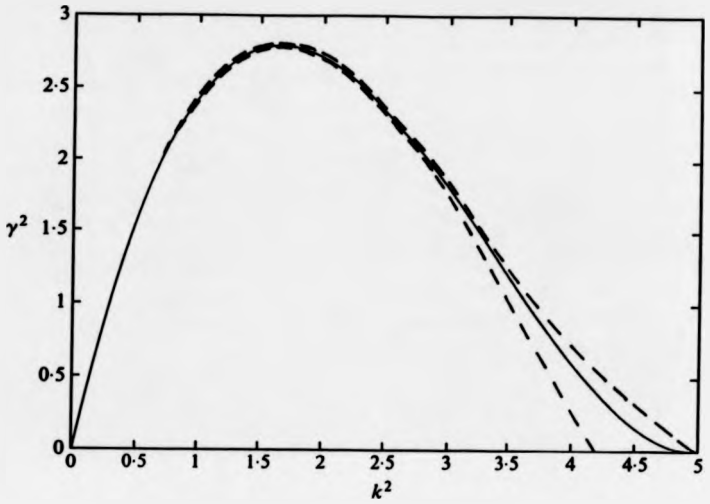

Figure 2.1: Growth rate curve for the linearized ZK equation. Solid line is the result of the numerical calculations; broken lines depict the Laedke & Spatschek upper and lower bounds obtained using complementary variational principles. (From Allen & Rowlands 1993)

As a by-product of determining γ for a given k numerically, we also obtain the eigenfunction. A selection of these are shown in Figure 2.2. We see that for $k = 0$, the eigenfunction has the form of $\mathrm{sech}^2 x \tanh x$ and is reasonably well approximated by this for small k. On increasing k, we see that the slow exponential decay for $x < 0$, which is a result of the algebraically secular terms, becomes more apparent. In particular, the decay is slower but of smaller amplitude as k^2 approaches 5. This enables the integral of the eigenfunction to remain equal to zero until $k^2 = 5$ at which point it suddenly becomes finite - the eigenfunction is then $\mathrm{sech}^3 x$.

Comparison of the analytical and numerical results

In Figure 2.3 we compare the nth order growth rates calculated analytically with the growth rate curve we obtained using our numerical method. It can be seen that the analytical curves approach the numerical curve as the order is increased. However, the fourth order result does not lie as close to the true growth rate curve as we might expect from the convergence of the lower order curves.

The anomalous behaviour at fourth order is very apparent when we fit a Pth order polynomial to the numerical data (see Table 2.1). The value of P was chosen to minimize γ_0. We see very good agreement for the γ_m up to third order, but not for γ_4. Since the numerical

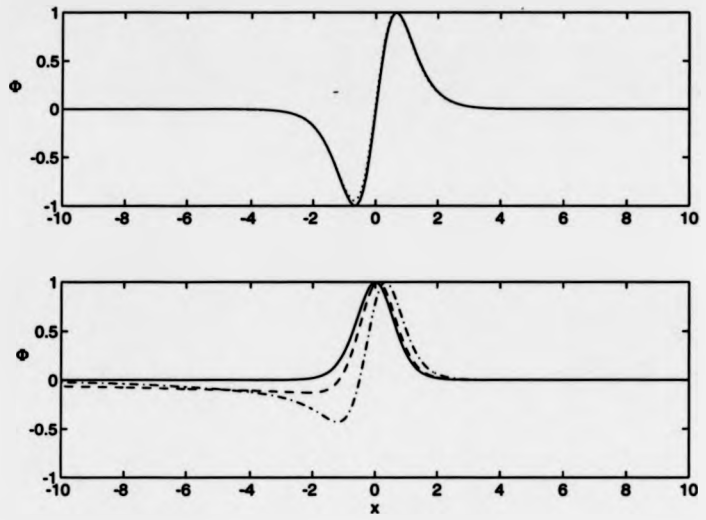

Figure 2.2: Eigenfunctions of linearized ZK equation for k equal to: 0 solid curve, upper graph; 0.1 dotted; 1.3 dash-dot; 2.0 dashed; $\sqrt{5}$ solid curve, lower graph.

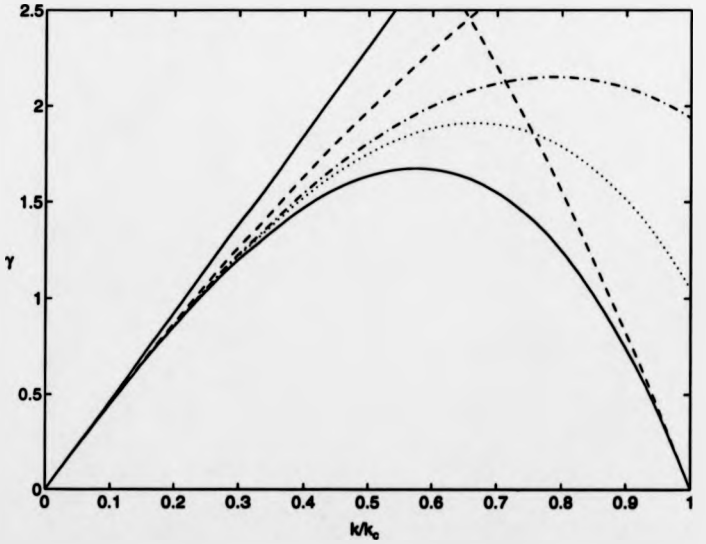

Figure 2.3: Growth rates given by the expansions about $k = 0$ and $k = k_c$. Lower solid curve - numerical results. Other curves emanating from origin are obtained from (2.70) to nth order: solid n=1; dashed n=2; dash-dot n=3; dotted n=4. Dashed curve passing through $k = k_c$ is from the second order result (2.72).

		analytical	numerical N=100; P=17	numerical N=1000; P=25
γ_0	0	0	-6×10^{-12}	-3×10^{-12}
γ_1	$8/\sqrt{15}$	2.0655911179	2.0655911161	2.0655911185
γ_2	$-4/15$	-0.2$\dot{6}$	-0.266666664	-0.266666668
γ_3	$-7/(15\sqrt{15})$	-0.1204928	-0.1204917	-0.1204935
γ_4	$-8/225$	-0.03$\dot{5}$	-0.167169	-0.167132
γ_5	?	?	0.055534	0.055159

Table 2.1: Estimates of γ_n obtained from a polynomial fit. N is the number of data points in growth rate curve; P is the order of the polynomial.

values of γ_4 and γ_5 do not change much on increasing the number of data points, it would seem that the numerical value of γ_4 we have obtained can be relied upon. Hence it seems possible that the series for γ we are obtaining analytically is in fact asymptotic, converging only for a finite number of terms.

A vastly improved analytical expression for γ for all $0 \leq k^2 \leq 5$ can be obtained by combining our analytical results for small k and $\bar{k}$ as a two-point Padé approximant. A Padé approximant is a rational function which approximates a given function over a certain range of the independent variable (see Baker & Graves-Morris 1984 for further details and applications). In our case, the Padé approximant is determined by demanding that its expansion agrees as well as possible with the analytically derived expansions of γ.

To ensure that the zeros of the approximant match those of γ, it must contain the factor $k(k-\sqrt{5})(k+\sqrt{5})$. We therefore choose our Padé approximant to be of the form

$$\gamma_p = \gamma_1 k(1-k^2/5)\left(\frac{1+a_1 k}{1+b_1 k}\right) \tag{2.79}$$

so that it also already has the same gradient at $k=0$ as the true γ. At $k^2=5$ we insist that $\gamma_p = \bar{\gamma}_2(5-k^2)$, where $\bar{\gamma}_2$ is given by (2.66). This leads to the relation

$$\frac{\gamma_1}{\sqrt{5}}\left(\frac{1+\sqrt{5}a_1}{1+\sqrt{5}b_1}\right) = \bar{\gamma}_2. \tag{2.80}$$

To obtain another equation for the unknowns a_1 and b_1, we choose to match the Padé approximant in the limit of small k with the series expansion obtained in §2.2; by equating coefficients of k^2 we find

$$(a_1 - b_1)\gamma_1 = \gamma_2. \tag{2.81}$$

From (2.80), (2.81) and the values of γ_1, γ_2 and $\bar{\gamma}_2$, we obtain $a_1 \approx 1.43976$ and $b_1 \approx 1.56886$.

The very close agreement between our Padé approximant and the numerical results can be seen in the plot of the percentage error shown in Figure 2.4. We see that the maximum error is less than 0.42%. We could consider a higher order Padé approximant and use the values of γ_3 and γ_4 to determine a_2 and b_2 but this seems unnecessary in view of the excellent agreement we find with the present order.

We also compare the numerically evaluated eigenfunction for $k=0.1$ with the small-k approximations obtained analytically. The maximum error in the eigenfunction obtained for

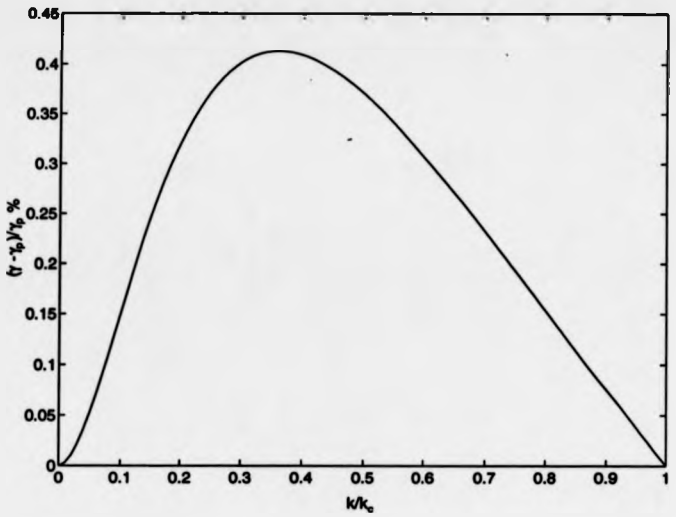

Figure 2.4: Percentage error in the Padé approximant.

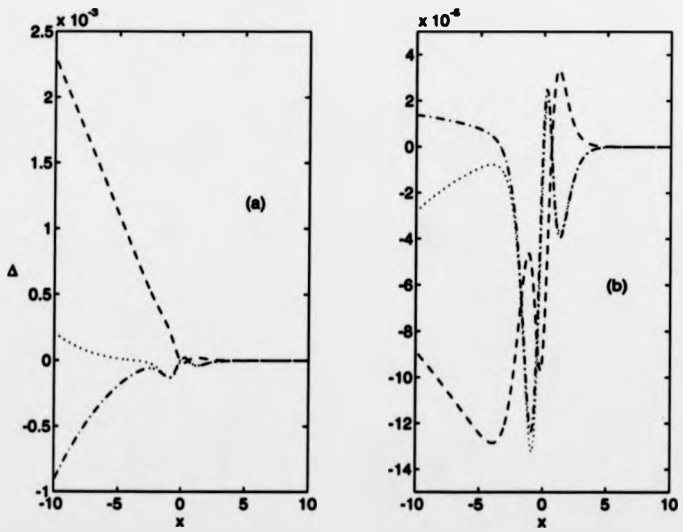

Figure 2.5: Comparison of the numerically generated eigenfunction for $k = 0.1$ with that derived analytically. $\Delta = \hat{\Phi}_{\text{numerical}} - \hat{\Phi}_{\text{analytical}}$, where the hat denotes normalization to unit amplitude. (a): $\hat{\Phi}_{\text{analytical}}$ is obtained from (2.71) to nth order: dashed n=2; dash-dot n=3; dotted n=4. (b): As in (a), but the $\mathcal{A}_0$ terms are replaced by Λ. Maximum values of Δ for zeroth and first order expressions are 0.08 and 0.003 respectively.

the test equation (2.76) for which the analytical form is known exactly was 10^{-8}. Hence we can be confident that discrepancies much larger than this between the numerical and analytical eigenfunctions obtained for the linearized ZK equation are predominantly due to having only an approximate analytical form.

In Figure 2.5(a), we plot the difference between the numerically obtained eigenfunction and our expression (2.71) for Φ to second, third, and fourth order. To obtain an improved approximation to the eigenfunctions, we replaced the three $\mathcal{A}_0$ terms in our expression for Φ by Λ (see equation (2.55)). (The values of $\mathcal{A}_2(x)$, $\mathcal{A}_3(x)$, and $\Lambda(k,x)$ were calculated using the numerical integration routine in *Mathematica*.) As Λ is equivalent to an infinite series of algebraic secularities, we have to be careful to subtract any higher order terms in its expansion which already appear in (2.71). As can be seen in Figure 2.5(b), the errors in the resulting analytical expression for Φ are significantly lower. In particular, the maximum error in the eigenfunction calculated from (2.71) as it stands is ten times larger than the maximum error in the second order expression for Φ with the algebraic secularity replaced by Λ. This backs up our conjecture that the leading algebraic secularities at each order are the first few terms in the expansion of the function $\Lambda(k,x)$. This is analogous to the better approximation to the true eigenfunction which one achieves by replacing the $x^n\varphi_0$ terms that appear in the ordinary perturbation analysis by the exponential h_0 on performing a multiple-scale analysis.

2.5 Oblique perturbation

We now determine the effect of applying a periodic perturbation at an angle θ to the magnetic field. Substituting

$$n = n_0 + \varepsilon\Phi(x)e^{i(k\cos\theta\, x + k\sin\theta\, y)}e^{\gamma t} \tag{2.82}$$

into the ZK equation (2.2) and neglecting ε^2 terms leads to

$$\frac{d}{dx}L_o\Phi = -\gamma\Phi - ik\cos\theta\,(n_0-4)\Phi - 3ik\cos\theta\,\frac{d^2\Phi}{dx^2} + k^2(1+2\cos^2\theta)\frac{d\Phi}{dx} + ik^3\cos\theta\,\Phi. \tag{2.83}$$

Using the same method as in §2.2, we again have at zeroth order $\partial_x L\Phi_0 = 0$ from which $\Phi_0 = h_0\varphi_0$. Note that Φ, γ, and h_0 are now also functions of θ. The first order equation is

$$\begin{aligned}\partial_x L\Phi_1 &= -3\Phi_{0,xx1} - 3i\cos\theta\,\Phi_{0,xx} - (n_0-4)\Phi_{0,1} - i\cos\theta\,(n_0-4)\Phi_0 - \gamma_1\Phi_0\\ &= -2\Phi_{0,xx1} - 2i\cos\theta\,\Phi_{0,xx} - \gamma_1\Phi_0\end{aligned}$$

and on removing the ghost secular terms from the solution we find

$$\Phi_1 = \frac{\gamma_1}{8}\operatorname{sech}^2 x$$

and

$$h_{0,1} = -\left(\frac{\gamma_1}{8} + i\cos\theta\right)h_0\,.$$

The second order equation can be written as

$$\begin{aligned}\partial_x L\Phi_2 &= -2\Phi_{0,xx2} - 3\Phi_{0,x11} - 3\Phi_{1,xx1} - (n_0-4)\Phi_{1,1} - \gamma_2\Phi_0 - \gamma_1\Phi_1\\ &\quad -3i\cos\theta\,\Phi_{1,xx} - 6i\cos\theta\,\Phi_{0,x1} - i\cos\theta\,(n_0-4)\Phi_1 + (1+2\cos^2\theta)\Phi_{0,x}.\end{aligned}$$

The exponentially secular terms in Φ_2 are removed by making

$$\gamma_1^2 = \frac{64}{15}\sin^2\theta.$$

This result agrees with the soliton limit of the analysis of perturbations to nonlinear waves done by Infeld (1985). After also removing the ghost secularities, we have

$$\Phi_2 = \frac{1}{15}\sin^2\theta\,(\tanh x - 1) + \left(\frac{1}{5}\sin^2\theta + \frac{\gamma_2}{8}\right)\operatorname{sech}^2 x.$$

On eliminating the exponential secularities from third order contribution, we find

$$\gamma_2 = -\frac{4}{15}\sin^2\theta.$$

We seem to be getting the same expressions for Φ and γ as before, but with k replaced by $k\sin\theta$ which is the component of the wavevector along the y-axis. This is what we might have expected since the KdV equation is stable to small perturbations (Benjamin 1972) and so plane ZK solitons will also be stable to perturbations along their direction of motion. Since we are examining the linearized equation, the x-component of the perturbation should therefore have no effect.

As was concluded by Infeld, we see that plane solitons propagating along the magnetic field are most unstable to perturbations applied perpendicular to their direction of motion.

2.6 Variational approach

A frequently used method for giving an estimate of the entire growth rate curve as opposed to the just the behaviour near its zeros is the variation of action method (see for example Anderson, Bondeson & Lisak 1979). In this section we see whether we can improve upon previous efforts to determine the growth rate curve for the ZK equation in this way.

The variation of action method can be used to investigate the stability of the solution $u_0(x,t)$ of the evolution equation $\mathcal{N}(u, u_t, u_x, u_y, u_{xx}, \ldots) = 0$ if the equation is derivable from a Lagrangian density $\mathcal{L}(u, u_t, u_x, u_y, u_{xx}, \ldots)$ via the variational principle

$$\delta \iiint \mathcal{L}\,dx\,dy\,dt = 0.$$

$u_0(x,t)$ is made into a trial function by rewriting it so that the properties such as amplitude, width and phase appear as independent parameters, A_j. One or more of these parameters is then considered to be a function of y and t. The trial function is inserted into the Lagrangian density and the x-dependence is integrated out to leave the reduced variational principle

$$\delta \iint \langle\mathcal{L}\rangle(A_j, A_{jy}, A_{jt}, \ldots)\,dy\,dt = 0$$

in which $\langle\mathcal{L}\rangle = \int_{-\infty}^{\infty}\mathcal{L}\,dx$. The resulting Euler-Lagrange equations $\delta\langle\mathcal{L}\rangle/\delta A_j = 0$ are then linearized about the unperturbed values of the parameters. The solution to these linearized equations finally yields the growth rate.

We now illustrate this method by applying it to the simplest form of trial function that gives meaningful results. This takes the form

$$n(x,y,t) = A(y,t)\operatorname{sech}^2(x - P(y,t)). \tag{2.84}$$

The following Lagrangian density, which is based on that obtained by Infeld (1985) for the ZK equation, generates the moving frame reduced version (equation (2.2)).

$$\mathcal{L} = \frac{1}{2}\psi_t\psi_x + \frac{1}{6}\psi_x^3 - 2\psi_x^2 - \frac{1}{2}\psi_{xx}^2 - \frac{1}{2}\psi_{xy}^2\,; \qquad \psi_x \equiv n. \tag{2.85}$$

Substituting the trial function (2.84) into (2.85) and integrating over all x, we obtain

$$\langle\mathcal{L}\rangle = -\frac{16}{5}A^2 + \frac{8}{45}A^3 - \frac{2}{3}A^2P_t - \frac{2}{3}A_y^2 - \frac{8}{15}A^2P_y^2. \tag{2.86}$$

The Euler-Lagrange equations for $A(y,t)$ and $P(y,t)$ yield the relations

$$\frac{32}{5}A - \frac{8}{15}A^2 + \frac{4}{3}AP_t + \frac{16}{15}AP_y^2 - \frac{4}{3}A_{yy} = 0 \tag{2.87}$$

and

$$\frac{4}{3}A_t + \frac{32}{15}A_yP_y + \frac{16}{15}AP_{yy} = 0 \tag{2.88}$$

respectively. Linearizing (2.87) and (2.88) by substituting in $A(y,t) = A_0 + \delta A(y,t)$ and $P(y,t) = \delta P(y,t)$ (our δ is no longer the variational operator) gives the expected zero order condition $A_0(A_0 - 12) = 0$ along with the coupled linear equations

$$-\frac{8}{5}\delta A - \frac{1}{3}\delta A_{yy} + 4\,\delta P_t = 0 \tag{2.89}$$

and

$$\delta A_t + \frac{48}{5}\delta P_{yy} = 0. \tag{2.90}$$

These are solved by making both δA and δP proportional to $e^{\hat{\gamma}t}e^{iky}$. We then obtain the dispersion relation

$$\hat{\gamma}^2 = \frac{96}{25}k^2\left(1 - \frac{5}{24}k^2\right). \tag{2.91}$$

This gives a reasonable approximation to the initial slope of the growth rate curve and the position of its other zero, k_c. The growth rate in the small-k limit is obtained exactly on varying more parameters as was done by Makhankov (1978) and Infeld & Frycz (1987), but both these attempts failed to give the correct value of k_c. To obtain the correct value, we incorporated an additional term into the trial function. This took the form of an infinitesimal quantity of the eigenfunction at $k^2 = 5$:

$$n = A\,\mathrm{sech}^2(B\,[x - \delta P(y,t)]) + \delta H(y,t)\,\mathrm{sech}^3(B\,[x - \delta P(y,t)]). \tag{2.92}$$

We tried all possible combinations of A, B, and δH as parameters which could vary. Only on varying all the available parameters do we get the correct value for both $d\gamma/dk$ at $k = 0$, and k_c. The results of this calculation along with those of the other combinations of parameters which lead to sensible dispersion relations are shown in Table 2.2. It turns out that these dispersion relations are always expressible in the form

$$\hat{\gamma}^2 = \hat{\gamma}_1^2k^2\left(1 - \frac{k^2}{k_c^2}\right)\left(\frac{1 + c_1k^2 + c_2k^4}{1 + d_1k^2 + d_2k^4}\right). \tag{2.93}$$

	A	B	δH	$\tilde{\gamma}_1/\gamma_1$	k_c/k_c	c_1	d_1	c_2	d_2
(a)	$A(y,t)$	1	0	0.9487	0.9798	0	0	0	0
(b)	$12B^2(y,t)$	$B(y,t)$	0	1	0.9502	0	0	0	0
(c)	$A(y,t)$	$B(y,t)$	0	1	0.9998	0.1185	0.1399	-0.06375	-0.06803
(d)	12	1	$\delta H(y,t)$	0.9801	1	0	0	0	0
(e)	$A(y,t)$	1	$\delta H(y,t)$	0.9991	1	0.3039	0.3236	0	0
(f)	$A(y,t)$	$B(y,t)$	$\delta H(y,t)$	1	1	0.4743	0.4958	0.04746	0.05063

Table 2.2: Results of a variational calculation with trial function (2.92). The parameters refer to (2.93). (b) Makhankov result. (c) Infeld & Frycz result.

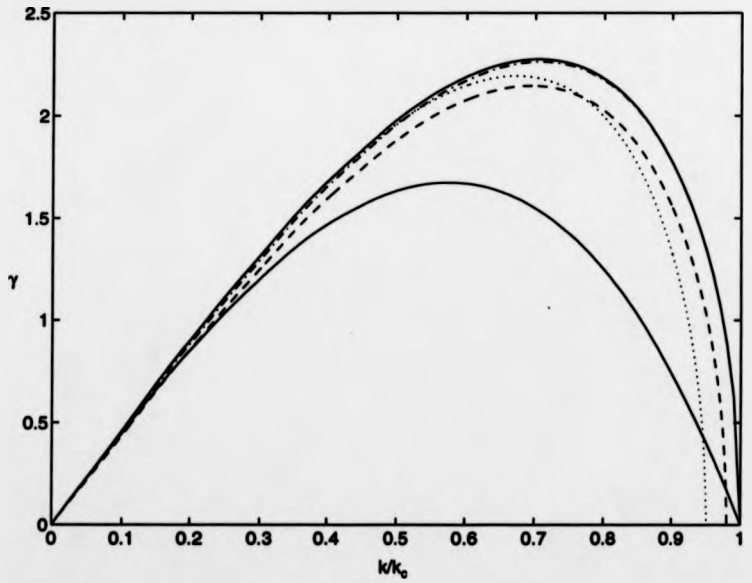

Figure 2.6: Comparison of numerical results with those obtained from a variational calculation using the trial functions detailed in Table 2.2. Lower solid curve - numerical results; dashed (a); dotted (b); dash-dot (d); upper solid curves (c),(e),(f).

As can be seen in Figure 2.6, the shape of the growth rate curves for all the calculations are fairly similar. In particular, we see that the addition of a small amount of the $k^2 = 5$ solution has very little effect on the overall form of the curve. They all, however, differ significantly from the true growth rate curve. None of the curves have the linear dependence of the growth rate at $k = k_c$ shown by the Padé approximant and the numerical results. The maximum growth rate is also about 40% too large and the variational estimate of the wavenumber at which this occurs is around 1.6 whereas the true value is 1.294.

The incorrect behaviour of the variational method curves at $k^2 = 5$ may be understood by noting that only by fine tuning c_j and d_j will (2.93) generate the linear dependence of γ on k near the cut-off value. Furthermore, it is impossible to choose these constants in such a way as to attain our ZK Padé approximant (2.79). The overshooting of the growth rate maximum is possibly due to the fact that because of the form of (2.93), we will always have

$$\hat{\gamma}_2 = \frac{1}{2!}\frac{d^2\hat{\gamma}}{dk^2}\bigg|_{k=0} = 0.$$

Our small-k analysis gives a negative γ_2 which results in the growth rate dropping from the linear k-dependence around the origin at a smaller value of k.

On the basis of our comparison with the numerical results, it seems that the variation of action method appears to be only of limited use in this case. In contrast, our Padé approximant would be practically indistinguishable from the numerical results if plotted in Figure 2.6.

Laedke & Spatschek (1979) have found that the variation of action method also gives wrong results for the KP$^+$ equation. They point out that the reason for its failure is that the variational principle is for the action rather than for the growth rate. An important property of variational methods in general is that the trial function does not have to be particularly accurate to give a reasonable estimate of the extremum. It would therefore seem that such trial functions cannot really be relied upon to give an accurate dispersion relation.

Before dismissing this method entirely, we should note that Anderson *et al.* (1979) used it to obtain a very reasonable approximation to the growth rate for the cubic nonlinear Schrödinger (NLS) equation. This is probably explained by the true NLS growth rate curve having approximately the form

$$\gamma_1^{\mathrm{NLS}} k \sqrt{1 - \left(\frac{k}{k_c^{\mathrm{NLS}}}\right)^2}. \tag{2.94}$$

This sort of dependence is generated naturally by the variation of action method applied to this type of problem as can be seen by comparing (2.94) with (2.93). We also note that for the linearized cubic NLS equation, we have shown† that the second order contribution to the growth rate vanishes. This offers a further explanation for the suitability of the method for that equation.

†For the cubic NLS equation, linearization about the soliton solution generates two coupled o.d.e.'s. A small-k expansion allowing for the fact that the odd and even parts of the eigenfunctions have different growth rates was used to determine γ^{NLS} to second order.

2.7 Discussion

We have studied the analytic form of the growth rate curve, $\gamma(k^2)$ for plane solitons in the neighbourhood of its two zeros $k^2 = 0$ and $k^2 = 5$. The results have been used to obtain a two-point Padé approximant to the growth rate which agrees with the numerical calculations to within 0.4%.

The important step in the method of analysis given in this chapter is that the perturbation theory is made to give the correct asymptotic form of the solution as $x \to \pm\infty$. As discussed in §2.2, this entails a regrouping of what we called the algebraic secularities. It is not sufficient just to regroup the terms of the form $x^n\varphi_0$ which we referred to as ghost secular terms.

There appear to be two other strategies that have been used to estimate the form of the growth rate curve analytically. The standard variational method which was used in §2.6 gives the correct value of $d\gamma/dk$ at $k = 0$ and position of the second zero once we vary sufficient parameters in our trial function. However, for all the trial functions we tested, the expression for γ so derived does not have the linear dependence on k at the second zero seen in both (2.79) (on factorizing $1 - k^2/5$) and the numerical results shown in Figure 2.6. Furthermore, the maximum of the curve is approximately 40% too large. A serious disadvantage of this approach, which is overcome in the other strategy, is that there is no way to gauge the accuracy of the results. Conclusions about stability drawn from its application alone can therefore only be tentative.

The other, more sophisticated strategy (Laedke & Spatschek 1982) is to use complementary variational principles to produce an upper and lower bound for the growth rate curve. Using a trial function with 20 variables they constrain γ to lie within a band which is reasonably narrow for k^2 up to around 3.5, as illustrated in Figure 2.1. A further disadvantage of both variational approaches is that they cannot be used to find the growth rate of oblique perturbations (see p.275 of Infeld & Rowlands 1990).

Our method of finding the gradients of γ at its zeros and then using a Padé approximant to interpolate gives a substantial improvement on the approaches mentioned above. We obtain a $\gamma(k)$ lying within the bounds generated by the Laedke & Spatschek variational calculations without having to resort to the extensive numerical computation that their method requires.

Chapter 3

Application of the new method

Before continuing our investigation of the ZK equation, we shall look at where the new method presented in the previous chapter can be applied. The reason for extending the multiple-scale perturbative expansion technique was the appearance of so-called algebraic secularities. Such terms can only arise if the linearized equations have both exponentially decaying *and* constant (i.e. 'e^0') asymptotic solutions to zeroth order in a small parameter. However, a series of algebraically secular terms will not necessarily arise in this case. In fact, on looking for suitable candidates for the new method, we found that a number of equations have a solution to the linearized equation that is relatively simple, containing only a finite number of terms. We then obtain the growth rate for all k automatically. This is discussed in §3.1.

We only need to carry out our regrouping procedure if there is an infinite series of algebraic secularities. Based on our experience in §3.1 and the fact that in principle the growth rate for all k can be determined exactly for integrable equations, it seems quite likely that such equations have only a finite number of terms in the solution to the linearized equation. Hence we postulate that the new method is most appropriate for investigating solitons of non-integrable equations whose linearized equation has at least one asymptotic solution that is a slowly decaying exponential. Since we have to carry out the regrouping of algebraic secularities explicitly, a further criterion is that the linearized equation must be solvable in terms of known functions. This rules out a number of otherwise promising candidates such as the Infeld-Rowlands equation (1991) which has been shown not to have the Painlevé property and therefore appears to be non-integrable (Faucher & Winternitz 1993). Unfortunately its soliton solution can only be obtained by series solution, and the linear operator is third order which makes finding its inverse in general impossible.

We managed to apply the new method to optical solitons in fibre optic cable couplers. As we shall discuss in §3.2, this system admits a number of branches of soliton solutions. Two of these, referred to as types 'A' and 'B', cannot be obtained explicitly, but since they join to branches which can, we are able to use perturbation theory in the neighbourhood of the bifurcation points. The 'A'-branch, which we deal with in §3.3, requires only ordinary perturbation theory applied about either end. The whole branch on the bifurcation diagram can then be reasonably accurately described by a Padé approximant. In §3.4 we show that the solution of the 'B'-branch at one of its ends requires a regrouping of algebraic secularities. This time, in contrast to the analysis in the previous chapter, a multiple-scale expansion performs the regrouping automatically. However the new method is used to find the correct

ordering in a situation where the usual approach of applying a consistency condition is no longer valid. The other end of the 'B'-branch presents more of a problem. Because of the nature of the solution found numerically, we argue in §3.5 that a conventional small-k expansion cannot be applied. We instead present our numerically derived results and offer a semi-quantitative explanation of their form.

3.1 Equations with a fully determined growth rate curve

It was mentioned in the introductory chapter that the two-dimensional KP$^+$ equation,

$$(n_t + nn_x + n_{xxx})_x - n_{yy} = 0, \tag{3.1}$$

is integrable. The growth rate for the linearized equation has already been obtained exactly for all k by Zakharov (1975) using inverse scattering methods. However, it turns out that we can obtain the same result in a simpler way once a multiple-scale small-k expansion has hinted at the full solution to the linearized equation.

Equation (3.1) again has the KdV soliton solution so we transform it to a reduced variable, moving-frame system in the same way as before to obtain:

$$(n_t + (n-4)n_x + n_{xxx})_x - n_{yy} = 0 \tag{3.2}$$

with the plane soliton solution $n_0 = 12\,\mathrm{sech}^2 x$. Linearization of (3.2) using $n = n_0 + \varepsilon\Phi(x)e^{iky}e^{\gamma t}$ results in:

$$\frac{d^2}{dx^2}L_o\Phi = -\gamma\frac{d\Phi}{dx} - k^2\Phi. \tag{3.3}$$

For large x, this can be approximated by

$$\frac{d^4\Phi}{dx^4} - 4\frac{d^2\Phi}{dx^2} + \gamma\frac{d\Phi}{dx} + k^2\Phi = 0,$$

which has the four solutions:

$$e^{2x-\gamma x/8}, \quad e^{-2x-\gamma x/8}, \quad \text{and} \quad e^{\left(\gamma \pm \sqrt{\gamma^2+16k^2}\right)x/8},$$

to first order in k. The two slowly decaying asymptotic forms are exponentials of opposite sign, and so we can no longer cavalierly integrate from ∞ to x as in §2.2, but must choose the constants of integration by trial and error.

Using a multiple-scale small-k expansion we expand Φ and γ using (2.32) and (2.7). Since the linearized KP$^+$ equation (integrated once) differs from the linearized ZK equation, (2.4), only at second order in k, the zeroth and first order results in both cases are the same (see equations (2.35), (2.37), and (2.38)). However, the second order equation is

$$\begin{aligned}\partial_x^2 L\Phi_2 \;=\; & -2\Phi_{0,xxx2} - 5\Phi_{0,xx11} - 4\Phi_{1,xxx1} - 2(n_0-4)\Phi_{1,x1} - 2n_{0,x}\Phi_{1,1} \\ & -\gamma_2\Phi_{0,x} - \gamma_1\Phi_{0,1} - \gamma_1\Phi_{1,x} - \Phi_0.\end{aligned} \tag{3.4}$$

As has been done implicitly in previous orders, we set the constant of the first integration to zero, as this would immediately give rise to an exponentially secular term. If at a later stage it appears that we have not obtained a bounded solution overall, we can always return to the

present order and reintroduce the constant. In this order, we do retain the second constant of integration. After (3.4) has been integrated twice, we apply L^{-1} (given by (2.31) but with indefinite integrals) to obtain

$$\Phi_2 = \frac{1}{128}\left(\frac{16}{3}-\gamma_1^2\right)h_0\sinh x\cosh x - \frac{C_2}{4} - \frac{\gamma_1^2}{128}h_0\tanh x + \left(\frac{3C_2}{4}+\frac{\gamma_2}{8}h_0\right)\operatorname{sech}^2 x - \left(\frac{3C_2}{4}+\frac{\gamma_2}{8}h_0+h_{0,2}\right)x\varphi_0. \tag{3.5}$$

To remove the exponential secularities at second order, we now have to make

$$\gamma_1^2 = \frac{16}{3}. \tag{3.6}$$

On examining (3.5) it can be seen that the $\tanh x$ term and therefore the whole expression does not have the correct underlying asymptotic form. This can be remedied by choosing C_2 so that Φ_2 contains the term $-\frac{1}{8}h_0(\tanh x+\sigma)$ in which the sign, $\sigma = \pm 1$, is yet to be determined - either sign gives an expression matching one of the asymptotic forms to zeroth order in k. With positive γ_1, $h_0 = h_0^{(1)}e^{-\gamma_1 x_1/8}$ is a negative exponential. This means that only when $\sigma = +1$ is Φ_2 bounded. Although, based on our experience gained from the linearized ZK equation, we can tolerate the unboundedness of Φ_m caused by algebraic secularities if they are part of a series, it seems more sensible to choose the bounded solution since it does not violate the asymptotic conditions and at this stage we do not know whether a series of algebraic secularities will arise at higher order. We are therefore left with

$$\Phi_2 = -\frac{h_0}{24}(\tanh x+1)+\frac{1}{8}(1+\gamma_2)h_0\operatorname{sech}^2 x \tag{3.7}$$

after removing the ghost secularities in the usual way.

On solving the third order equation in a similar manner, we find that Φ_3 is given by an expression of a similar form to the right hand side of (3.5). The $\sinh x\cosh x$ terms are removed by choosing

$$\gamma_2 = -\frac{2}{3}, \tag{3.8}$$

and using the same rationale as for the previous order, the constant of integration is chosen so that Φ_3 is bounded:

$$\Phi_3 = -\frac{\gamma_1}{192}h_0(\tanh x+1)+\left(\frac{\gamma_1}{96}+\frac{\gamma_3}{8}\right)h_0\operatorname{sech}^2 x\,. \tag{3.9}$$

We see that Φ_3 is very similar to Φ_2. This suggests that the higher order contributions to Φ will also be of the same form.

The expansion for Φ so far can be written as

$$\Phi = e^{-\alpha x}\{\varphi_0 + b\operatorname{sech}^2 x + c(\tanh x+1)\} \tag{3.10}$$

for some α, b, and c. If we substitute this into (3.3) we find that the linearized KP$^+$ equation has the exact solution

$$\Phi = e^{-\alpha x}\left\{\operatorname{sech}^2 x\tanh x + \alpha\operatorname{sech}^2 x - \frac{\alpha^2}{2}(\tanh x+1)\right\} \tag{3.11}$$

when

$$\gamma = 4\alpha(\alpha-1)(\alpha-2) \tag{3.12}$$

and

$$3\alpha^2(\alpha-2)^2 = k^2. \tag{3.13}$$

On inspecting (3.11) we see that for bounded solutions, Re α must lie between 0 and 2, which leaves us with two possible solutions for α. The one which gives a positive growth rate,

$$\gamma = \frac{4}{\sqrt{3}} k \sqrt{1 - k/\sqrt{3}}\,, \tag{3.14}$$

is

$$\alpha = 1 - \sqrt{1 - k/\sqrt{3}}\,. \tag{3.15}$$

Expanding (3.14) and (3.15) for small k, we find agreement with the results from the perturbation analysis. Our expression for γ, allowing for differences in scaling, is the same as that obtained by Zakharov (1975).

Kuznetsov *et al.* (1984) showed that the growth rate may be determined for all k for any equation which can be written using the Zakharov-Shabat formalism (and is therefore integrable). They worked through the KP equations as an example. However, our method of using a multiple-scale small-k expansion to suggest the form of the solution to the linearized equation is much easier, provided that the solution itself turns out to be simple enough.

A similar scenario arose when we attempted the same procedure on a two-dimensional Boussinesq equation (Boussinesq 1871; Makhankov 1978):

$$q_{tt} - q_{xx} - q_{yy} - (q^2)_{xx} - q_{xxxx} = 0. \tag{3.16}$$

This has plane soliton solutions of the form

$$q_0 = \frac{3}{2}\left(v^2 - 1\right) \operatorname{sech}^2 \frac{\sqrt{v^2-1}}{2}(x - vt) \qquad |v| > 1,$$

where v is the soliton velocity and can be of either sign. Transforming (3.16) to a coordinate system moving with the soliton in which the soliton width has been scaled out, and then linearizing, we obtain

$$\frac{d^2}{dx^2} L_o \Phi = -\frac{16v}{(v^2-1)^{\frac{1}{2}}} \gamma \frac{d\Phi}{dx} + \frac{16}{(v^2-1)^2}(\gamma^2 + k^2)\Phi. \tag{3.17}$$

Due to the similarity between (3.17) and (3.3), we tried substituting (3.10) into the linearized equation. We again find an exact solution to (3.17) of the form (3.11) but this time the relationships between γ, α, and k are rather more complicated:

$$\gamma = \frac{(v^2-1)^{\frac{1}{2}}}{4v}\alpha(\alpha-1)(\alpha-2)$$

$$\alpha^2(\alpha-2)^2\left(3v^2 + (\alpha-1)^2(v^2-1)\right) = -\frac{16v^2}{(v^2-1)^{\frac{1}{2}}}k^2.$$

In this case we see that γ and α will be complex. As far as we are aware, the growth rate for this generalization of the Boussinesq equation has not been obtained previously.

3.2 Solitons in optical fibre couplers

A very important application of solitons is in the field of nonlinear optics. Hasegawa & Tappert (1973) showed that the envelope of a light wave propagating down a fibre obeys the cubic nonlinear Schrödinger equation:

$$i\frac{\partial E}{\partial \xi} + \frac{1}{2}\frac{\partial^2 E}{\partial \tau^2} + |E|^2 E = 0$$

where the normalized quantities E, ξ, and τ are proportional to the envelope function of the electric field, the distance along the fibre, and the time, respectively, and the coordinate system is moving with the group velocity. The nonlinearity is a result of the Kerr effect which is the distortion of the electron orbitals due to an applied electric field. It produces a nonlinear refractive index, $n = n_0 + n_2|E|^2$, and this results in the wavenumber having a nonlinear dependence on the signal amplitude.

If two fibres are placed next to each other, optical signals propagating along them will be coupled via the evanescent fields. Trillo *et al.* (1988) have shown that this form of nonlinear dual-core directional coupler can exhibit soliton switching and therefore has potential applications in optical processing. They show that the system may be described in terms of two linearly coupled NLS equations:

$$iU_\xi + \frac{1}{2}U_{\tau\tau} + |U|^2 U + KV = 0, \qquad iV_\xi + \frac{1}{2}V_{\tau\tau} + |V|^2 V + KU = 0, \tag{3.18}$$

where U, V are the electric field envelopes in the two fibres and K is the normalized coupling coefficient. Insisting on stationary pulse-like solutions by making

$$U(\xi,\tau) = u(\tau,q)e^{iq\xi}, \qquad V(\xi,\tau) = v(\tau,q)e^{iq\xi},$$

where q is a soliton parameter, Akhmediev & Ankiewicz (1993) obtained the reduced equations for soliton states:

$$\frac{1}{2}\ddot{f} - f + f^3 + \kappa g = 0, \qquad \frac{1}{2}\ddot{g} - g + g^3 + \kappa f = 0 \tag{3.19}$$

where $f \equiv u/\sqrt{q}$, $g \equiv v/\sqrt{q}$, $\kappa \equiv K/q$, and the dot denotes the derivative with respect to the reduced variable $t \equiv \tau\sqrt{q}$. It is sometimes helpful to rewrite equations (3.19) as

$$\ddot{x} - \alpha^2 x + x^3 + 3xy^2 = 0, \qquad \ddot{y} - \mu^2\alpha^2 y + y^3 + 3yx^2 = 0, \tag{3.20}$$

where

$$x = \frac{1}{\sqrt{2}}(f+g), \qquad y = \frac{1}{\sqrt{2}}(f-g),$$

and

$$\alpha^2 = 2(1-\kappa), \qquad \mu^2 = \frac{1+\kappa}{1-\kappa}. \tag{3.21}$$

They pointed out that equations (3.20) describe the motion of a particle in a two-dimensional potential well. The Hamiltonian for this motion is

$$\mathcal{H} = \frac{1}{2}\dot{x}^2 + \frac{1}{2}\dot{y}^2 - (x^2+y^2) + \kappa(x^2-y^2) + \frac{1}{2}(x^2+y^2)^2 - \frac{1}{4}(x^2-y^2)^2 \tag{3.22}$$

which may be re-expressed as

$$\mathcal{H} = \frac{1}{2}(\dot{f}^2 + \dot{g}^2) + \frac{1}{2}(f^4 + g^4) - (f^2 + g^2) + 2\kappa fg. \tag{3.23}$$

From (3.19) it is apparent that both symmetric (f=g) and antisymmetric (f=-g) solutions exist. They take the forms

$$(x, y) = (\sqrt{2\alpha}\,\mathrm{sech}\ \alpha t, 0), \qquad 0 < \kappa < 1, \tag{3.24}$$

and

$$(x, y) = (0, \sqrt{2\alpha\mu}\,\mathrm{sech}\ \alpha\mu t), \qquad \kappa > 0, \tag{3.25}$$

respectively. Akhmediev & Ankiewicz found that there are also two branches of asymmetric states. They appear as a result of bifurcations from the symmetric states at $\kappa = 0.6$ and from the antisymmetric states at $\kappa = 1$. The two branches are referred to as 'A' and 'B' respectively. All the asymmetric states can be conveniently parameterized by

$$\phi_0 \equiv \tan^{-1}\frac{y_0}{x_0}, \tag{3.26}$$

where $x_0 \equiv x(0)$ and $y_0 \equiv y(0)$.

We repeated their numerical determination of the asymmetric states before attempting to describe the states analytically. Since the solitons are even functions of t, the first derivatives of f and g are zero at $t = 0$. We therefore integrate equations (3.19) from $t = 0$. Once $f(0)$ is chosen, $g(0)$ is determined using (3.23) with $\mathcal{H} = 0$. In a similar way to the numerical method of §2.4, for fixed κ, we find the value $f(0)$ for which the solution remains close to zero for the largest value of t.

As a check on the accuracy of our solutions for f and g, we calculated $\mathcal{H}$ for all t. For optimum settings of the tolerances, it was never more than 2×10^{-14}. The bifurcation diagram we derived numerically is plotted in Fig. 3.1 and is in agreement with that obtained by Akhmediev & Ankiewicz.

The asymmetric states are of particular interest because for some values of ϕ_0 their shape deviates significantly from the sech-form usually associated with non-topological solitons. This is important, as many calculations had been done with the assumption that the two solitons had sech-function shapes.

3.3 Analysis of the 'A'-type asymmetric states

As can be seen from the figure, the two branches of asymmetric states meet at $\kappa = 0$ which corresponds to the decoupled states. One such state is a single soliton $(f, g) = (\sqrt{2}\,\mathrm{sech}\ \sqrt{2}t, 0)$. It turns out that if we perturb about this state, we obtain the 'A'-branch.

After introducing the new variables $(F, G) = \frac{1}{\sqrt{2}}(f, g)$ and $T = \sqrt{2}t$, from (3.19) we obtain:

$$F'' - F + 2F^3 = -\kappa G \quad \text{and} \quad G'' - G + 2G^3 = -\kappa F, \tag{3.27}$$

where the prime denotes differentiation with respect to T. Using κ as our small parameter, we carry out an ordinary small-κ perturbation analysis and expand the envelope functions as

$$F = F_0 + \kappa F_1 + \kappa^2 F_2 + \ldots; \qquad G = \kappa G_1 + \kappa^2 G_2 + \ldots.$$

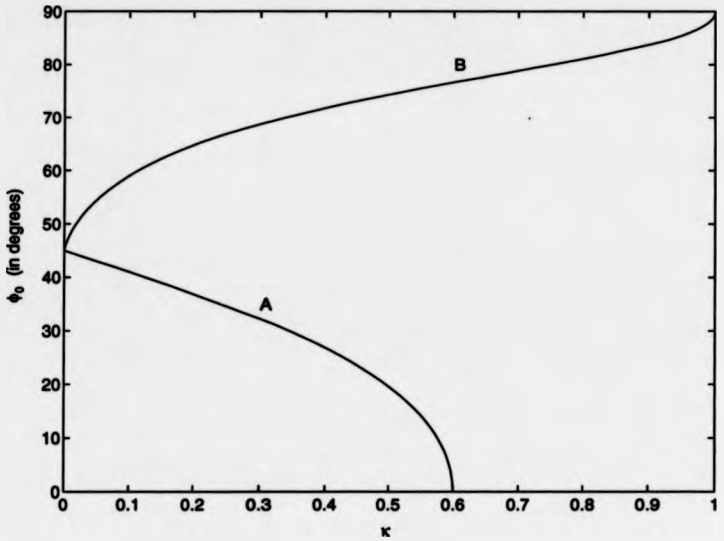

Figure 3.1: Soliton bifurcation diagram

The zeroth order solution is the state we are perturbing about, namely $F_0 = \operatorname{sech} T$. To first order we find

$$L_o(1)F_1 = 0 \tag{3.28}$$

and

$$G_1'' - G_1 = -F_0, \tag{3.29}$$

where we have denoted $d^2/dT^2 + 6\operatorname{sech}^2 T - p$ by $L_o(p)$. The solution to (3.28) is $F_1 = AF_0'$, but F must be even and therefore $A = 0$. Using (2.12) with $u_0 = \cosh T$ we find that the only solution to (3.29) which decays to zero at infinity is

$$G_1 = \cosh T \ln(2\cosh T) - T\sinh T. \tag{3.30}$$

We now have enough information to determine the small-κ behaviour of ϕ_0 to first order for the 'A'-type asymmetric states. From our definition of ϕ_0 and our expression for G_1, we have:

$$\tan\phi_0 = \frac{y(0)}{x(0)} = \frac{F(0) - G(0)}{F(0) + G(0)} \simeq \frac{1 - \kappa\ln 2}{1 + \kappa\ln 2} \approx 1 - 2\kappa\ln 2 \tag{3.31}$$

from which

$$\phi_0 \simeq \frac{\pi}{4} - \kappa\ln 2. \tag{3.32}$$

The gradient, $d\phi_0/d\kappa$, at $\kappa = 0$ agrees with that obtained numerically for the 'A'-type asymmetric states.

At the other end of the 'A'-branch is one of the symmetric soliton states, $y = 0$. To perturb about such a state, it is most convenient to use (3.20) rewritten using the reduced

variables $(X,Y) = (x,y)/(\sqrt{2}\alpha)$ and $T = \alpha t$:

$$\frac{d^2X}{dT^2} - X + 2X^3 + 6XY^2 = 0, \qquad \frac{d^2Y}{dT^2} - \mu^2 Y + 2Y^3 + 6YX^2 = 0. \tag{3.33}$$

Introducing an expansion parameter $\epsilon^2 = \mu_0^2 - \mu^2$ (a consistency condition at second order cannot be satisfied if $\epsilon = \mu_0^2 - \mu^2$ is used), we write

$$X = X_0 + \epsilon X_1 + \ldots ; \qquad Y = \epsilon Y_1 + \ldots .$$

The zeroth order equation derived from (3.33) is

$$X_0'' - X_0 + 2X_0^3 = 0 \tag{3.34}$$

and has the solution $X_0 = \operatorname{sech} T$. The first order equations are

$$X_1'' + 6X_0^2 X_1 - X_1 \equiv L_o(1)X_1 = 0 \tag{3.35}$$

and

$$Y_1'' + 6X_0^2 Y_1 - \mu_0^2 Y_1 \equiv L_o(\mu_0^2)Y_1 = 0. \tag{3.36}$$

The solution to (3.35) is $X_1 = A \operatorname{sech} T \tanh T$. As with the small-$\kappa$ analysis, since X must be an even function of T, we have to make $A = 0$.

$L_o(p)$ can be transformed into the associated Legendre operator with $N = 2$ and eigenvalue p (see equation (2.5)). From this it can be deduced that (3.36) has exactly two solutions which decay at infinity. The non-trivial solution is $Y_1 = B_1 \operatorname{sech}^2 T$ with $\mu_0^2 = 4$ (which corresponds to $\kappa = 3/5$). This is the result obtained by Akhmediev & Ankiewicz.

To describe the asymmetric states, however, we need to proceed to higher order. The second order equations are

$$L_o(1)X_2 = -6X_0Y_1^2 \tag{3.37}$$

and

$$L_o(4)Y_2 = 0. \tag{3.38}$$

The solution of (3.37) is

$$X_2 = B_1^2(\operatorname{sech}^3 T - 2\operatorname{sech} T) \tag{3.39}$$

and from (3.38), Y_2=0. To third order we have

$$L_o(1)X_3 = 0 \tag{3.40}$$

and

$$L_o(4)Y_3 = Y_1 - 2Y_1^3 - 12Y_1X_0X_2. \tag{3.41}$$

To determine B_j we can use the consistency condition

$$\langle Y_1 L_o(4) Y_{j+2} \rangle = 0 \quad \text{where} \quad \langle\, \rangle \equiv \int_{-\infty}^{\infty} dx \tag{3.42}$$

derived from the self-adjoint property of $L_o(4)$. Applying (3.42) to (3.41) gives

$$B_1(5 - 48B_1^2) = 0. \tag{3.43}$$

from which we obtain $B_1 = \sqrt{5/48}$.

The expansion for X and Y so far is

$$X = \text{sech } T + \epsilon^2 B_1^2(\text{sech}^3 T - 2\,\text{sech } T) + \ldots \tag{3.44}$$

$$Y = \epsilon B_1 \,\text{sech}^2 T + \ldots . \tag{3.45}$$

To compare these results with the numerical results of Fig 3.1 we must determine ϕ_0:

$$\tan\phi_0 = \frac{y(0)}{x(0)} = \frac{Y(0)}{X(0)} \simeq \frac{\epsilon B_1}{1-\epsilon^2 B_1^2}. \tag{3.46}$$

Expressing $\epsilon(=\sqrt{4-\mu^2})$ in terms of κ using (3.21) we then obtain

$$\phi_0 \approx \tan\phi_0 \approx \sqrt{\frac{25}{32}\left(1-\frac{5}{3}\kappa\right)} \tag{3.47}$$

for κ near 3/5.

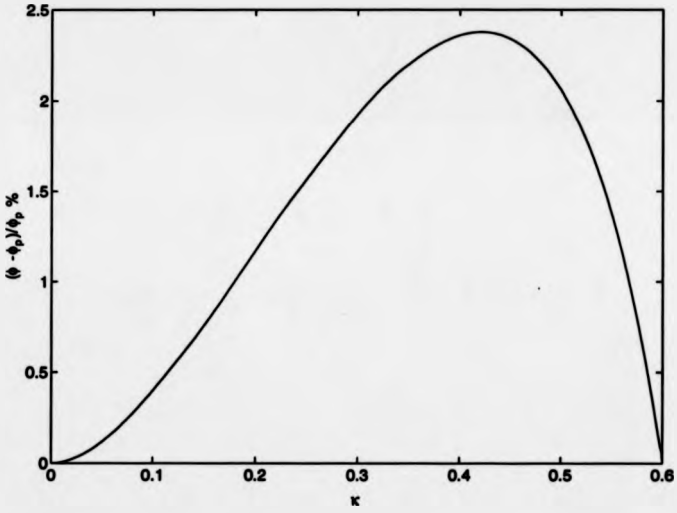

Figure 3.2: Percentage error in Padé approximant to 'A'-type states. $\phi_p \equiv \sqrt{\tan^{-1} P}$.

As in §2.4 we can combine the results (3.31) and (3.47) using a two-point Padé approximant. Given the form of the equations, it seemed most natural to obtain an approximant, P, for $\tan^2\phi_0$. We therefore write

$$P = \left(1-\frac{5}{3}\kappa\right)\left(\frac{1+a_1\kappa}{1+b_1\kappa}\right). \tag{3.48}$$

so that P automatically has a zero at $\kappa = 5/3$ and the correct value at κ=0. Matching the expansion to first order of the Padé approximant with that of $\tan^2\phi_0$ for small κ gives

$$a_1 - b_1 - \frac{5}{3} = -4\ln 2\,,$$

and to ensure that P has the correct gradient around its zero we must have

$$\frac{1+3a_1/5}{1+3b_1/5} = \frac{25}{32}.$$

From these two relations we obtain the Padé coefficients $a_1 \simeq 2.28305$ and $b_1 \simeq 3.38898$. Fig. 3.2 shows that the error in ϕ_0 obtained using (3.48) is less than 2.5%.

3.4 Analysis of the 'B'-type asymmetric states about $\kappa = 1$

In the case of the antisymmetric state we have $f = -g$ and so $x = 0$. We now rewrite (3.20) in terms of the reduced variables $(X, Y) = (x, y)/(\sqrt{2}\alpha\mu)$, $T = \alpha\mu t$:

$$\frac{d^2X}{dT^2} - \nu X + 2X^3 + 6XY^2 = 0, \tag{3.49}$$

$$\frac{d^2Y}{dT^2} - Y + 2Y^3 + 6YX^2 = 0, \tag{3.50}$$

in which we have put $\nu = 1/\mu^2$. Notice that these equations are the same as (3.33) but with X and Y exchanged and μ^2 replaced by ν. Demanding a solution with κ non-zero and X_1 vanishing at infinity, would similarly result in $\nu_0 = 4$ which would imply a negative κ. The numerical results suggest that we should insist that $\nu_0 = 0$ (i.e. $\kappa = 1$). Hence we use ν as our small parameter and write

$$X = \nu X_1 + \nu^2 X_2 + \ldots \tag{3.51}$$

$$Y = Y_0 + \nu Y_1 + \nu^2 Y_2 + \ldots . \tag{3.52}$$

To zeroth order in ν, we have $Y_0 = \operatorname{sech} T$. To first order we obtain

$$L_o(0)X_1 = 0 \tag{3.53}$$

which has the general solution

$$X_1 = A_1\left(\frac{3}{2}\operatorname{sech}^2 T - 1\right) + H_1\left(\frac{3}{2}T\operatorname{sech}^2 T - T + \frac{3}{2}\tanh T\right). \tag{3.54}$$

Although this does not blow up for large T (with H_1 set to zero), it still does not vanish at infinity. It is therefore an algebraic secularity, and based on our experience of the linearized ZK equation we would hope that it can be regrouped with other such terms at higher order to give an expression which does tend to zero overall for large T.

We therefore apply a multiple-scale analysis so that A_1 is now a function of the scaled variables T_1, etc., where $T_m \equiv \nu^m T$. The quantities X_i and Y_i are now functions of T_m as well as of T and so we must expand the derivatives in (3.49) and (3.50) using

$$\frac{d}{dT} \equiv \frac{\partial}{\partial T} + \nu\frac{\partial}{\partial T_1} + \nu^2\frac{\partial}{\partial T_2} + \ldots .$$

Apart from A_1 and H_1 no longer being constants, the results obtained so far for the ordinary analysis are still valid. The solution to the other first order equation,

$$L(1)Y_1 = 0, \tag{3.55}$$

where we now have $\mathrm{L}(p) \equiv \partial_T^2 + 6\,\mathrm{sech}^2 T - p$, is

$$Y_1 = B_1 \,\mathrm{sech}\; T \tanh T + J_1 \left(\frac{1}{2}\cosh T - \frac{3}{2}\,\mathrm{sech}\, T + \frac{3}{2} T \,\mathrm{sech}\, T \tanh T\right). \tag{3.56}$$

Evidently we must make $J_1 = 0$. All that we can say about $A_1 = A_1(T_1, T_2, ...)$, $H_1 = H_1(T_1, T_2, ...)$ and $B_1 = B_1(T_1, T_2, ...)$ so far is that their parities must be such as to ensure that X_1 and Y_1 are even.

The second order equations are

$$L(0)X_2 = X_1 - 2X_{1,T1} - 12X_1 Y_0 Y_1 \tag{3.57}$$

and

$$L(1)Y_2 = -2Y_{1,T1} - 6Y_0 Y_1^2 - 6X_1^2 Y_0. \tag{3.58}$$

As was the case for the $k^2 = 5$ expansion in §2.1, we cannot use a consistency condition of the type used in the previous section because X_1 is not zero at infinity. To determine whether we have chosen the correct ordering we must continue in the hope of finding out how the algebraic secularities regroup. Applying $L(0)^{-1}$ to (3.57) gives an expression that has the leading terms

$$H_1 \frac{T^2}{6}\left\{\left(\frac{3}{2}\,\mathrm{sech}^2 T - 1\right) T + \frac{3}{2}\tanh T\right\} - A_1 \frac{T^2}{2}\left(\frac{3}{2}\,\mathrm{sech}^2 T - 1\right)$$

after we have put $H_{1,1} = A_1$. Notice that the most divergent term in X_2 is $-\frac{1}{6}H_1 T^3$. This, in conjunction with the leading term of X_1, is hinting at an exponential, but to be more certain, we need to find X_3. After determining Y_2, we obtain an expression for X_3 whose most divergent term is $-\frac{1}{120}H_1 T^5$. Now consider the sum of the most divergent terms in our expansion of X so far:

$$-H_1\left(\nu T + \frac{1}{6}\nu^2 T^3 + \frac{1}{120}\nu^3 T^5\right).$$

This expansion is consistent with X containing the term $-\sqrt{\nu}H_1 \sinh\sqrt{\nu}T$. This will grow exponentially with T since we cannot have negative ν, and H_1 is an exponential function of $m\nu T$ (where m is an integer) which will always be overwhelmed by $\sinh\sqrt{\nu}T$ for small enough ν. If we start by insisting that $H_1 \equiv 0$, we instead find that X appears to contain the term $-\nu A_1 \cosh\sqrt{\nu}T$. This unphysical behaviour in either case shows that we have chosen the wrong ordering.

For our new ordering we make $\nu = 1/\mu$. We leave the expansions for X and Y unchanged but (3.49) is replaced by

$$\frac{d^2 X}{dT^2} - \nu^2 X + 2X^3 + 6XY^2 = 0. \tag{3.59}$$

With the new ordering we have the same first order results. However, at second order we find

$$\begin{aligned} X_2 \;=\; & \frac{3}{2}A_{1,1}\tanh T + 3A_1 B_1 \,\mathrm{sech}^2 T \tanh T + 3B_1 H_1\left(\mathrm{sech}^2 T - 1 + T\,\mathrm{sech}^2 T \tanh T\right) \\ & + H_{1,1}\left\{(1-T^2)\left(\frac{3}{2}\,\mathrm{sech}^2 T - 1\right) - \frac{3}{2}T\tanh T\right\}. \end{aligned} \tag{3.60}$$

Since the $H_{1,1}$ term cannot be removed by making it a function of A_1, B_1, or H_1, we put $H_1 = 0$. Our equation for Y_2 is then

$$\begin{aligned} Y_2 &= A_1^2\left(\frac{9}{4}\operatorname{sech}^3 T - 3\operatorname{sech} T + 3T\operatorname{sech} T\tanh T\right) \\ &\quad + B_1^2\operatorname{sech} T - B_1^2\operatorname{sech}^3 T - B_{1,1}T\operatorname{sech} T\tanh T. \end{aligned} \tag{3.61}$$

Given the form of Y_1, it can be seen that the $T\operatorname{sech} T\tanh T$ terms in Y_2 are ghost secularities. Their removal gives a relation between B_1 and A_1:

$$B_{1,1} = 3A_1^2. \tag{3.62}$$

At third order we obtain

$$\begin{aligned} X_3 &= \left(A_{1,11} - A_1 + 2A_1^3\right)\left\{\left(\frac{3}{4} - \frac{T^2}{2}\right)\left(\frac{3}{2}\operatorname{sech}^2 T - 1\right) - \frac{3}{2}T\tanh T\right\} \\ &\quad - \frac{A_1}{2} - A_{1,1}B_1 + 2A_1B_1^2 - \frac{9}{5}A_1^3\left(\frac{3}{2}\operatorname{sech}^2 T - 1\right) \\ &\quad - \frac{63}{20}A_1^3\operatorname{sech}^2 T + \left(\frac{27}{8}A_1^3 - \frac{9}{2}A_1B_1^2\right)\operatorname{sech}^4 T + A_{1,2}\tanh T. \end{aligned} \tag{3.63}$$

It is then most natural to choose

$$A_{1,11} - A_1 + 2A_1^3 = 0 \tag{3.64}$$

as this will remove the most divergent terms. The only bounded solutions to (3.64) are

$$A_1 = \pm\operatorname{sech} T_1. \tag{3.65}$$

Notice that this has no dependence on the higher order scaled variables and so, for instance, the last term in (3.63) vanishes. From (3.62) and (3.65) we see that $B_1 = 3\tanh T_1$.

If we look at the ordinary perturbation analysis again and expand up to fifth order, ignoring the mounting algebraic secularities, we find that the leading terms in each order in the expansion of X sum to give

$$-\nu A\left(1 - (2A^2 - 1)\frac{1}{2}\nu^2T^2 + (2A^2 - 1)\frac{6A^2 - 1}{24}\nu^4T^4\right)$$

which is consistent with the expansion of $-\nu A\operatorname{sech}\nu T$ if $A = \pm 1$. The positive solution in (3.65) is the one we have been taking throughout the previous analyses.

Using the results we have obtained so far, we find that

$$\tan\phi_0 \simeq \frac{1 - \frac{3}{4}\nu^2}{\frac{1}{2}\nu} \quad \text{with} \quad \nu = \sqrt{\frac{1-\kappa}{1+\kappa}}. \tag{3.66}$$

This agrees with the numerical results for κ close to unity as can be seen in Fig. 3.3.

In Figure 3.4 we compare the state calculated numerically with that obtained from the expansion to second order. As was the case in the previous chapter, the slow decay for large T is a result of the regrouped algebraic secularities. The agreement between the numerical and analytical results is acceptable, but not particularly good. For some values of T, the functions obtained using only the first order expression are closer to the numerical results. This suggests that the expansion is an asymptotic one.

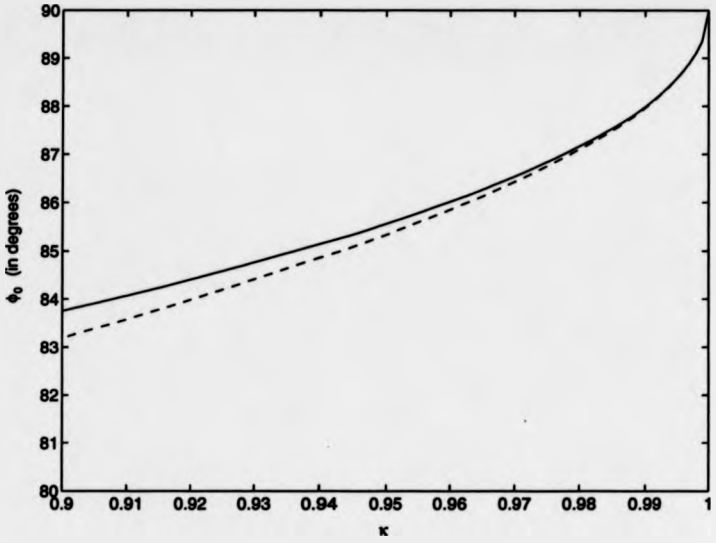

Figure 3.3: Solid line is numerical results; dotted line obtained using equation (3.66).

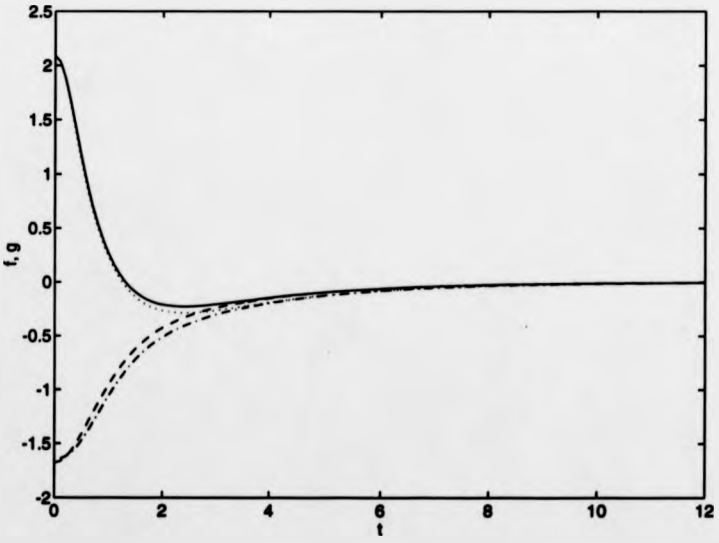

Figure 3.4: 'B'-type asymmetric state at $\kappa = 0.9$. Solid - numerically derived f; dotted - analytically derived f; dashed - numerically derived g; dash-dot - analytically derived g.

3.5 The 'B'-type asymmetric states near $\kappa = 0$

The analysis of the 'B'-type asymmetric states about the decoupled state has proved to be much more difficult. As κ approaches zero, the numerical calculations show that F tends to a $\operatorname{sech} T$ function while G has two sech-like humps (symmetrically placed about the origin) whose separation increases with decreasing κ (see Fig. 3.5). To carry out a small-κ analysis like that in §3.3 we would have to perturb about a state, G_0, that has two sech-like humps at infinity. With the G_m independent of κ, it is difficult to imagine what form they could take to relocate G_0's humps at infinity to some finite, κ-dependent distance from the origin.

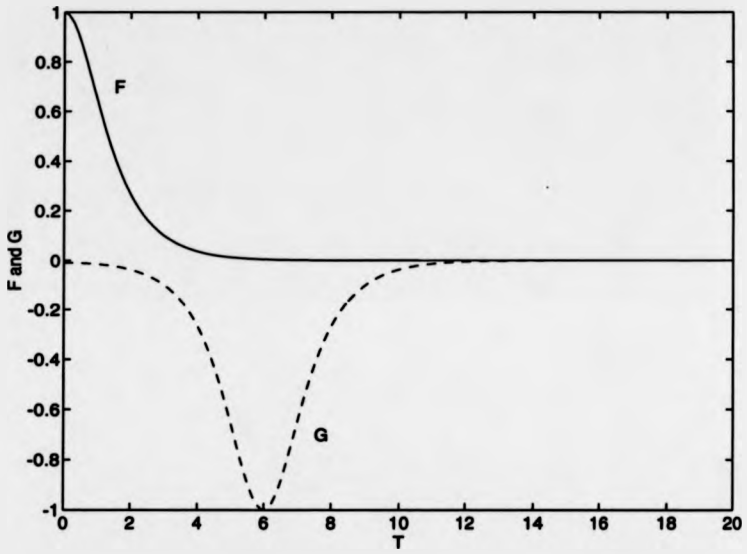

Figure 3.5: 'B'-type asymmetric state at $\kappa = 10^{-3}$.

We can, however, apply a small-κ perturbation analysis locally and then match the solutions in the region in between. Around the origin we can use the same variables and expansions as in the corresponding analysis for the 'A'-type states. As before, we therefore have

$$G_1'' - G_1 = -F_0 \tag{3.67}$$

where $F_0 = \operatorname{sech} T$ and $G_0 = 0$. Since we must have $G(0) < 0$ and the particular integral of (3.67) is positive at $T = 0$, we include some of the homogeneous solution with even parity to give:

$$G = \kappa G_1 + O(\kappa^2) = \kappa \cosh T \ln 2 \cosh T - \kappa T \sinh T - c\kappa \cosh T + O(\kappa^2). \tag{3.68}$$

This extra $\cosh T$ term is permitted since we will not use the expression for large T. From the numerical results it can be seen that for larger T, G is given approximately by

$$G = -\operatorname{sech}(T - \lambda). \tag{3.69}$$

Equating the asymptotic forms of (3.68) and (3.69) for $0 \ll T \ll \lambda$ we have

$$-\frac{c\kappa}{2}e^T = -2e^{T-\lambda}$$

from which

$$\lambda = \ln \frac{4}{c\kappa}. \tag{3.70}$$

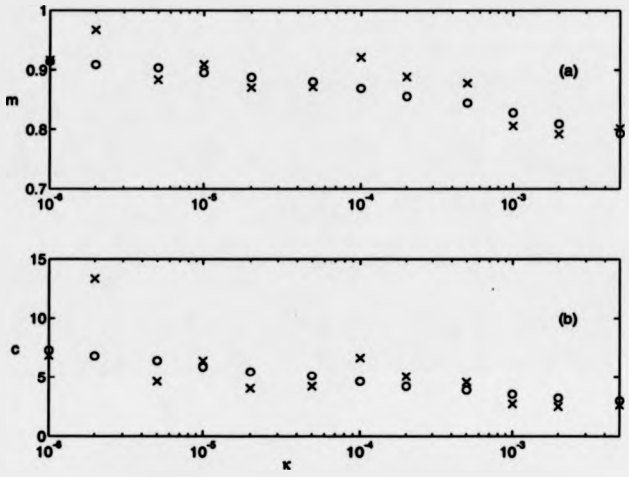

Figure 3.6: Numerical results for 'B'-type asymmetric state near κ=0. Circles refer to a $(\ln\kappa, \ln(\tan\phi_0 - 1))$ plot; crosses to a $(\ln\kappa, -\lambda)$ plot. (a) gradients derived from the plots; (b) values of c derived from the intercepts.

For κ ranging from 0.01 to 5×10^{-7} we numerically determined $\tan\phi_0$ and λ. From (3.68) and (3.70), we would expect a $\ln(\tan\phi_0 - 1)$ versus $\ln\kappa$ plot to have a gradient of one and intercept $\ln(2c - 2\ln 2)$, and a $(\ln\kappa, -\lambda)$ plot to have unit gradient and intercept $\ln(c/4)$. In Figure 3.6(a) we show the gradients, m, determined from the tangent at each data point of such plots as a function of κ. It can be seen that the gradients are not unity, but approach it as κ decreases. The value of c derived from the intercepts is plotted in Figure 3.6(b). As we would hope, it appears to have approximately the same value for both plots, and also does not vary greatly as κ changes by several orders of magnitude. The fluctuations in the $(\ln\kappa, -\lambda)$ plot data are due to numerical errors.

3.6 Discussion

In this chapter we have seen that our new method can be applied to problems differing from that for which it was originally formulated. We found that a small-k multiple-scale perturbation analysis applied to some linearized equations can rapidly lead to their exact solution and hence an exact expression for the growth rate of instabilities. This is simpler than the conventional, Zakharov-Shabat method of determining the growth rate exactly for integrable equations.

The new method was applied to a problem involving two coupled cubic NLS equations bearing unusual soliton states. The method was used to determine the correct ordering of the small quantities involved in the expansion. As a result we could obtain the analytical behaviour of the 'B'-type asymmetrical states near to $\kappa = 1$. We were, however, unable to analytically describe the states at the other end of the branch. The behaviour at both ends of the 'A'-branch could be understood on applying ordinary perturbation theory, and the results were combined using a two-point Padé approximant. This gives a good approximation to the whole branch on the bifurcation diagram.

Chapter 4

Stability of obliquely propagating ZK plane solitons

As was mentioned in the introductory chapter, in addition to the plane solitons discussed in Chapter 2, the ZK equation admits obliquely propagating plane soliton solutions of the form

$$n = 12\eta^2 \operatorname{sech}^2\eta((x - 4\eta^2 t)\cos\alpha + y\sin\alpha) \tag{4.1}$$

where α is the angle between the direction of motion and the magnetic field. In this chapter we investigate the stability of such solitons to small perturbations.

Das & Verheest (1989) have determined the growth rate for long wavelength disturbances using a small-k expansion and ordinary perturbation theory. They show that plane solitons travelling at angles up to some α_0 are unstable, but do not determine the stability of solitons propagating at larger angles. This is because the authors only determine the growth rate to first order and this becomes pure imaginary for $\alpha \geq \alpha_0$. We extend their work by analytically determining the stability of plane solitons to small-k perturbations for all α.

Before addressing the analytical side, we give details of the numerical calculation of the growth rate. These along with the numerically determined dependence of the growth rate on both k and α are presented in §4.1. We carry out a multiple-scale perturbation analysis in §4.2 to determine the growth rate in the limit of small k for $k \ll \cos\alpha$. Das & Verheest obtained the first order growth rate from a consistency condition at second order. A similar condition applied to the third order equation yields a second order growth rate with a singularity at α_0. To prevent this, part of the third order exponential secularity which causes γ_2 to diverge is regrouped with such terms at second order, and is then removed, along with the other second order exponentially secular terms, by assigning a new first order growth rate which now depends on k. This technique requires us to keep track of the exponential secularities explicitly and so consistency conditions cannot be used. Using this method, we obtain a growth rate which is in very good agreement with the numerical results for α up to and some way beyond α_0. In this section we also attempt to expand about the other zero of the growth rate, but we almost immediately run into difficulties.

The analysis in §4.2 is only valid if k is small in comparison to $\cos\alpha$. If this is not the case, we have to use a different ordering. This is done in §4.3. We obtain good agreement with the numerical results for α close to $\pi/2$, but fail to describe analytically the region where $\pi/2 - \alpha$ and k are comparable.

In §4.4 we derive the small-k dependence of the growth rate on perturbations applied at

an angle to the direction of propagation, and in §4.5 we briefly examine how well a variation of action calculation fares at generating the growth rate curves as a function of α.

4.1 The numerical methods and results

We begin by rotating the reduced variable moving frame coordinate system we employed in §2.1 by applying the transformation

$$(x\cos\alpha + y\sin\alpha, -x\sin\alpha + y\cos\alpha) \mapsto (x, y)$$

to the transformed two-dimensional ZK equation (2.2). The resulting equation is

$$n_t + (\cos\alpha\,\partial_x - \sin\alpha\,\partial_y)\left(\frac{1}{2}n^2 - 4n + \nabla^2 n\right) = 0 \tag{4.2}$$

in which our obliquely propagating plane soliton now moves along the x-axis. As before, we apply a perturbation so that

$$n = n_0 + \varepsilon\Phi(x)e^{iky}e^{\gamma t}. \tag{4.3}$$

Substituting (4.3) into (4.2) and linearizing gives

$$\frac{d}{dx}L_o\Phi = -\gamma\sec\alpha\,\Phi + k^2\frac{d\Phi}{dx} + ik\tan\alpha\,(L_o - k^2)\Phi. \tag{4.4}$$

On rearranging, we obtain

$$\left(\frac{d}{dx} - ik\tan\alpha\right)(L_o - k^2)\Phi = -\gamma\sec\alpha\,\Phi$$

from which we see that we have the same eigenvalue problem for γ=0 as when $\alpha = 0$. Hence the cut-off wavenumber, k_c, is still $\sqrt{5}$.

For large $|x|$ (4.4) reduces to

$$\frac{d^3\Phi}{dx^3} - ik\tan\alpha\frac{d^2\Phi}{dx^2} - (4+k^2)\frac{d\Phi}{dx} + \left\{\gamma\sec\alpha + ik(4+k^2)\tan\alpha\right\}\Phi = 0. \tag{4.5}$$

The solutions of (4.5) for small k and γ are $e^{p_1 x}$, $e^{-p_2 x}$, and $e^{p_3 x}$ where $p_1 \simeq 2 - \frac{1}{8}\gamma\sec\alpha$, $p_2 \simeq 2 + \frac{1}{8}\gamma\sec\alpha$, and $p_3 \simeq \frac{1}{4}\gamma\sec\alpha + ik\tan\alpha$.

To determine the value of γ numerically we use a similar method to that presented in §2.4. However, since the linearized equation is now complex, we firstly need to rewrite (4.4) as two separate equations for the real and imaginary parts. They can then be integrated with the Runge-Kutta routine we used before. There is only one exponentially decaying asymptotic form as $x \to \infty$, and so we again start our integration from a large and positive x_0, and calculate our initial boundary conditions from the approximation $\Phi(x_0) \simeq Ae^{-p_2 x}$ in which A is arbitrary and $-p_2$ is the root that has a negative real part of the auxiliary equation,

$$p^3 - ik\tan\alpha\,p^2 - (4+k^2)p + \gamma\sec\alpha + ik(4+k^2)\tan\alpha = 0.$$

The eigenvalue problem for the equation we solved in §2.4 was one-dimensional and hence we could use a simple technique, namely, the method of false position, to obtain a closer approximation to the true γ on the basis of the previous estimates. This was done by

attempting to find the zero of the function $\mathrm{sgn}[\Phi(\gamma, x_1)]/\Phi(\gamma, x_1)$, where $x_1 = x_1(\gamma)$ is the value of $x(< 0)$ at which the eigenfunction starts to grow exponentially.

In the present case, γ is complex, and so there are now two values to be chosen to maximize the distance from the origin at which the eigenfunction starts to grow exponentially. We therefore have to use the more involved Newton-Raphson (NR) technique. This method cannot be used to find the zero of the function we used in the one-dimensional problem. Instead, we have to integrate the equations up to a fixed large negative value of x which we call x_1. To provide an improved next estimate of the real and imaginary parts of γ, we use the NR method to find γ such that $\Phi(\gamma, x_1)$ is as small as possible. The primary drawback of this method is that there are a number of eigenfunctions and hence values of γ for which $\Phi(\gamma, x_1) = 0$. We therefore require fairly accurate starting estimates of Re γ and Im γ in order to home in on the desired solution. Nevertheless, when this method is applied to the one-dimensional case, we can obtain practically the same accuracy given a large enough x_1.

The growth rate curve for a given α is determined in the same way as before, incrementing k in small steps and using the values of γ for the previous few values of k to generate an estimate of the next. We also determine the growth rate as a function of α for fixed k. Starting at α=0, the first estimate of the real part of γ is most conveniently obtained from the Padé approximant (2.79) we derived earlier, and Im $\gamma(\alpha = 0)$ is just zero.

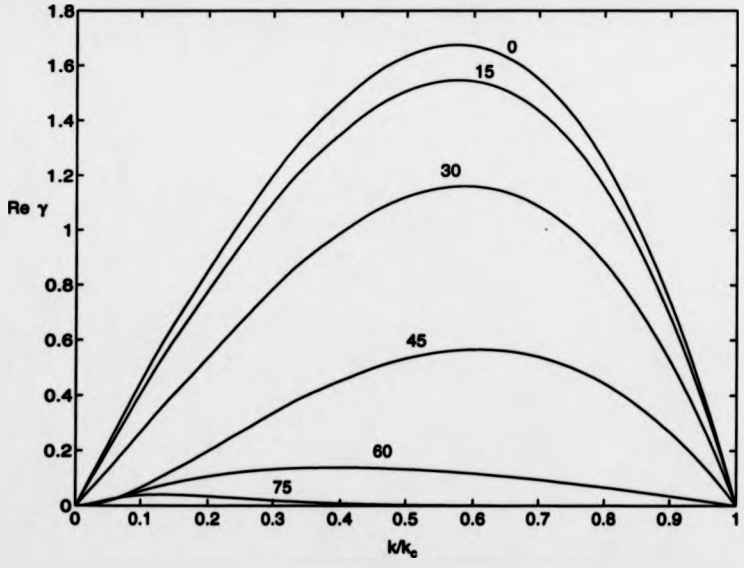

Figure 4.1: Growth rate curves for various values of α (in degrees).

We used the method to determine the growth rate curves for a range of angles and some of these are shown in Fig. 4.1. The maximum growth rates for various values of α are plotted in Fig. 4.2.

We see that the larger the angle, the smaller the maximum growth rate of perturbations. The value of k/k_c corresponding to the maximum growth rate initially increases slightly on

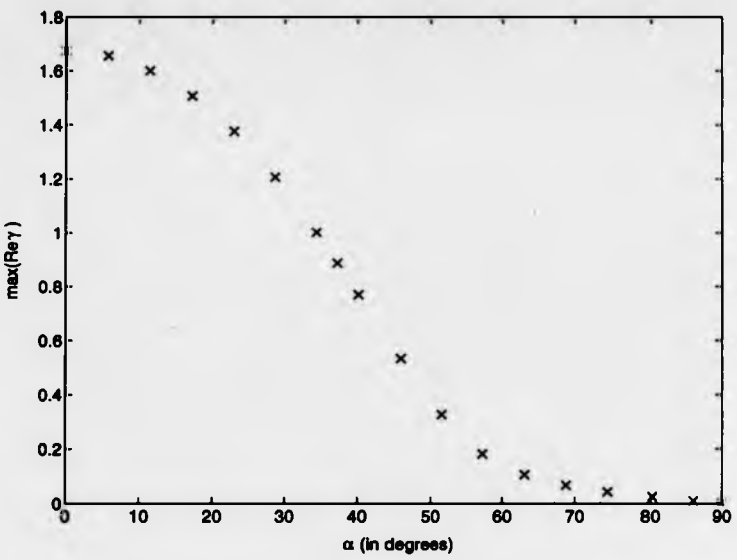

Figure 4.2: Dependence of maximum growth rate on α.

increasing α and then drops markedly for plane solitons propagating at large angles to the magnetic field.

4.2 Small-k expansion for $k \ll \cos\alpha$

We start by carrying out a similar multiple-scale expansion on the linearized equation (4.4) to that in §2.2. The zeroth order solution is again

$$\Phi_0 = h_0 \operatorname{sech}^2 x \tanh x. \tag{4.6}$$

To first order in k, the linearized equation yields

$$\partial_x L\Phi_1 = -2\Phi_{0,xx1} - \gamma_1 \sec\alpha\, \Phi_0 \tag{4.7}$$

from which we obtain

$$\Phi_1 = \frac{\gamma_1 \sec\alpha}{8} h_0 \operatorname{sech}^2 x \tag{4.8}$$

and

$$h_{0,1} = -\frac{\gamma_1 \sec\alpha}{8} h_0. \tag{4.9}$$

The second order equation is

$$\begin{aligned} \partial_x L\Phi_2 \;=\; & -2\Phi_{0,xx2} - 3\Phi_{0,x11} - 3\Phi_{1,xx1} - (n_0-4)\Phi_{1,1} - \gamma_2\Phi_0 - \gamma_1\Phi_1 \\ & + i\tan\alpha\,(2\Phi_{0,x1} + \Phi_{1,xx} + (n_0-4)\Phi_1) + \Phi_{0,x} \end{aligned} \tag{4.10}$$

and gives

$$\Phi_2 = h_0\left\{\frac{\sec^2\alpha}{256}\left(\gamma_1^2 - \frac{16\gamma_1 i}{3}\sin\alpha - \frac{64}{15}\cos^2\alpha\right)e^{-2x} + \frac{1}{640}(64 - 5\gamma_1^2\sec^2\alpha)A_0 + \left(\frac{1}{4} - \frac{\gamma_1 i\sec\alpha\tan\alpha}{16} - \frac{3\gamma_1^2\sec^2\alpha}{256} + \frac{\gamma_2\sec\alpha}{8}\right)\operatorname{sech}^2 x\right\} - \left(\frac{h_0}{4} - \frac{\gamma_1 i\sec\alpha\tan\alpha\, h_0}{16} - \frac{3\gamma_1^2\sec^2\alpha\, h_0}{256} + \frac{\gamma_2\sec\alpha\, h_0}{8} + h_{0,2}\right)x\varphi_0. \quad (4.11)$$

Using the conventional method we would now remove the exponentially secular terms by making

$$\gamma_1 = \frac{8}{3}\left(\sqrt{\frac{8}{5}\cos^2\alpha - 1} + i\sin\alpha\right). \quad (4.12)$$

We now have a γ_1 that is pure imaginary for $\alpha > \alpha_0$ where

$$\alpha_0 = \cos^{-1}\sqrt{\frac{5}{8}} \approx 37.8°. \quad (4.13)$$

These results are in line with those obtained by Das & Verheest.

In order to determine whether solitons propagating at angles greater than α_0 to the magnetic field are stable, we must find the sign of Re γ in this region. This will involve finding the growth rate to higher order. However, if we attempt this using the conventional perturbation method, we encounter difficulties.

As we shall see shortly, part of the exponentially secular terms at higher order, if left as they are, give rise to a singularity in γ_m for $m > 1$. Because the exponential secularities are all proportional to e^{-2x}, we can deal with this by grouping all the troublesome terms at higher order with the second order exponential secularities. The essential step in the method is to anticipate this regrouping by dealing with all the troublesome exponential secularities before they arise. When they do appear at higher order, we can just remove them since they will have already been accounted for. We therefore treat the following exponential secularities at second order

$$\frac{\sec^2\alpha}{256}\left\{\gamma_1^2 - \frac{16\gamma_1 i}{3}\sin\alpha - \frac{64}{15}\cos^2\alpha - \frac{64}{9}(E_3 k + E_4 k^2 + \ldots)\right\}h_0 e^{-2x}.$$

To remove them, we must choose

$$\gamma_1 = \frac{8}{3}\left(\sqrt{\frac{8}{5}\cos^2\alpha - 1 + E_3 k + E_4 k^2 + \ldots} + i\sin\alpha\right). \quad (4.14)$$

The unknowns E_3, E_4, etc. will be determined later from the troublesome exponentially secular terms. We are now ready to proceed to next order.

On solving the third order equation, we find that the exponential secularity in Φ_3 is

$$\frac{\sec^2\alpha}{2160}\left\{(45\gamma_2 + 32\cos\alpha - 20\sec\alpha)\sqrt{\frac{8}{5}\cos^2\alpha - 1 + E_3 k + E_4 k^2 + \ldots} - 4\left(5 + 4\cos^2\alpha + 5E_3 k + 5E_4 k^2 + \ldots\right)i\tan\alpha\right\}h_0 e^{-2x}. \quad (4.15)$$

We see that if the E_m were zero, this expression could not be made to vanish when $\alpha = \alpha_0$, and the γ_2 required to remove the whole expression would take the form:

$$\frac{4}{9}\sec\alpha\left(1-\frac{8}{5}\cos^2\alpha\right)+\frac{4\,(5+4\cos^2\alpha)\,i\tan\alpha}{45\sqrt{\frac{8}{5}\cos^2\alpha-1}} \tag{4.16}$$

and hence become very large near $\alpha = \alpha_0$. It is for this reason that we made allowances for regrouping third order exponential secularities with the second order ones. The last two k-independent terms in (4.15) are the troublesome ones and have already been accounted for at second order. They are therefore used to determine E_3 and then discarded. Having found E_3, we can now write γ_1 as

$$\gamma_1 = \frac{8}{3}\left(\sqrt{\frac{8}{5}\cos^2\alpha-1+\frac{1}{15}ik(5+4\cos^2\alpha)\tan\alpha+O(k^2)}+i\sin\alpha\right). \tag{4.17}$$

To remove the k-dependent terms outside the square root in (4.15), we move them to the order to which they belong. This leaves the terms multiplied by the square root. These are removed by choosing

$$\gamma_2 = \frac{4}{9}\sec\alpha\left(1-\frac{8}{5}\cos^2\alpha\right). \tag{4.18}$$

If we were to proceed to fourth order, we would use the same procedure, except we also have to remember to include exponentially secular terms that we promised to move to this order from the previous order. The exponentially secular terms which would have given rise to a singularity in γ_3 if we had used the conventional method are moved back to second order, and so determine E_4. The k-dependent exponential secularities which remain are moved to higher order and the other exponentially secular terms are removed by appropriate choice of γ_3.

When using this method, to minimize the complexity of the analysis, it is important not to replace γ_1 by the expressions we have derived for it (such as (4.14)) until either we need to explicitly evaluate the coefficient of the exponential secularity (as in (4.15)), or we have reached the required order and wish to have an explicit expression for the eigenfunction.

Before we examine the numerical results, notice that if we expand (4.17) for small k, the first k-dependent term we find corresponds to the troublesome term in γ_2 obtained using the conventional analysis (see (4.16)). Hence it appears that we could achieve the results (4.18) and (4.17) by using the conventional method and then replacing the troublesome term in γ_2 by an additional k-dependent term in γ_1. However this method lacks rigour - as α approaches α_0, we can no longer expand the square root in γ_1.

An alternative approach to dealing with the singularity at $\alpha = \alpha_0$ would be to carry out another expansion about this point. However, using the method we have developed, we rigorously obtain a *single* expression for the growth rate which is valid from α=0 up to some $\alpha > \alpha_0$.

The results of the numerical calculations compared with values found from the analytical expression $\gamma_1 k + \gamma_2 k^2$ for k=0.1 are shown in Figure 4.3 (γ_1 and γ_2 are given by (4.17) and (4.18) respectively). We see good agreement between numerical and analytical results except as α approaches $\pi/2$. This will be dealt with in the next section.

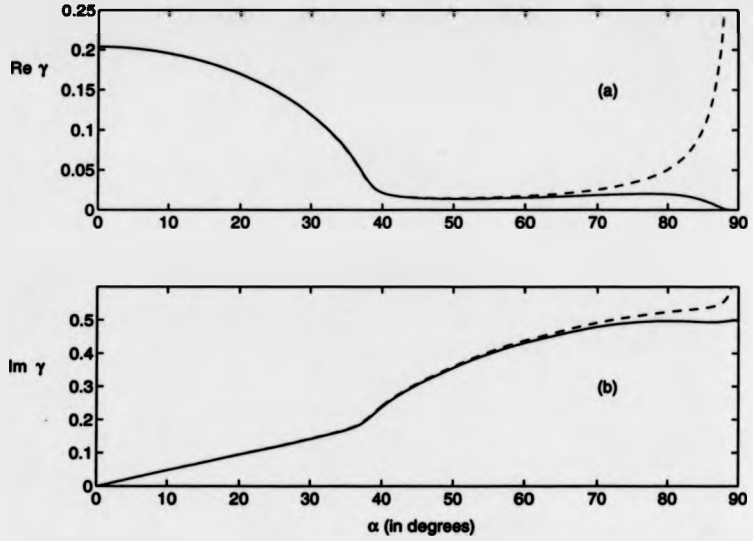

Figure 4.3: (a) Re γ and (b) Im γ for k=0.1. Solid curves - numerical results; dashed curves - analytic results.

As was mentioned in the previous section, when $\gamma = 0$, (4.4) also has the solution $\Phi = \mathrm{sech}^3 x$ for $k^2 = 5$. We therefore attempt to expand about this zero of the growth rate as well. To avoid the small quantity we are expanding in terms of appearing inside square roots, we choose our small quantity to be $\bar{k} = \sqrt{5} - k$ rather than writing $\bar{k}^2$ in terms of k^2 as was done in §2.3.

The linearized equation is now

$$\left\{\frac{d}{dx} - i\sqrt{5}\tan\alpha\right\}\bar{L}_o\Phi = -\gamma\sec\alpha\,\Phi + (\bar{k}^2 - 2\sqrt{5}\bar{k})\left\{\frac{d}{dx} - i(\sqrt{5}-\bar{k})\tan\alpha\right\}\Phi - i\bar{k}\tan\alpha\,\bar{L}_o\Phi. \tag{4.19}$$

The zeroth order equation is

$$(\partial_x - i\sqrt{5}\tan\alpha)\bar{L}\bar{\Phi}_0 = 0 \tag{4.20}$$

and may be rewritten as

$$\frac{\partial}{\partial x}\left(e^{-i(\sqrt{5}\tan\alpha)x}\bar{L}\bar{\Phi}_0\right) = 0. \tag{4.21}$$

As we are carrying out a definite integration, the exponential is lost and we are left with

$$\bar{\Phi}_0 = \bar{h}_0\,\mathrm{sech}^3 x \tag{4.22}$$

as we would expect. With the first order equation we run into difficulties. To find $\bar{\Phi}_1$ we have to solve

$$\frac{\partial}{\partial x}\left(e^{-i(\sqrt{5}\tan\alpha)x}\bar{L}\bar{\Phi}_1\right) = (-\bar{\gamma}_1\sec\alpha\,\bar{\Phi}_0 + 19i\tan\alpha\,\bar{\Phi}_0 - i\tan\alpha\,n_0\bar{\Phi}_0 - 2\sqrt{5}\bar{\Phi}_{0,x} - i\tan\alpha\,\bar{\Phi}_{0,xx} + i2\sqrt{5}\tan\alpha\,\bar{\Phi}_{0,x1} - 2\bar{\Phi}_{0,xx1})\,e^{-i(\sqrt{5}\tan\alpha)x}.$$

The integral we are required to perform cannot be expressed in terms of elementary functions and so we cannot proceed any further with the analysis.

4.3 Stability of plane solitons propagating almost perpendicular to the magnetic field

On inspecting (4.4) it can be seen that as α approaches $\pi/2$, the terms proportional to $\sec\alpha$ and $\tan\alpha$ can no longer be taken as small, and so a new ordering is required. We therefore fix k and choose $\beta \equiv \pi/2 - \alpha$ as our small expansion parameter. Equation (4.4) can then be rewritten as

$$\tan\beta\frac{d}{dx}(L_o - k^2)\Phi = -\gamma\sec\beta\,\Phi + ik(L_o - k^2)\Phi. \tag{4.23}$$

We will now carry out a small-β multiple-scale perturbation expansion. Rearranging (4.23) and expanding the functions of β gives

$$\left(L_o - \frac{\gamma}{ik} - k^2\right)\Phi = \frac{\gamma}{ik}\left(\frac{\beta^2}{2} + \frac{5\beta^4}{24} + \ldots\right)\Phi + \frac{1}{ik}\left(\beta + \frac{\beta^3}{3} + \ldots\right)\frac{d}{dx}(L_o - k^2)\Phi \tag{4.24}$$

in which Φ and γ are now expanded as

$$\Phi = \tilde{\Phi}_0 + \beta\tilde{\Phi}_1 + \beta^2\tilde{\Phi}_2 + \ldots \tag{4.25}$$

$$\gamma = \tilde{\gamma}_0 + \beta\tilde{\gamma}_1 + \beta^2\tilde{\gamma}_2 + \ldots \tag{4.26}$$

and the $\tilde{\Phi}_j$ are functions of x and the scaled variables $\tilde{x}_m \equiv \beta^m x$. Substituting the above two expansions into (4.24) and equating the zeroth order coefficients of β, we obtain

$$\left(L_o - \frac{\tilde{\gamma}_0}{ik} - k^2\right)\tilde{\Phi}_0 = 0. \tag{4.27}$$

This is satisfied by both

$$\tilde{\Phi}_0 = \tilde{\Phi}_0^- \equiv \tilde{h}_0^-\tilde{\varphi}_0^- \equiv \tilde{h}_0^-(\tilde{x}_1, \tilde{x}_2, \ldots)\,\mathrm{sech}^2 x\tanh x\,, \qquad \tilde{\gamma}_0 = \tilde{\gamma}_0^- \equiv -ik^3 \tag{4.28}$$

and

$$\tilde{\Phi}_0 = \tilde{\Phi}_0^+ \equiv \tilde{h}_0^+\tilde{\varphi}_0^+ \equiv \tilde{h}_0^+(\tilde{x}_1, \tilde{x}_2, \ldots)\,\mathrm{sech}^3 x\,, \qquad \tilde{\gamma}_0 = \tilde{\gamma}_0^+ \equiv ik(5 - k^2). \tag{4.29}$$

Before continuing with the expansion, we note that the above are solutions corresponding to a linearization about a soliton whose n=constant planes are parallel to the magnetic field. The ZK equation (2.2) also has the solution $n = f(y)$ where f is an arbitrary function of y only. Linearizing about this in an analogous way to before, we obtain

$$\frac{d^2}{dy^2}\Phi + (f(y) - 4)\Phi = -\frac{\gamma}{ik}\Phi + k^2\Phi. \tag{4.30}$$

If $f(y)$ is chosen to be $12\,\mathrm{sech}^2 y$, we arrive at the solutions (4.28) and (4.29), but this time in terms of the unrotated y-co-ordinate and with $\tilde{\gamma}_0$ of the opposite sign. From (4.30) we see that for any real f, γ must be pure imaginary. Hence if a solution to the ZK equation has no x-dependence, it appears to be stable.

The existence of two values for $\tilde{\gamma}_0$ can be understood on considering our crude expression for γ_1 derived in the previous section. When $\alpha = \pi/2$, (4.12) gives $\gamma = 16ik/3$ for the positive root and zero for the other. These are close to the values of $\tilde{\gamma}_0$. Furthermore, it can be seen from the numerical results of Figure 4.3 that for $\alpha = 90°$, the imaginary part of the growth rate is close to $5k$. On the other hand, if we numerically determine the growth rate as a function of angle starting at $\alpha = 90°$ with $\gamma = \tilde{\gamma}_0^-$, we instead generate a growth rate curve with a negative real part. Hence it is the positive branch of solutions which is of interest to us.

The first order equation derived from (4.24) for the positive branch is

$$\bar{L}\tilde{\Phi}_1 = -2\tilde{\Phi}_{0,x1} - \frac{i\tilde{\gamma}_1}{k} - \frac{i}{k}\partial_x L\tilde{\Phi}_0 + ik\tilde{\Phi}_{0,x}. \tag{4.31}$$

in which $\bar{L} \equiv \partial_x^2 + n_0 - 9$ and we have dropped the '+' superscripts. To determine $\tilde{\gamma}_1$ we find it most convenient to use the consistency condition

$$\left\langle \tilde{\Phi}_0 \bar{L} \tilde{\Phi}_j \right\rangle = 0. \tag{4.32}$$

From this with j=1 we find that $\tilde{\gamma}_1 = 0$. Solving (4.31) then leaves us with a ghost secularity:

$$\tilde{\Phi}_1 = \left(-\frac{i}{2k}(5 - k^2)\bar{h}_0 - \bar{h}_{0,1} \right) x\bar{\varphi}_0. \tag{4.33}$$

In the usual fashion we assign $\bar{h}_{0,1} = -i(5 - k^2)\bar{h}_0/2k$ to leave $\tilde{\Phi}_1 = 0$.

Applying (4.32) to the second order equation

$$\begin{aligned} \bar{L}\tilde{\Phi}_2 \;=\; & -2\tilde{\Phi}_{0,x2} - \tilde{\Phi}_{0,11} - 2\tilde{\Phi}_{1,x1} - \frac{i\tilde{\gamma}_2}{k}\tilde{\Phi}_0 - \frac{i}{k}\left(\partial_x L\tilde{\Phi}_1 + 3\tilde{\Phi}_{0,xx1} + (n_0 - 4)\tilde{\Phi}_{0,1} \right) \\ & + ik(\tilde{\Phi}_{0,1} + \tilde{\Phi}_{1,x}) + \frac{5 - k^2}{2}\tilde{\Phi}_0 \end{aligned} \tag{4.34}$$

gives us

$$\tilde{\gamma}_2 = -\frac{i}{28k}(5 - k^2)(1 + 21k^2). \tag{4.35}$$

After putting $\bar{h}_{0,2} = 12(5 - k^2)\bar{h}_0/7k^2$, we obtain

$$\tilde{\Phi}_2 = \frac{12}{7k^2}(5 - k^2)\bar{h}_0 A_1(x)\bar{\varphi}_0. \tag{4.36}$$

At third order we again have $\tilde{\gamma}_3 = 0$. After evaluating $\tilde{\Phi}_3$, with the help of *Mathematica*, the fourth order consistency condition yields

$$\tilde{\gamma}_4 = -\frac{i}{8232k^3}(5 - k^2)(1011 + 1153k^2 + 1029k^4). \tag{4.37}$$

We see that this branch gives γ with zero real part to order β^4 at least. The numerical and analytical calculations for small β are shown in Figure 4.4. Not surprisingly, the agreement breaks down as β (in radians) becomes comparable with k.

To investigate the case where β and k are comparable, we tried various orderings, but were unable to obtain any sensible results.

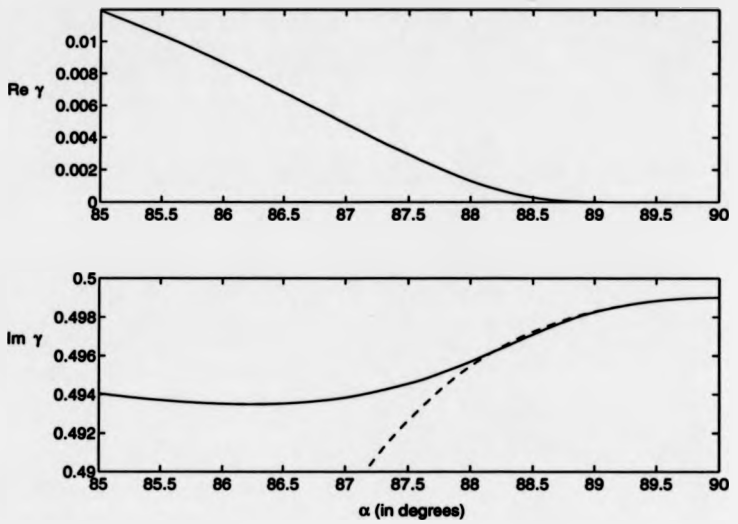

Figure 4.4: (a) Re γ and (b) Im γ for k=0.1. Solid curves - numerical results; dashed curve (and Re $\gamma = 0$ in (a)) - analytic results.

4.4 Oblique perturbation

We have also determined the effect of a periodic perturbation applied at an angle θ to the direction of propagation. Substituting

$$n = n_0 + \varepsilon\Phi(x)e^{i(k\cos\theta\, x + k\sin\theta\, y)}e^{\gamma t} \tag{4.38}$$

into (4.2) gives

$$\begin{aligned}\frac{d}{dx}L_o\Phi &= -\gamma\sec\alpha\,\Phi - ik\cos\theta\,(n_0-4)\Phi - 3ik\cos\theta\,\frac{d^2\Phi}{dx^2} + ik\sin\theta\tan\alpha\,(L_o - k^2)\Phi \\ &\quad + k^2(1+2\cos^2\theta - 2\sin\theta\cos\theta\tan\alpha)\frac{d\Phi}{dx} + ik^3\cos\theta\,\Phi. \end{aligned}\tag{4.39}$$

Using the same method as in §4.2 our results for the growth rate indicate that

$$\gamma(k,\alpha,\theta) = \gamma(k\sin\theta,\alpha,\frac{\pi}{2}). \tag{4.40}$$

Hence we can say that in general a plane soliton is most unstable to perturbations perpendicular to its direction of propagation.

4.5 Variational method results

The variation of action method used in §2.6 gave the correct value of the slope of the growth rate curve at $k = 0$. Hence there is the possibility that it would be successful in estimating

the small-k growth rate for obliquely propagating solitons. The Lagrangian density for (4.2) is

$$\mathcal{L} = \frac{1}{2}\psi_t\psi_x + \left(\frac{1}{6}\psi_x^3 - 2\psi_x^2 - \frac{1}{2}\psi_{xx}^2 - \frac{1}{2}\psi_{xy}^2\right)\cos\alpha - \left(\frac{1}{6}\psi_y^3 - 2\psi_y^2 - \frac{1}{2}\psi_{xy}^2 - \frac{1}{2}\psi_{yy}^2\right)\sin\alpha. \tag{4.41}$$

Using the simplest trial function which gives meaningful results,

$$n(x,y,t) = A(y,t)\,\mathrm{sech}^2(x - P(y,t))\,,$$

we obtain the dispersion relation

$$\gamma^2 = \frac{96}{25}k^2(\cos\alpha - 6\sin\alpha)\left\{\left(1 - \frac{5}{24}k^2\right)\cos\alpha - \frac{25}{24}k^2\sin\alpha\right\}. \tag{4.42}$$

This gives only vague agreement with the first order real part of γ found in §4.2 in that it shows that Re γ_1 is zero for α greater than some cut-off angle, α_0. From (4.42) we obtain $\alpha_0 = \tan^{-1}\sqrt{\frac{1}{6}} \simeq 9°$ as compared with the correct value of approximately 38°. Even if we use the more general trial function (2.92) and allow all the parameters to vary, we do not obtain an improved estimate of α_0.

4.6 Discussion

Numerical studies have shown that the maximum growth rate of a perturbation decreases as the angle between the plane soliton direction of motion and the magnetic field increases. For large angles, the value of k for which the maximum growth rate occurs decreases with increasing angle.

We have extended previous analytical studies on the stability of plane solitons propagating at $\alpha < \alpha_0$ to long wavelength disturbances by determining the growth rate to second order. As a result, we have shown that the solitons are also unstable when propagating at angles greater than α_0. To obtain in a consistent way an expression for the growth rate to second order that lacks singularities, we had to carry out a new type of regrouping of terms. This time it was necessary to regroup exponential secularities before they were removed by appropriate choice of γ_m.

An alternative approach of moving the troublesome parts of the higher order γ_m (obtained using consistency conditions) to γ_1 gives the same result. However this method lacks rigour; the new, k-dependent γ_1 cannot be expanded when α lies close to the singularity, and so strictly, this regrouping of part of γ_2 to the previous order is only permitted when this singular term is not causing problems.

The method we have developed should be generally applicable to any problem where the first consistency condition to give a meaningful result does not present any difficulties with singularities, but consistency conditions applied at higher order do generate expressions with singularities. On finding a problem of this nature, to apply our method we would redo the calculation, determining the exponential secularities explicitly rather than using consistency conditions.

Chapter 5

The formation of cylindrical solitons

In this chapter we finally turn to the solution of the full two-dimensional ZK equation. Since the equation is nonlinear and non-integrable, we cannot expect to be able to advance very far on the analytical side. As we shall see in §5.1, for a perturbation with an amplitude much larger than k, we immediately run into difficulties. Only if we consider a perturbation of a size comparable to k can we proceed. However, to obtain results from this weakly nonlinear analysis, we end up having to substitute our results from the linear analysis into the functions that remain undetermined. Nevertheless, these results describe a form of behaviour of the perturbation not shown by those of the purely linear analysis of Chapter 2. We interpret the results as the preliminary stages of the formation of a cylindrical soliton.

To determine the subsequent evolution of a perturbed plane soliton we have to resort to solving the full equation numerically. The numerical method we use is described in §5.2. After discussing its accuracy, we use the method to see how well the growth rates obtained from the linear analysis agree with the values derived numerically from the full equation. We also compare the numerical data with the results of the analysis in §5.1.

As has now been shown by a number of authors, the most interesting feature of the two-dimensional ZK equation is the emergence of coherent structures in the form of cylindrical solitons as a result of the application of a relatively arbitrary perturbation to a plane soliton. In §5.3 we illustrate the transformation of a sinusoidally perturbed plane soliton into a periodic array of pulse-like solutions. The properties of these solutions are shown to match those theoretically predicted for cylindrical solitons. We also show numerically that the number and speed of the emerging solitons depends on the wavenumber of the perturbation. We then make use of two of the conservation laws the ZK equation obeys to offer an explanation for some of this behaviour.

5.1 Analysis of the nonlinear equation for perturbed plane solitons

In the nonlinear analysis of the ZK equation we must now insist upon the more general ansatz of

$$n = n_0 + \varepsilon\Phi(x, y, t) \tag{5.1}$$

in which ε is no longer small compared with k, and $n_0 \equiv 12\,\mathrm{sech}^2 x$ is again the equilibrium plane soliton solution. Substituting (5.1) into the reduced moving frame ZK equation (2.2) gives

$$\partial_x L\Phi = -\partial_t \Phi - \partial_x \partial_y^2 \Phi - \varepsilon \Phi \partial_x \Phi \,. \tag{5.2}$$

We expand Φ as

$$\Phi = \Phi_0 + k\Phi_1 + k^2\Phi_2 + \ldots \tag{5.3}$$

where

$$\Phi_i \equiv \Phi_i(x_0, x_1, \ldots y_1, \ldots t_1, t_2, \ldots) \tag{5.4}$$

and $x_m \equiv k^m x$, etc. are treated as independent variables. Proceeding in the same way as the linear case, we try

$$\begin{aligned} \partial_t &= k\partial_{t_1} + k^2\partial_{t_2} + \ldots \\ \partial_y &= k\partial_{y_1} + \ldots \\ \partial_x &= \partial_{x_0} + k\partial_{x_1} + \ldots \,. \end{aligned}$$

To zeroth order in k we have

$$\partial_{x_0} L\Phi_0 = -\frac{\varepsilon}{2}\partial_{x_0}(\Phi_0^2) \tag{5.5}$$

from which

$$\frac{\partial^2 \Phi_0}{\partial x_0^2} + (n_0 - 4)\Phi_0 + \frac{\varepsilon}{2}\Phi_0^2 = C_0. \tag{5.6}$$

Unfortunately, we do not know how to solve this equation. We can however try making the perturbation of order k by replacing the ε in (5.1) by εk. This leads to

$$\partial_x L\Phi = -\partial_t \Phi - \partial_x \partial_y^2 \Phi - \varepsilon k \Phi \partial_x \Phi \,. \tag{5.7}$$

Then to zeroth order in k this yields,

$$\partial_{x_0} L\Phi_0 = 0 \tag{5.8}$$

with solution

$$\Phi_0 = H_0\varphi_0 \equiv H_0(x_0, x_1, \ldots y_1, \ldots t_1, t_2, \ldots)\,\mathrm{sech}^2 x \tanh x. \tag{5.9}$$

The first order equation is

$$\partial_{x_0} L\Phi_1 = -2\Phi_{0,xx1} - \Phi_{0,t_1} - \frac{\varepsilon}{2}(\Phi_0^2)_x \tag{5.10}$$

where we have extended the notation used in the linear analysis; we continue to write $\Phi_{0,x1} \equiv \partial^2\Phi_0/\partial x_0 \partial x_1$, etc. but we now also have $\Phi_{0,t_1} \equiv \partial\Phi_0/\partial t_1$ and $\Phi_{0,y_1y_1} \equiv \partial^2\Phi_0/\partial y_1^2$, etc.

As can be seen from the solution of (5.10),

$$\Phi_1 = -x\varphi_0 H_{0,1} + \frac{1}{8}H_{0,t_1}(\,\mathrm{sech}^2 x - x\varphi_0) - \frac{1}{48}\varepsilon H_0^2 \varphi_{0,x}\,, \tag{5.11}$$

we still have ghost secularities. We can remove them by making $H_{0,1} = -H_{0,t_1}/8$ which leaves

$$\Phi_1 = \frac{1}{8}H_{0t_1}\,\mathrm{sech}^2 x - \frac{1}{48}\varepsilon H_0^2 \varphi_{0,x}. \tag{5.12}$$

To second order we have

$$\partial_{x_0} L\Phi_2 = -2\Phi_{1,xx1} - 3\Phi_{0,x11} - 2\Phi_{0,xx2} - L\Phi_{1,1} - \Phi_{0,t_2} - \Phi_{1,t_1} - \Phi_{0,y_1y_1} - \frac{\varepsilon}{2}(\Phi_0^2)_{,1} - \varepsilon\Phi_0\Phi_1 . \tag{5.13}$$

Applying the consistency condition $\langle n_0 \partial_{x_0} L\Phi_2 \rangle = 0$ we obtain

$$H_{0,t_1t_1} = -\frac{64}{15} H_{0,y_1y_1} . \tag{5.14}$$

The $x\varphi_0$ terms we find in Φ_2 are removed by choosing

$$H_{0,2} = \frac{1}{5} H_{0,y_1y_1} - \frac{1}{8} H_{0,t_2} \tag{5.15}$$

which then leaves us with

$$\Phi_2 = -\frac{1}{15} H_{0,y_1y_1} \mathcal{A}_0 + \left(\frac{1}{5} H_{0,y_1y_1} - \frac{1}{8} H_{0,t_2} \right) \operatorname{sech}^2 x - \frac{\varepsilon^2}{288} H_0^3 \operatorname{sech}^4 x \tanh x . \tag{5.16}$$

Notice that on replacing H_0 by $h_0 e^{iky} e^{\gamma t}$ and putting $\varepsilon = 0$ we recover the results of the linear theory.

The total expression for Φ so far is

$$\begin{aligned} \Phi \;=\; & H_0\varphi_0 - \frac{\varepsilon k}{48} H_0^2 \varphi_{0,x} - \frac{\varepsilon^2 k^2}{288} H_0^3 \operatorname{sech}^4 x \tanh x + \frac{k H_{0,t_1}}{8} \operatorname{sech}^2 x \\ & + k^2 \left\{ \left(\frac{1}{5} H_{0,y_1y_1} - \frac{1}{8} H_{0,t_2} \right) \operatorname{sech}^2 x - \frac{1}{15} H_{0,y_1y_1} \mathcal{A}_0 \right\} + O(k^3). \end{aligned} \tag{5.17}$$

We see that the first two terms are the same as the expansion of $\varphi_0(x - \varepsilon k H_0/48)$ to first order. However, to second order,

$$\varphi_0(x - \varepsilon k H_0/48) = \varphi_0 - \frac{\varepsilon k}{48} H_0 \varphi_{0,x} + \varepsilon^2 k^2 H_0^2 \left(\frac{1}{1152} \varphi_0 - \frac{1}{384} \operatorname{sech}^4 x \tanh x \right) + O(k^3). \tag{5.18}$$

In order to make the ε^2 term in Φ_2 compatible with the above, we add the appropriate amount of φ_0 to it, which we are permitted to do since $L\varphi_0 = 0$. We then have

$$\Phi_2 = -\frac{1}{15} H_{0,y_1y_1} \mathcal{A}_0 + H_{0,2} \operatorname{sech}^2 x + \frac{1}{2} \left(\frac{\varepsilon H_0}{48} \right)^2 H_0 \varphi_{0,xx} - \frac{\varepsilon^2}{1152} H_0^3 \operatorname{sech}^4 x \tanh x . \tag{5.19}$$

On applying the consistency condition to the third order equation, we obtain

$$H_{0,t_1t_2} + \frac{64}{15} H_{0,y_1y_2} = \frac{4}{15} H_{0,y_1y_1t_1} . \tag{5.20}$$

On solving the third order equation, we find that the only ε-dependent terms which Φ_3 contains are

$$\varepsilon^3 H_0^4 \left(\frac{5}{27648} \operatorname{sech}^6 x - \frac{1}{6912} \operatorname{sech}^4 x \right) .$$

The contents of the brackets may be re-expressed as

$$\frac{1}{48} \frac{1}{1152} \frac{d}{dx} (\operatorname{sech}^4 x \tanh x) - \frac{1}{3! \, 48^3} \varphi_{0,xxx} + \frac{1}{165888} \varphi_{0,x} . \tag{5.21}$$

The first term in the above may again be included as a phase change of $-\varepsilon k H_0/48$ to the 'left over' $\mathrm{sech}^4 x \tanh x$ term in the previous order (see (5.19)). The second term is what we would expect from taking the (5.18) expansion to next order. The presence of the final term in (5.21) indicates that the phase of the zeroth order term, Φ_0, also has an ε^3-dependence.

If we now include our third order results, we see that the dominant part of the perturbation has the form $H_0\varphi_0(\xi)$ where

$$\xi = x - \frac{\varepsilon k H_0}{48} + \frac{2}{3}\left(\frac{\varepsilon k H_0}{48}\right)^3 + O(\varepsilon^4). \tag{5.22}$$

With H_0 of the form taken in the linear régime, we have

$$n \simeq n_0 + \varepsilon k h_0 \cos ky\, e^{\gamma t}\, \varphi_0(\xi_{\mathrm{lin}}) + O(k^2). \tag{5.23}$$

where

$$\xi_{\mathrm{lin}} = x - \frac{\varepsilon k}{48} h_0 \cos ky\, e^{\gamma t} + \frac{2}{3}\left(\frac{\varepsilon k h_0 \cos ky\, e^{\gamma t}}{48}\right)^3 + O(\varepsilon^4)$$

and h_0 and γ are the results from the linear analysis. This indicates that as the perturbation grows, it will exhibit a y-dependent phase shift or 'bending'. As will be shown shortly, this behaviour is seen in the numerical solution of the full equation.

5.2 Numerical solution of the two-dimensional ZK equation

The time evolution of the two-dimensional ZK equation was obtained numerically using a method similar to that employed by others (see e.g. Iwasaki *et al.* 1990). The equation is discretized in time and space and periodic boundary conditions in both spatial coordinates are imposed. This is perfectly natural for the y-direction when we are applying a periodic perpendicular perturbation. However, since the soliton solutions we are investigating are not periodic in the direction of motion, we must ensure that the periodicity in x is large enough to have little effect on the results.

The solution is advanced in time by using the leap-frog scheme:

$$\begin{aligned} n(x,y,t+\Delta t) \;=\; & n(x,y,t-\Delta t) - 2\,\Delta t \left\{[n(x,y,t)-4]\,\partial_x n(x,y,t)\right. \\ & \left. + \partial_x^3 n(x,y,t) + \partial_x \partial_y^2 n(x,y,t)\right\}. \end{aligned}$$

The derivatives are calculated using spectral methods. With a discrete Fourier transform defined by

$$\tilde{n}_q = \sum_{p=0}^{N_x-1} n(p\,\Delta x, y, t) e^{2\pi i p q/N_x},$$

the rth derivative with respect to x is given by

$$\partial_x^r n(x,y,t) = \frac{1}{N_x} \sum_{q=0}^{N_x-1} \left(-\frac{2\pi i q}{l_x}\right)^r \tilde{n}_q e^{-2\pi i p q/N_x}$$

where N_x is the number of lattice points in the x-direction, Δx is the spacing between them, and $l_x \equiv N_x \Delta x$. The derivatives with respect to y are found in a similar way.

In order that the standard fast-Fourier transform can be implemented, the spatial lattice must be a $(N_x, N_y) = (2^{m_x}, 2^{m_y})$ array where $m_{x,y}$ are integers. We used an array of at least 256×32 for our calculations.

To test the numerical method, we firstly examined the fate of the unperturbed plane soliton solution $n(x,y,t) = 12\,\mathrm{sech}^2 x$. The solution did not significantly change its form over time-scales typical of the simulations we later carried out. Specifically, at $t = 8$, the error in height was found to be 3.5×10^{-6} and was growing approximately linearly at a rate of 5×10^{-7} per unit time.

We also used three of the conservation laws mentioned in the introductory chapter as a check on the accuracy. For the two-dimensional system with periodic boundary conditions the conserved quantities mass, momentum in the x-direction, and energy are given by

$$M \equiv \int_0^{l_x}\int_0^{l_y} n\,dx\,dy \tag{5.24}$$

$$P \equiv \frac{1}{2}\int_0^{l_x}\int_0^{l_y} n^2\,dx\,dy \tag{5.25}$$

$$H \equiv \frac{1}{2}\int_0^{l_x}\int_0^{l_y} \left\{n_x^2 + n_y^2 - \frac{1}{3}n^3\right\} dx\,dy \tag{5.26}$$

respectively. The energy was found to be the most sensitive test of the numerical accuracy. Comparing the final and initial energies, we found that at worst the relative error was 2×10^{-7}, although the typical value was 10^1-10^3 times smaller than this.

The purpose of the analysis in Chapter 2 was to find out how fast perturbations to plane solitons grow. We now look at how well those results apply to the numerical solutions of the full equation. As the initial condition for the calculation we used

$$n(x,y,t=0) = n_0(x) + \hat{\varepsilon}\dot{\Phi}(x)\cos ky$$

where $\dot{\Phi}$ is the eigenfunction associated with the linearized equation with periodic boundary conditions. We chose the initial condition to be of this form so that the perturbation was the best approximation to the fastest growing eigenfunction of the full equation. $\dot{\Phi}$ was numerically determined using the method employed by Infeld & Frycz (1987) (see §2.4) since this generates an eigenfunction that is periodic in x. The eigenfunction obtained was then normalized to unit amplitude and hence $\hat{\varepsilon}$ is the amplitude of the perturbation.

To find the growth rate in the context of the full equation, the amplitude of the perturbation as a function of time was fitted to an exponential at a time sufficient for transient effects to have died away. In Table 5.1 we show the effect of $\hat{\varepsilon}$ on the initial growth rate of the perturbation. We see that the larger the perturbation, the larger the growth rate. Hence the perturbation grows at a rate faster than exponential initially. However, for $\hat{\varepsilon}$ very small compared to k, the growth rate is in agreement with that obtained numerically for the linearized equation with periodic boundary conditions. For a sufficiently large period, this growth rate is very close to that given by the Padé approximant we obtained in Chapter 2.

We also saw in Chapter 2 that plane solitons should be stable for perturbations with $k^2 > 5$. When such a perturbation was added to a plane soliton, no exponential growth was observed in the numerical solution to the full equation. In §4.3 we showed analytically that the solution $n = 12\,\mathrm{sech}^2 y$ is stable to x-dependent perturbations. This was also demonstrated numerically.

We now use our numerical method to test the predictions of the analysis in the previous section. The analysis is only valid for small k and $\hat{\varepsilon}$ and hence small growth rates. This

$\hat{\varepsilon}$	$\gamma(k=0.1)$	$\gamma(k=1)$
1	0.37	1.72
0.1	0.22	1.58
0.01	0.206	1.565
0.001	0.2038	1.563
linear	0.2036	1.563

Table 5.1: Growth rate measured from numerical solution of the full ZK equation. The linear result is obtained from the numerical solution of the linearized equation with periodic boundary conditions.

means that before the perturbation gets too large for the analysis to apply, the bending of the eigenfunction will be very small. It would seem that we would require a very small stepsize for x to obtain a quantitative comparison of the numerical and analytical results. However, decreasing the stepsize gives rise to a large increase in the running time for two reasons. Firstly, in order to maintain the same domain size, l_x, we would need to increase N_x. Secondly, the numerical method is only stable for

$$\frac{\Delta t}{(\Delta x)^3} < 0.03$$

(Canuto *et al.* 1988). Hence halving the stepsize would require us to decrease Δt by a factor of eight, and so the program would take eight times as long to run. Rather than decrease the stepsize, we instead used the spline interpolation routine in the software package *Matlab* to interpolate between the data points and hence effectively increase the resolution in x.

We determined the phase of the perturbation along $y = 0$ and $y = \pi/k$ by finding the position of its maximum and minimum respectively for those values of y. From (5.23) we see that the change in position of the maximum and minimum are given by

$$\Delta x_{\pm} = \pm\frac{\varepsilon k}{48}\left(e^{\gamma t_2} - e^{\gamma t_1}\right) \mp \frac{2}{3}\left(\frac{\varepsilon k}{48}\right)^3\left(e^{3\gamma t_2} - e^{3\gamma t_1}\right). \tag{5.27}$$

where the upper and lower signs refer to the maximum and minimum of the perturbation respectively. Since h_0 is a slowly varying exponential, we have approximated it by $h_0(0) = 1$.

Initially the change in position of the extremum is very slow. We therefore choose our t_1 to be the time at which the extremum is first observed to change by $\Delta x/s$ where s is the number of points at which the spline is evaluated (in order to test for its extremum) per data point. We found that it was sufficient to choose $s = 10$, and hence obtain a factor of ten increase in the x-resolution. Now that t_1 is fixed, t_2 are the times at which the position of the extremum advances by $\Delta x/s$ or more. Hence the values of $\Delta x_{\pm}$ determined from our numerical calculations will equal $m\Delta x/s$ for some integer m. We compare these values with those obtained from (5.27) in Figure 5.1 for $k = 0.1$ and $\hat{\varepsilon} = 0.1$. Note that because the eigenfunction in the analysis in the previous section is not normalized, we have $\hat{\varepsilon}/(\varepsilon k) \approx \max\varphi_0 = 2/\sqrt{27}$.

We see that initially there is fairly good agreement between the numerical and analytical results. For larger times, the numerically derived distance increases faster than the analytical one for the perturbation maximum along $y = 0$. On the other hand, the rate at which the

perturbation minimum moves in the opposite direction along $y = \pi/k$ soon falls below the analytical prediction. This leads to an asymmetrical bending - it is more pronounced in the positive x-direction. We shall see in the next section that this corresponds to the birth of a cylindrical soliton.

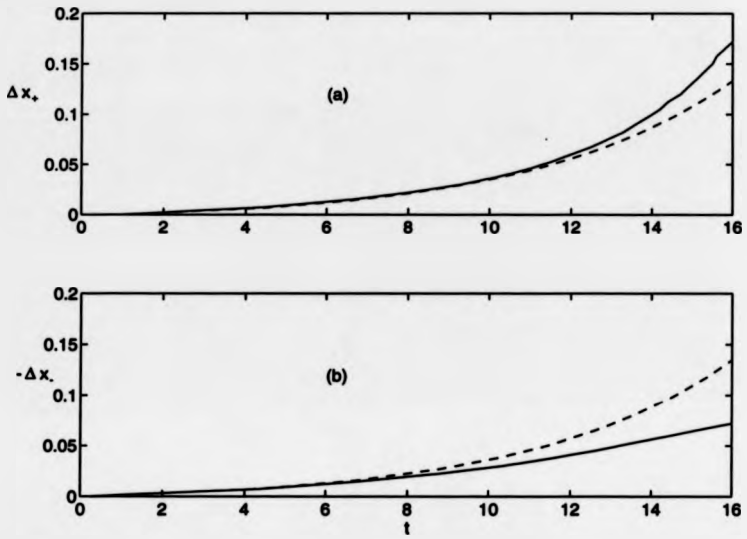

Figure 5.1: Change in position of the extremum of the perturbation for k=0.1. Solid curve - numerical results; dashed curve - analytic results. (a) perturbation maximum along $y = 0$; (b) perturbation minimum along $y = \pi/k$.

5.3 Cylindrical solitons

As was first demonstrated numerically by Frycz & Infeld (1989), a plane soliton to which a perpendicular perturbation with $k < k_c$ has been applied will eventually evolve into cylindrical solitons. We used the numerical method described in the previous section to observe this process for various values of k. In Figures 5.2 and 5.3 we show some of the steps in the formation of a cylindrical soliton when $k = 1$.

In the Figure 5.3(a) contour plot we can see the presence of the initial perturbation. By $t = 2$ (Figure 5.3(b)), the contour lines have a noticeable y-dependence. The bending we described analytically in §5.1 is the preliminary stage of this. However, the contour lines at t=2 are bent more in the positive x-direction than in the negative direction - this effect was not present in the analytical solution. The maximum of the perturbation becomes ever more pronounced until it finally saturates, breaks free and becomes a two-dimensional pulse with an elliptical cross-section as is apparent in (c) and (d) of both figures.

Zakharov & Kuznetsov (1974) showed that the radial dependence of a cylindrical soliton

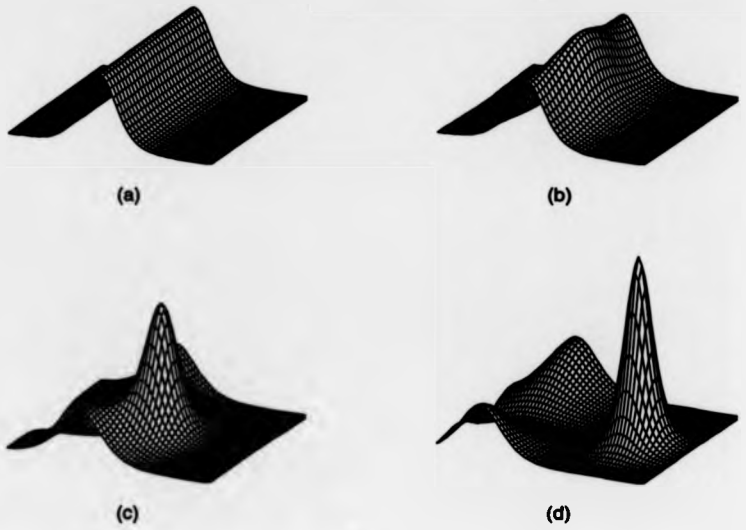

Figure 5.2: Evolution of a perturbed plane soliton. $k = 1.0$, $\hat{\epsilon} = 0.1$. (a) t=0; (b) t=2; (c) t=3; (d) t=4.

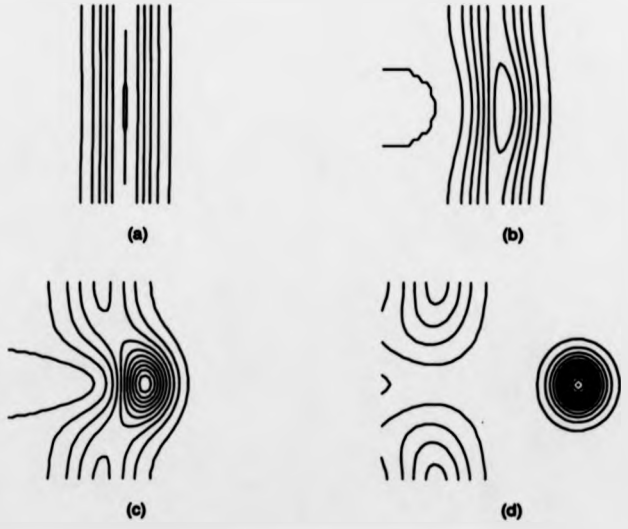

Figure 5.3: Contour plots for Figure 5.2.

is given by the solution to

$$\frac{d^2 n_c}{dr^2} + \frac{1}{r}\frac{dn_c}{dr} - v_c n_c + \frac{1}{2} n_c^2 = 0 \tag{5.28}$$

where v_c is the speed of the cylindrical soliton. The solution takes the form

$$n_c = v_c U(\sqrt{v_c} r) \tag{5.29}$$

in which $U(r)$ can only be determined numerically. A plot of $U(r)$ is shown in Figure 5.4 along with two suitably scaled vertical cross-sections obtained from Figure 5.2(d). The striking agreement, which has also been verified by others (e.g. Frycz & Infeld 1989), is a strong indication that the structures we are seeing are indeed the cylindrical solitons described by (5.28).

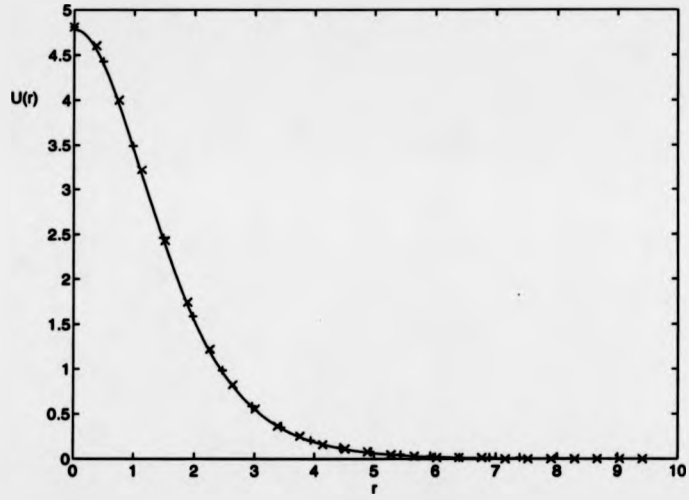

Figure 5.4: Radial dependence of a cylindrical soliton. Solid curve - theoretical $U(r)$; ×,+ - obtained from vertical sections parallel to the x and y axes respectively through the cylindrical soliton in Figure 5.2(d) after rescaling using (5.29).

From the numerical solution of (5.28) Iwasaki *et al.* (1990) obtained the relation

$$n_c(0) = 4.783 v_c. \tag{5.30}$$

We were able to test this relation against the behaviour of the cylindrical solitons generated using the numerical solution since for the various values of k we tried, we obtained cylindrical solitons travelling at different speeds. A graph of their height versus speed is shown in Figure 5.5. We see that the behaviour of the cylindrical solitons that appear in the numerical solution of the full equation match the theoretical prediction very well. As previous work has not focussed on the k-dependence of the soliton speed and number, it appears that this is the first time that such a test has been carried out.

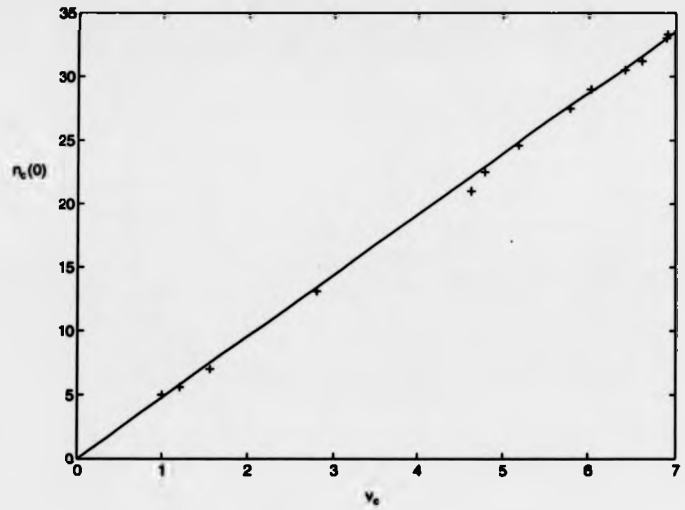

Figure 5.5: Speed-height relationship for cylindrical solitons. Solid line is the theoretical result (5.30). The crosses are determined from the numerical simulation of the full equation for various values of the perturbation wavenumber.

It was also shown by Iwasaki *et al.* (1990) that all cylindrical solitons have the same mass, M_c, which is defined by

$$M_c = \int_0^\infty U(r) 2\pi r \, dr \, .$$

Using numerical methods we find that M_c=61.87.

Consider the effect of a periodic perturbation of wavenumber k. By symmetry, if cylindrical solitons are to be formed as a result of its application, there must be at least one formed per wavelength. As was mentioned in Chapter 1, the total mass (given by (5.24)) is conserved. This leads to a criterion for the formation of cylindrical solitons - if k is too large, the total mass in a wavelength of the flat soliton will not be enough to form a cylindrical soliton. In other words, we have the condition

$$\frac{2\pi}{k} \int_{-\infty}^{\infty} n_0 \, dx > N_c M_c, \tag{5.31}$$

where N_c is the number of cylindrical solitons formed and n_0 is the number density of the flat soliton. Putting $N_c = 1$, this rather simplistic analysis gives an upper limit on k of

$$\hat{k}_c = \frac{48\pi}{M_c} \simeq 2.44 \tag{5.32}$$

for the formation of cylindrical solitons as compared with the true value of $k_c \simeq 2.24$.

The results of the numerical simulations for various values of k are shown in Figure 5.6. The number of structures that eventually emerge increases with the wavelength of the perturbation. We determined the nature of each 'hump' which arose by finding its mass, speed,

and height. For entities which turned out to be cylindrical solitons on the basis of their amplitude to speed ratio, their mass never differed from M_c by more than a few percent except in the cases where the degree of rippling in the neighbourhood of the soliton made an accurate estimate of its mass impracticable.

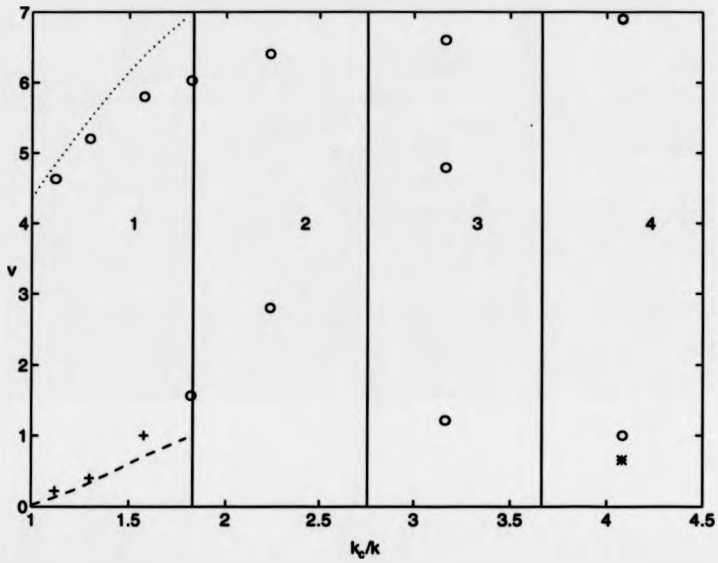

Figure 5.6: Diagram showing the types and speeds of solitons produced as a function of the wavelength of the perturbation. Circles - cylindrical solitons; crosses - flat solitons; * - possibly a bisoliton. Dotted line - theoretical v_c given by (5.35); dashed line - theoretical speed of flat soliton. The numbers refer to the theoretical maximum number of cylindrical solitons that can be produced by a perturbation of a given wavelength within that zone of the diagram.

The zone boundaries in Figure 5.6 are given by $k = k_c/N_c$ which is obtained from (5.31) and (5.32). We see that in the first three zones, the number of cylindrical solitons generated agrees with the theory. However, at k_c/k=4.1, only three cylindrical solitons appear on the diagram. A contour plot of the situation at $t = 23$ is shown in Figure 5.7. The structures labelled 1 and 2 are both large amplitude cylindrical solitons while structure 3 is an example of one with a much smaller amplitude. The mass of structure 4 is approximately $1.5M_c$ and so cannot be regarded as two separate cylindrical solitons. However its amplitude to speed ratio of 4.6 is remarkably close to that for cylindrical solitons, and the level curves at the peaks are circular to within 5%. These results together with the form of the contour plot of Figure 5.8, which shows the structure in more detail, suggest that it might be a 'bisoliton'. Bisoliton solutions are known for the KP^+ equation (Pelinovsky & Stepanyants 1993b). Their nature, however, does not closely resemble what we see here. In particular, the peaks of the KP^+ bisoliton are aligned with the direction of motion, and their existence can be directly attributed to the fact that the two-dimensional soliton solution drops below zero in some places.

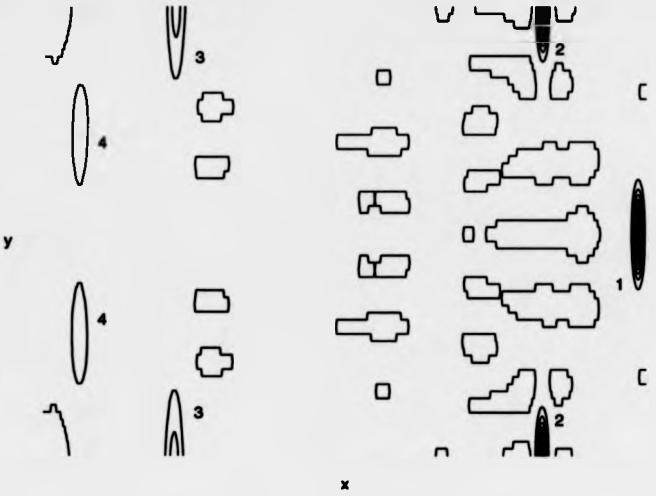

Figure 5.7: Contour plot of numerically evolved perturbed plane soliton at $t = 23$. $k_c/k = 4.1$. The structures labelled 1, 2, and 3 are cylindrical solitons; the nature of that labelled 4 is uncertain.

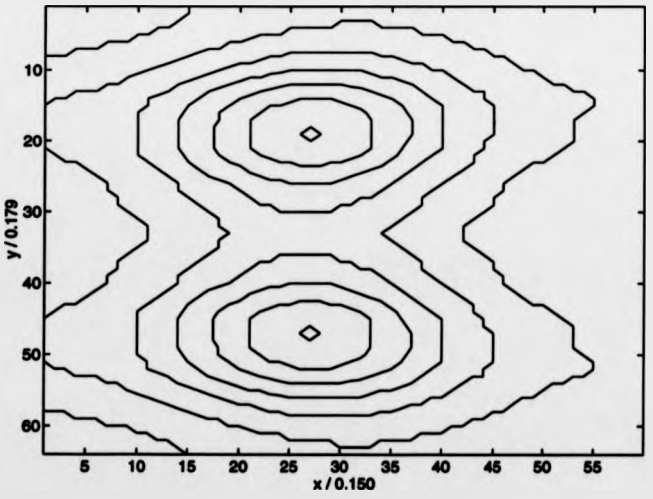

Figure 5.8: Contour plot of structure 4 of Figure 5.7.

Although once the bisoliton-type structure formed, it was not observed to change significantly, it is still possible that it is only a transient phenomenon and that the two humps will eventually coalesce to form a single cylindrical soliton plus some rippling. The domain size we used for this calculation was 2048×64; a further investigation of this structure would require a significantly longer domain and therefore much larger amounts of computer time and memory. It is for this reason that we ceased to investigate the long term behaviour for perturbations with k_c/k greater than 4.1.

Before moving on, we remark upon two other features of Figure 5.7. Firstly, the irregularly shaped level curves are due to 'ripples' in the solution. In general, we have found that there is a significant amount of this produced when more than one cylindrical soliton is permitted. Notice also that the two largest solitons are half a wavelength apart. For the ZK equation, the mass along an element parallel to the field,

$$M(y) = \int_{-\infty}^{\infty} n\,dx\ ,$$

is constant. Such an element passing through a high peak will have to become negative in some regions. Since there are no soliton solutions which ever have a negative value of n, the negative contribution will be generated by much less coherent ripples. It seems that the system favours producing coherent structures, and hence to minimize the amount of rippling, the largest coherent structures are arranged as evenly as possible in the y-direction.

We now turn to the case when only one cylindrical soliton per wavelength is produced. It was mentioned earlier that the amount of rippling is small for k close to k_c; we find instead that a perturbed plane soliton is always generated, appearing to travel in the opposite direction from the cylindrical soliton when viewed from the frame moving with the original plane soliton (see Figure 5.9). This phenomenon is also seen in the recent analytical results of Pelinovsky & Stepanyants (1993a) and the numerical results of Infeld *et al.* (1994) in the context of the KP^+ equation. This perturbed flat soliton persists because it does not have enough mass to decay into a cylindrical soliton.

The lack of a significant amount of rippling allows us to use the conservation of mass and conservation of momentum laws to obtain a relation between the emerging soliton speeds and the wavenumber of the perturbation. Equating the initial and total final masses and momenta leads to

$$\frac{48\pi}{k} = \frac{48\pi\eta}{k} + M_c \tag{5.33}$$

and

$$\frac{192\pi}{k} = \frac{192\pi\eta^3}{k} + M_c v_c \tag{5.34}$$

respectively. We have taken the emerging flat soliton to be of the form $12\eta^2\,\mathrm{sech}^2\eta(x-x_0)$. Solving the two equations and using (5.32) gives us

$$v_c = 4 + 4\eta(1+\eta) \tag{5.35}$$

where

$$\eta = 1 - \frac{k}{k_c}\,. \tag{5.36}$$

The speed of the emerging flat soliton is just $4\eta^2$. Both this and the theoretical value of v_c are plotted in Figure 5.6. The agreement with the numerically obtained data is not particularly

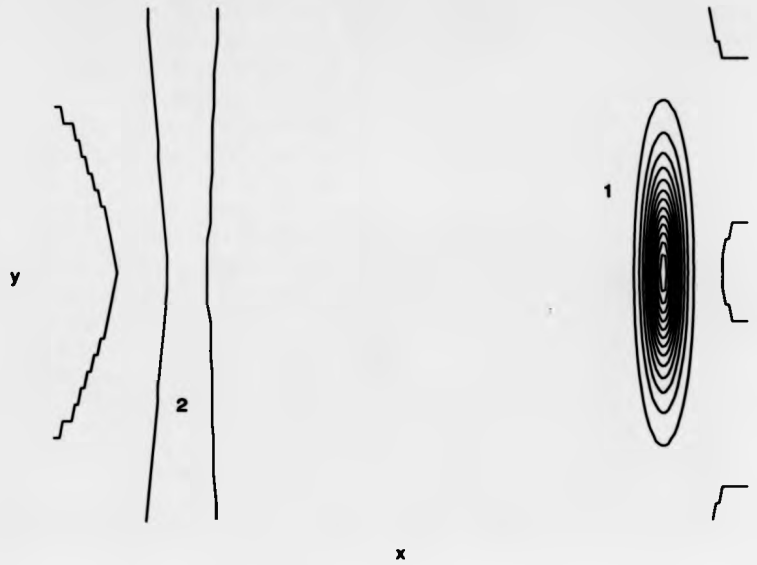

Figure 5.9: Contour plot of numerically evolved perturbed plane soliton at $t = 7.5$. $k_c/k = 1.6$. 1 - cylindrical soliton; 2 - plane soliton.

good, but this is hardly surprising since k_c differs from k_c by about 10%. Also, in deriving the mass and momentum of the ejected flat soliton we have neglected the fact that it can be quite severely perturbed (the contour lines in Figure 5.9 show this). Finally, we have not been able to include any effects of the ripples, although in this case their contribution to the discrepancy is probably not very large.

It is apparent from the plot that as the boundary between the first and second zone is approached, the flat soliton is replaced by the second cylindrical soliton. The transition occurs via the perturbation of the flat soliton growing more prominent as k_c/k increases, so that the soliton appears more and more localized, until the distinction between the two types of soliton becomes ill-defined just before the zone boundary. The presence of two cylindrical solitons at a value just inside the first zone can be attributed to a net negative contribution from the rippling to the total mass.

Notice finally that as k approaches the cut-off value, the speed of the cylindrical soliton approaches 4 which is the speed of the initial plane soliton, and the amplitude of the emerging plane soliton tends to zero. This is what we might have predicted on physical grounds, as for the cylindrical soliton to travel at a different speed from the initial soliton, mass (in the form of the plane soliton) would have to be ejected in the opposite direction. Since there is not much mass to spare when k is close to k_c, the system will try to minimize the amount of mass it ejects.

5.4 Discussion

In the nonlinear analysis we carried out, we performed a third type of regrouping of terms. This time the terms were not secular and there were no problems with the boundedness of the solution or singularities that had not already been dealt with. The regrouping was done merely in order to show that the perturbation undergoes a y-dependent phase shift.

The remainder of the chapter was based around the results of the numerical solution of the full two-dimensional ZK equation. Our numerical method was shown to be accurate and we were able to reproduce the generation of cylindrical solitons seen by others. The numerical results we obtained showed good agreement with both the linear and nonlinear analyses for small times.

The most important results we have presented here concern the effect of k on the subsequent emergence of organized structures. We have seen that the system tries to produce the maximum number of coherent structures that are theoretically possible. We have also presented tentative numerical evidence for the existence of a bisoliton solution to the ZK equation.

The theoretical maximum number of cylindrical solitons for a given perturbation wavenumber can be calculated because the mass of all cylindrical solitons is the same and because the overall mass of the system is conserved. The ideas involved are reminiscent of problems in particle physics in which a certain elementary particle can only come into existence if the total energy available is equivalent to its mass. Using, in addition to mass conservation, only the conservation of momentum, we can predict the nature of the coherent structures a perturbed plane soliton decays into when k is close enough to k_c.

Chapter 6

Conclusion

6.1 Conclusions

In this thesis we have examined both analytically and numerically the evolution of a perturbed plane soliton in the context of the Zakharov-Kuznetsov equation. Much of the analysis has involved the application of perturbation theory to the case when the growth rate of the perturbation is small. For periodic problems, multiple-scale perturbation theory is used to remove secular terms by implicitly regrouping the secular terms of the ordinary expansion. The corresponding terms in the non-periodic case are no longer strictly secular - we called them ghost secularities - but are still regrouped into slowly varying functions in a multiple-scale analysis. The central theme of the analytical techniques we have developed has been a *further* regrouping of terms in a perturbative expansion. We have presented three types of regrouping.

Chapter 2 was concerned with finding the growth rate of linear instabilities of a plane soliton. The method for solving such nonperiodic problems in the past has been to find the growth rate for the periodic case and then take the limit of infinite wavelength. This method is algebraically very involved and for the present problem had been used to find the growth rate to only first order. If, instead, an ordinary perturbation analysis is applied to the soliton solution directly, it is found that what we referred to as algebraically secular terms arise. These terms cannot be removed, and considered individually do not decay to zero at infinity. To circumvent this difficulty we developed a method centred around a multiple-scale perturbation analysis.

The key idea behind our new method is to choose the arbitrary constants of integration in such a way that the terms in the expansion have the correct behaviour to zeroth order in a small quantity as $x \to \pm\infty$. If this not done, one obtains incorrect results for the growth rate. The algebraically secular terms are dealt with by regrouping them so that their asymptotic forms constitute the expansion of an exponential function of a scaled variable. This, in conjunction with the arbitrary function of scaled variables whose nature is determined by the conventional multiple-scale analysis, gives an overall expression that has the correct asymptotic form.

Our new method is applicable to equations which have at least one asymptotic solution that is constant to zeroth order in a small parameter, and whose linearization results in an equation which can be solved analytically. We were able to use it to characterize part of one of the branches of asymmetric soliton states occurring in optical fibre couplers. Its use also

led us to discover that a multiple-scale approach can sometimes hint at an exact solution for certain linearized equations. An exact analytical expression for the growth rate for all wavenumbers can then be obtained easily.

We needed to carry out another type of regrouping of terms in order to find the growth rate for obliquely propagating solitons. To obtain an expression for the growth rate to second order that is free of singularities it was necessary to regroup some of the exponential secularities in addition to the algebraically secular terms. The method we developed is applicable to any situation where the first order expression obtained is free from singularities, but the higher order terms found by the conventional method are not.

Finally, in Chapter 5 we performed a regrouping of non-secular terms in order to simplify the overall expression and hence demonstrate that the perturbation of finite size undergoes a bending. This was as far as the analysis was able to take us towards an understanding of the mechanism behind the generation of cylindrical solitons.

In two instances we obtained an analytical description of a curve in the neighbourhood of its endpoints. The first instance was for the growth rate curve in Chapter 2, the other arose in connection with one of the branches of asymmetric states in the optical fibre problem. In both cases we found that a two-point Padé approximant chosen in a natural way gave an analytic expression for the entire curve which agreed well with the numerically derived results. To test the analytical results we derived for the growth rate, in Chapter 2 we also developed a numerical method based on the shooting method. It was found to give very accurate results while remaining computationally inexpensive.

In the final section of the thesis we looked at the coherent structures that emerge as a result of perturbing a plane soliton. It was found that in some cases the structures could be analysed as particles obeying the laws of mass and momentum conservation.

6.2 Future studies

During the course of this study, a number of problems worthy of further investigation arose. First of all, we saw in Chapter 2 that we have to regroup the algebraic secularities ourselves to form a slowly varying exponential in contrast to the automatic regrouping of ghost secularities which occurs by virtue of the multiple-scale expansion. One would hope that a formalism for regrouping algebraic secularities automatically could also be found. In this chapter we showed that the value of γ_4 differed significantly from its numerically determined value. Further work needs to be done to see whether after the third order, the series for the growth rate then diverges.

In Chapter 3 we failed to completely describe one end of one of the branches of solutions analytically. It would be interesting to see whether the difficulties inherent in this problem could be overcome. We postulated in this chapter that the solutions to linearized integrable equations contain only a finite number of terms (and hence our straightforward method to find the growth rate exactly can be applied). Further analysis could perhaps show whether this conjecture is true.

We are still a long way from a deep understanding of the transition from perturbed plane solitons to cylindrical solitons. However, the recent complete analytical description of the analogous process for the KP^+ equation (Pelinovsky & Stepanyants 1993a) surely holds some important clues. It would also be interesting to look at the dependence of soliton formation on k for that equation. Presumably the situation would be a lot simpler - due to the integrability

of the equation and hence the infinite number of conservation laws it possesses, the amount of rippling would be minimal, even for small k.

Finally, we have only been considering the two-dimensional equation. The plane to spherical soliton and cylindrical to spherical soliton transitions that have been observed numerically have yet to be analysed.

Appendix A

Higher order analysis for the linearized ZK equation

The fourth order contribution to Φ is obtained from

$$\begin{aligned}\partial_x L\Phi_4 &= -2\Phi_{0,xx4} - 6\Phi_{0,x13} - 3\Phi_{0,xx2} - 3\Phi_{0,112} - 3\Phi_{1,xx3} - 6\Phi_{1,x12} - \Phi_{1,111} \\ &\quad -3\Phi_{2,xx2} - 3\Phi_{2,x11} - 3\Phi_{3,xx1} - (n_0-4)(\Phi_{1,3} + \Phi_{2,2} + \Phi_{3,1}) \\ &\quad -\gamma_4\Phi_0 - \gamma_3\Phi_1 - \gamma_2\Phi_2 - \gamma_1\Phi_3 + \Phi_{0,2} + \Phi_{1,1} + \Phi_{2,x}. \end{aligned} \tag{A.1}$$

With the help of *Mathematica* this is solved in the same way as before and gives

$$\begin{aligned}\Phi_4 &= h_0\left\{\frac{1}{128}\left(\frac{56}{225} + \gamma_1\gamma_3\right)e^{-2x} + \frac{1}{25}\mathcal{A}_2 + \frac{1}{75}\mathcal{A}_1 - \frac{1}{50}\mathcal{A}_1\tanh x\right. \\ &\quad + \frac{\gamma_1\gamma_3}{64}\mathcal{A}_0 + \frac{1}{300}\left(\mathcal{A}_1 e^{2x} - 1\right) + \left(\frac{47}{1200} - \frac{3\gamma_1\gamma_3}{128} + \frac{\gamma_4}{8}\right)\operatorname{sech}^2 x \\ &\quad \left. - \frac{3}{100}\mathcal{A}_1\operatorname{sech}^2 x - \frac{2}{25}\mathcal{A}_2\operatorname{sech}^2 x + \frac{3}{100}\mathcal{A}_2\varphi_0 + \frac{3}{25}\mathcal{A}_3\varphi_0\right\} \\ &\quad + \left(-\frac{11h_0}{1200} + \frac{3\gamma_1\gamma_3 h_0}{128} - \frac{\gamma_4 h_0}{8} - h_{0,4}\right)x\varphi_0. \end{aligned} \tag{A.2}$$

To remove the e^{-2x} term we put

$$\gamma_3 = -\frac{7}{120}\gamma_1 = -\operatorname{sgn}(k)\frac{7}{15\sqrt{15}}. \tag{A.3}$$

Note that the $\mathcal{A}_1 e^{2x} - 1$ term tends to zero as $x \to \infty$ (see equation (2.47)) and so does not present a problem. Using (A.3) and removing the ghost secularities from (A.2) by assigning

$$h_{0,4} = \left(-\frac{3}{200} - \frac{\gamma_4}{8}\right)h_0 \tag{A.4}$$

leaves

$$\begin{aligned}\Phi_4 &= h_0\left\{\frac{1}{25}\mathcal{A}_2 + \frac{1}{75}\mathcal{A}_1 - \frac{1}{50}\mathcal{A}_1\tanh x + \frac{7}{1800}\mathcal{A}_0 + \frac{1}{300}\left(\mathcal{A}_1 e^{2x} - 1\right)\right. \\ &\quad \left. + \left(\frac{9}{200} + \frac{\gamma_4}{8} - \frac{3}{100}\mathcal{A}_1 - \frac{2}{25}\mathcal{A}_2\right)\operatorname{sech}^2 x + \left(\frac{3}{100}\mathcal{A}_2 + \frac{3}{25}\mathcal{A}_3\right)\varphi_0\right\} \end{aligned} \tag{A.5}$$

By considering terms in $L\Phi_5$ whose inverses contain exponential secularities, we also obtain

$$\gamma_4 = -\frac{8}{225}. \tag{A.6}$$

As a further check on our *Mathematica* manipulations, the same result was obtained via the consistency condition

$$\int_{-\infty}^{\infty} \operatorname{sech}^2 x \, \partial_x L\Phi_5 \, dx = 0. \tag{A.7}$$

Appendix B

Use of computer algebra

The software package *Mathematica* can be used to perform a wide variety of symbolic manipulations. It is particularly useful for dealing with problems in algebra that are straightforward but lengthy. However its real power lies in its ability to be used as a programming language.

We wrote a library of *Mathematica* routines to help with the solution of equations by either an ordinary or a multiple-scale perturbative approach. The routines were extensively tested by comparing the results they gave with calculations done by hand. We now illustrate the use of our routines by describing the procedure by which the calculations detailed in Appendix A were performed.

Using *Mathematica* the expansions to whatever order we desire of γ and Φ and the total derivative with respect to x can be substituted into the linearized equation and terms of the same order in k collected together. We can select the coefficient of k^4 and then subtract it from $\partial_x L\Phi_4$ to obtain the right hand side of (A.1). The Φ_m and their derivatives have so far been processed in symbolic form as we have defined rules by which they are transformed under differentiation. In order to be able to integrate the right hand side, the functional forms of Φ_m for $m < 4$ are substituted in.

As *Mathematica* is not very good at evaluating limits as the argument tends to infinity, we used it to evaluate the indefinite integral of (A.1). To find the required definite integral we used our own routine to find the limit of the integral as $x \to \infty$. We should point out that once we have supplied the properties of the $\mathcal{A}_n$ to *Mathematica*, it is able to manipulate these functions like any other.

We defined the function $L^{-1}(R(x))$ using (2.31) and the fact that it is a linear operator. This means, for instance, that $L^{-1}(Af(x)+Bg(x))$ is evaluated as $AL^{-1}(f(x))+BL^{-1}(g(x))$. As the evaluation of this operator using (2.31) is rather time-consuming and sometimes too difficult for *Mathematica*, we arranged for the results to be stored for future use so that they only ever need to be calculated once. We calculated the results which *Mathematica* could not find ourselves and added them to the L^{-1} database. The contents of the database were of course checked by applying L to them.

With the use of our L^{-1} function we can then obtain Φ_4, and γ_3 is determined from the coefficient of e^{-2x}. To check our result for γ_3 we can use *Mathematica* to solve the consistency condition equation

$$\int_{-\infty}^{\infty} \operatorname{sech}^2 x \, \partial_x L\Phi_4 \, dx = 0$$

by again using our own limit finding routines once the indefinite integral has been performed.

Bibliography

ABLOWITZ, M.J., KAUP, D.J., NEWELL, A.C. & SEGUR, H. 1974 *Stud. Appl. Math.* **53**, 249-315.

ABLOWITZ, M.J., RAMANI, A. & SEGUR, H. 1980 *J. Math. Phys.* **21**, 715-21.

AKHMEDIEV, N. & ANKIEWICZ, A. 1993 *Phys. Rev. Lett.* **70**, 2395-8.

ALLEN, M.A. & ROWLANDS, G. 1993 *J. Plasma Phys.* **50**, 413-24.

ANDERSON, D., BONDESON, A. & LISAK, M. 1979 *J. Plasma Phys.* **21**, 259-66.

BAKER, G.A. & GRAVES-MORRIS, P. 1984 *Padé Approximants* (CUP, Cambridge).

BENJAMIN, T.B. 1972 *Proc. Roy. Soc.* **328**, 153-83.

BOUSSINESQ, J. 1871 *Compte Rendus Acad. Sci.* **72**, 755-9.

BUTCHER, P.N. 1967 *Rep. Prog. Phys.* **30**, 97-148.

CANUTO, C., HUSSAINI, M.Y. & QUATERONI, M.Y. 1988 *Spectral Methods in Fluid Dynamics* (Springer-Verlag, New York).

DAS, K.P. & VERHEEST, F. 1989 *J. Plasma Phys.* **41**, 139-155.

DAVIDSON, R.C. 1972 *Methods in nonlinear plasma theory* (Academic, New York).

DAVIES, P.C.W. 1987 *The Cosmic Blueprint* (Heineman, London).

DAVYDOV, A.S. 1982 *Biology and Quantum Mechanics* (Permagon Press, Oxford).

DRAZIN, P.G. & JOHNSON, R.S. 1989 *Solitons: an introduction* (CUP, Cambridge).

FAUCHER, M. & WINTERNITZ, P. 1993 *Phys. Rev.* **E 48**, 3066-71.

FORSYTH, A.R. 1888 *Treatise on Differential Equations* (Macmillan, London).

FRYCZ, P. & INFELD, E. 1989 *Phys. Rev. Lett.* **63**, 384-5.

FRYCZ, P., INFELD, E. & SAMSON, J.C. 1992 *Phys. Rev. Lett.* **69**, 1057-60.

GARDNER, C.S., GREENE, J.M., KRUSKAL, M.D. & MIURA, R.M. 1967 *Phys. Rev. Lett.* **19**, 1095-7.

HASEGAWA, A. 1989 *Optical solitons in fibers* (Springer-Verlag, Berlin).

HASEGAWA, A. & TAPPERT F. 1973 *Appl. Phys. Lett.* **23**, 142.

IKEZI, H., TAYLOR, R.J. & BAKER, D.R. 1970 *Phys. Rev. Lett.* **25**, 11-14.

INFELD, E. 1985 *J. Plasma Phys.* **33**, 171-82.

INFELD, E. & FRYCZ, P. 1987 *J. Plasma Phys.* **37**, 97-106.

INFELD, E. & ROWLANDS, G. 1977 *Plasma Phys.* **19**, 343-8.

INFELD, E. & ROWLANDS, G. 1990 *Nonlinear waves, solitons and chaos* (CUP, Cambridge).

INFELD, E. & ROWLANDS, G. 1991 *Phys. Rev.* **A 43**, 4537-9.

INFELD, E., SENATORSKI, A. & SKORUPSKI, A.A. 1994 *Phys. Rev. Lett.* **72**, 1345-7.

IWASAKI, H., TOH, S. & KAWAHARA, T. 1990 *Physica* **D 43**, 293-303.

KADOMTSEV, B.B. & PETVIASHVILI, V.I. 1970 *Sov. Phys. Dokl.* **15**, 539-41.

KORTEWEG, D.J. & DE VRIES, G. 1895 *Phil. Mag.* **39**, 422-3.

KRUMHANSL, J.A. & SCHRIEFFER, J.R. 1975 *Phys. Rev.* **B 11**, 3535-45.

KUZNETSOV, E.A., SPECTOR, M.D. & FAL'KOVICH, G.E. 1984 *Physica* **D 10**, 379-86.

LAEDKE, E.W. & SPATSCHEK, K.H. 1979 *J. Math. Phys.* **20**, 1838-41.

LAEDKE, E.W. & SPATSCHEK, K.H. 1982 *J. Plasma Phys.* **28**, 469-84.

LONNGREN, K. & SCOTT, A. 1978 *Solitons in Action* (Academic, New York).

MAKHANKOV, V.G. 1978 *Phys. Reports* **35**, 1-128.

MANAKOV, S.V., ZAKHAROV, V.E., BORDAG, L.A., ITS, A.R. & MATEEV, V.B. 1977 *Phys. Lett.* **63A**, 205-6.

MELKONIAN, S. & MASLOWE, S.A. 1989 *Physica* **D 34**, 255-69.

MELKONIAN, S. & WINTERNITZ, P. 1991 *J. Math. Phys.* **32**, 3213-27.

MIURA, R.M., GARDNER, C.S. & KRUSKAL, M.D. 1968 *J. Math. Phys.* **9**, 1204-9.

NAYFEH, A.H. & MOOK D.T. 1979 *Nonlinear Oscillations* (Wiley, New York)

NOZAKI, K. 1981 *Phys. Rev. Lett.* **46**, 184-7.

PELINOVSKY, D.E. & STEPANYANTS, Y.A. 1993a *Soviet Phys. JETP* **77**, 602-8.

PELINOVSKY, D.E. & STEPANYANTS, Y.A. 1993b *Soviet Phys. JETP Lett.* **57**, 24-8.

PRESS, W.H., FLANNERY, B.P., TEUKOLSKY, S.A. & VETTERLING, W.T. 1988 *Numerical Recipes in C* (CUP, Cambridge).

PRIGOGINE, I. 1980 *From Being to Becoming: Time and Complexity in the Physical Sciences* (Freeman, San Francisco).

RAYCHAUDHURI, S., HILL, J., FORSHING, P., CHANG, H.Y., SUKARTO, S., LIEN, C. & LONNGREN, K.E. 1987 *Physica Scripta* **36**, 508-12.

ROWLANDS, G. 1969 *J. Plasma Phys.* **3**, 567-76.

RUSSELL, J.S. 1844 *Reports of the Meetings of the British Association for the Advancement of Science* (John Murray, London) pp. 311-90.

SHIVAMOGGI, B.K. 1989 *J. Plasma Phys.* **41**, 83-88.

SHIVAMOGGI, B.K., ROLLINS, D.K. & FANJUL, R. 1993 *Physica Scripta* **47**, 15-17.

SPATSCHEK, K.H., SHUKLA, P.K. & YU, M.Y. 1975 *Phys. Lett.* **A 54**, 419-20.

TABOR, M. 1989 *Chaos and Integrability in Nonlinear Dynamics* (Wiley, New York).

TRILLO, S., WABNITZ, S., WRIGHT, E.M. & STEGEMAN, G.I. 1988 *Opt. Lett.* **13**, 672-4.

WASHIMI, H. & TANIUTI, T. 1966 *Phys. Rev. Lett.* **17**, 966-8.

WEISS, J., TABOR, M. & CARNEVALE, G. 1983 *J. Math. Phys.* **24**, 522-6.

WOLFRAM, S. 1991 *Mathematica* (Addison-Wesley, Redwood City).

ZABUSKY, N.J. & KRUSKAL, M.D. 1965 *Phys. Rev. Lett.* **15**, 240-3.

ZAKHAROV, V.E. 1975 *JETP Lett.* **22**, 172-3.

ZAKHAROV, V.E. & KUZNETSOV, E.A. 1974 *Soviet Phys. JETP* **39**, 285-6.

ZAKHAROV, V.E. & RUBENCHIK, A.M. 1974 *Soviet Phys. JETP* **33**, 494-500.

ZAKHAROV, V.E. & SHABAT, A.B. 1974 *Funct. Anal. Appl.* **8**, 226-35.

4